

^{12th}
Targetry Workshop



12th International Workshop on Targetry and Target Chemistry

July 21-24, 2008

Seattle, Washington

ABSTRACT BOOK

[Home](#)

Organizing Committee

[Registration](#)

[Location](#)

[Accommodation](#)

[Program](#)

[Abstracts](#)

[Practicum](#)

Committee

[Contact](#)

Jeanne M. Link

Univ. of Washington

Kenneth R. Buckley

TRIUMF

Salma Jivan

TRIUMF

Kenneth A. Krohn

Univ. of Washington

James P. O'Neil

Univ. of California, LBNL

Thomas J. Ruth

TRIUMF



International Organizing Committee

Jeanne M. Link

Seattle, USA

John Clark

United Kingdom

Sven-Johan Heselius

Finland

Mikael Jensen

Denmark

Thomas J. Ruth

Vancouver, Canada

Didier Le Bars

France

Mario Martarrese

Italy

Olof Solin

Finland

Jean-Luc Morelle

Belgium

James P. O'Neil

Berkeley, USA

And Special Thanks to the Following Individuals

Michael J. Welch
 Gregory Gaehle
 Sven-John Heselius
 Olof Solin
 Didier LeBars
 Todd Barnhart
 Sandi Miller
 Shirley Reeve

John Clark
 David J Schlyer
 Robert J Nickles
 Hannu Sipila
 Todd Barnhart
 Linda Kimura
 Michelle Hilliker
 Libby Nielsen

***We Gratefully Thank our Sponsors for their Generous Support
that made this Targetry Workshop Possible.***

GE Healthcare

MDS Nordion

IBA Molecular

Bioscan

Eckert & Ziegler Eurotope

Sumitomo

Veenstra

Siemens Healthcare

AAPS - Advanced Applied Physics Solutions

COMECER

Advion

ABX

Von Gahlen

MONROL

Capintec, Inc.

ACF Metals

Isoflex

Medical Isotopes Inc.

D-Pace

Carroll & Ramsey Associates

Table of Contents

GAS TARGETS

Comparing the Results, Durability, and Production During the Evolution of C-11 targets on the RDS-111 Cyclotron Starting with the RDS111 Targets through the Progression to the Eclipse targets. Page 1

*Robert C. Dennett, Greg G. Gaehle, Robert H. Mach
Mallinckrodt Institute of Radiology, St Louis, MO*

Experiences Upgrading the RDS111 to an RDS Eclipse with Continuing Improvements to the Gas Targets Reliability and Production Page 2

*Greg G. Gaehle, Robert C. Dennett, Robert H. Mach, Michael J. Welch
Mallinckrodt Institute of Radiology, St. Louis, MO*

High yield [¹¹C]-CO₂ on a commercial cyclotron enhances possibilities for clinical tracer usage. Page 3

*Norling J¹, Dahlstrom K¹, Eriksson T¹, Nilsson R¹, Kilbourn M², Moskwa J², Smith RD³
¹GE Healthcare, Uppsala, Sweden; ²University of Michigan, Ann Arbor, MI, USA; ³GE Healthcare, Pewaukee, WI, USA*

A flexible [¹¹C]methane target Page 4

*Jacek Koziarowski¹, Peter Larsen², Holger Jensen³, Nic Gillings³
¹Herlev Hospital, University of Copenhagen, Herlev, Denmark; ²Scansys Laboratorieteknik, Vaerloese, Denmark; ³Copenhagen University Hospital, Righospitalet, Denmark*

Upgrading RDS-111 Turret Style Gas Targets: Experience with a New ¹⁸O₂-¹⁸F₂ Target Page 7

*James P. O'Neil and Christopher A. Ramsey
Biomedical Isotope Facility, Lawrence Berkeley National Laboratory, Berkeley, CA*

Improvement of the ¹¹C target at the Department of Nuclear Medicine at the University at Buffalo, the State University of New York. Page 9

*Erol Bars, Dr Sajjad M., Dr Mike Haka, Steve Toonrongian
University at Buffalo, the State University of New York, NY*

WATER TARGETS

Multi-kilowatt Recirculating Targets for the Production of ¹⁸F Page 11

*J. Michael Doster and Robert P. Newman
Department of Nuclear Engineering, North Carolina State University*

Experiences from using a PETtrace cyclotron at 130 μ A (2 x 65 μ A) with niobium targets producing ¹⁸F / FDG Page 14

*Eriksson T¹, Norling J¹, Eberl S², Husnu M³, Chicoine R³
¹GE Healthcare, Uppsala, Sweden; ²Royal Prince Alfred Hospital, Sydney, Australia;
³Cardinal Health, Ft. Lauderdale, Florida, USA*

High Current F-18 Water Target with Liquid Spray-Cooled Window Page 16

*Alexander Zyuzin¹, Erik van Lier¹, Richard Johnson¹, Jay Burbee¹, John Wilson²
¹Advanced Cyclotron Systems Inc., Richmond, BC, Canada; ²Cross Cancer Institute, Edmonton, AB, Canada*

- Deployment, Testing and Analysis of Advanced Thermosyphon Target Systems for Production of Aqueous [^{18}F]Fluoride via $^{18}\text{O}(\text{p},\text{n})^{18}\text{F}$** Page 19
Matthew Stokely^{1,2,3}, Johanna Peeples¹, J. Michael Doster¹, Gerald Bida², Bruce Wieland^{1,2,3}
¹Department of Nuclear Engineering, North Carolina State University, Raleigh, NC;
²Department of Nuclear Medicine, Duke University Medical Center, Durham, NC;
³Bruce Technologies Inc., Chapel Hill, NC
- Pressurized Water Target for high beam currents and multi Ci $^{18}\text{F}^-$ production** Page 22
A. Cambriani, Y. Jongen, M. Degeyter, B. Lambert
 Ion Beam Application SA
- Scaling up F-18 fluoride production in recirculating O-18 target** Page 27
Kiselev M, Botov S, Sokolovski E, Lai D, Vantos T, Schreiner E, Jongen Y
 IBA Molecular, Sterling, VA, USA
- Development and Validation of Computer Models for Design of Batch Boiling Targets for Production of ^{18}F** Page 29
Johanna Peeples, Matthew Stokely, Michael Doster
 North Carolina State University
- Ionic contaminants in irradiated [^{18}O]water generated with Havar and Havar-Nb foils** Page 31
J.S. Wilson¹, M.A. Avila-Rodriguez^{1,2}, S.A. McQuarrie¹
¹Edmonton PET Centre, Edmonton, AB, Canada; ²Turku PET Centre, Turku, Finland

SOLID TARGETS

- Comparison between different temperature measurement methods for a solid targetry irradiation system** Page 34
S. Chan, D. Cryer, R. I. Price, & RAPID GROUP
 Department of Medical Technology and Physics, Sir Charles Gairdner Hospital, Perth, Western Australia
- A rotating target for the irradiation of Ra-226** Page 37
Dr. M. Harfensteller¹, Dr. J. Moreno², Dr. R. Henkelmann², Dr. M. Mentler³, Dr. E. Huenges³, Dr. V. Bechtold¹, Prof. Dr. A. Tuerler², Dr. E. Kaba², Dipl.-Ing. A. Eursch⁴
¹Actinium Pharmaceuticals, API; ²Institute of Radiochemistry, Technische Universität München; ³Institute E17, Technische Universität München; ⁴Institute for Machine Tools and Industrial Management, Technische Universität München
- Production of ^{64}Cu on the CC18/9 Cyclotron at TPC, a work in progress** Page 38
M.A. Avila-Rodriguez^{1,2}, J. Rajander^{2,3}, S. Johansson^{2,3}, P.O. Eriksson^{2,3}, T. Wickstrom³, S. Vauhkala^{1,2}, E. Kokkomaki^{1,2}, J. Schlesinger^{1,2}, O. Solin^{1,2}
¹Turku PET Centre, University of Turku, Turku, Finland; ²Centre of Excellence on Molecular Imaging in Cardiology and Metabolic Research; ³Accelerator Laboratory, Abo Akademi University, Turku, Finland
- Design and construction of a compact semi automated solid target irradiation system for the production of ^{124}I , ^{64}Cu plus various solid-targetry based radioisotopes, using an 18/9 MeV IBA cyclotron.** Page 41
D. Cryer, S. Chan, R.I. Price, & RAPID Group
 Department of Medical Technology and Physics, Sir Charles Gairdner Hospital, Perth, Western Australia

- Thermal Modeling of an ^{124}I Solid Cyclotron Target** Page 44
K. Gagnon¹, M.A. Avila-Rodriguez³, S.A. McQuarrie²
¹Department of Physics, University of Alberta, Edmonton, Canada; ²Faculty of Medicine and Dentistry, University of Alberta, Edmonton, Canada; ³Turku PET Centre, Turku, Finland
- Multi Purpose Solid Target System for a MC 17 Scanditronix Cyclotron Pneumatic Manoeuvrable for Low Personnel Doses** Page 45
Jonathan Siikanen¹, Tomas Ohlsson², Anders Sandell²
¹University of Lund, Department of Medical Radiation Physics; ²Lund University Hospital, Sweden
- Investigation of Failure Mechanisms in Niobium-Encapsulated Gallium Targets for the Production of Germanium-68 Radioisotope** Page 47
Hong T. Bach¹, Thomas N. Claytor¹, Michael A. Connors¹, James F. Hunter¹, Francois M. Nortier¹, Donna M. Smith¹, Frank O. Valdez¹, John W. Lenz², Chuck Moddrell³, Paul A. Smith³
¹Los Alamos National Laboratory, Los Alamos, NM; ²John W. Lenz & Associates, Waxahachie, TX; ³P.A. Smith Concepts & Designs, Los Alamos, NM
- Efficient Separation of ^{64}Cu from ^{67}Ga Waste Product with Solvent Extraction and Chromatography: Co-production of ^{64}Cu and ^{67}Ga** Page 49
K.S. Chun, H. Park, J.H. Kim
 Dept of Radiopharmaceutical, Korea Institute of Radiological & Medical Sciences, Seoul, Korea
- Development of Tandem Targets for a Vertical Beam Target Station** Page 51
G.F. Steyn¹, C. Vermeulen¹, E. Isaacs¹, S. DeWindt¹, D. Saal¹, H.P. Burger², C. van Rooyen², F.C. de Beer³, H. Knox⁴, J. Isobe⁵
¹iThemba LABS, Somerset West, South Africa; ²National Laser Centre, CSIR, Pretoria, South Africa; ³Nuclear Technology Division, Necsa, Pretoria, South Africa; ⁴EB Welding CC, Pelindaba, Pretoria, South Africa; ⁵MDS Nordion, Vancouver, BC, Canada
- ACCELERATORS, BEAMLINES**
- A Simple Method for Measuring the Beam Profile of Charged Particle Accelerators** Page 54
M.A. Avila-Rodriguez, J.S. Wilson, S.A. McQuarrie
 Edmonton PET Centre Edmonton, AB, Canada
- Proton Beam Monitoring via (p,xn) Reactions in Niobium** Page 57
M.A. Avila-Rodriguez^{1,3}, J.S. Wilson¹, S.A. McQuarrie¹, M.J. Schueller², J.O. Lill³, J. Rajander³, O. Solin³
¹Edmonton PET Centre, Edmonton, AB, Canada; ²Brookhaven National Laboratory, Upton, NY; ³Turku PET Centre, Turku, Finland
- Decommissioning the Birmingham Nuffield cyclotron** Page 60
D.B. Mackay¹, N. Berovic², D. Parker²
¹University of Edinburgh, QMRI, Edinburgh; ²University of Birmingham, Edgbaston, Birmingham, UK
- Optimization of the Pulsar-7 a 7MeV linear accelerator** Page 63
Eyal Gimshi, Dr. Alex Tsechanski, Dr. Eli Shalom
 Engineering Sciences, Department of Nuclear Engineering, Ben-Gurion University of the Negev, Israel

CHEMISTRY, AUTOMATION, ETC.

- Raclopride synthesis conducted on a microfluidic chip** Page 66
S. Haroun, T.J. Ruth, and Paul D.H. Li
Department of Chemistry, Simon Fraser University, Burnaby, BC, Canada
- Synthera: A versatile platform for Nucleophilic Substitution Labeling Reactions** Page 67
Alexander Schmitz and Richard Freifelder
Department of Radiology, University of Pennsylvania
- Relatively Inexpensive Platform for Building Automated Chemistry Modules to Synthesize C-11 and F-18 Radiopharmaceuticals** Page 70
Greg G. Gaehle, Chris Bogner, Jeff Willits, Robert H. Mach
Mallinckrodt Institute of Radiology, St Louis, MO
- Commercial production of FDG in four cyclotron facilities serving forty PET centers** Page 72
Ayfer Soyulu, Harun Küçükmidil
MONROL Nuclear Products Industry and Trade Inc., Turkey
- Performance of a preloaded cassette based synthesis module for F-18 FDG production** Page 73
Paul E. Christian, H. Eric Smith, Brandon S. Buckway, John Gibby, Melissa L. Brooks, Kathryn A. Morton, John M. Hoffman
Huntsman Cancer Institute, University of Utah, Salt Lake City, UT
- A proportional counter for blood radioactivity measurements** Page 74
H.T. Sipila¹, A. Roivainen¹, J. Johansson¹, S-J. Heselius²
¹Turku PET Centre, Turku University Central Hospital, Turku, Finland; ²Turku PET Centre, Accelerator Laboratory, Turku, Finland
- Method of distribution of radioactive liquid product from the cyclotron targets to the hotcell labs at the Department of Nuclear Medicine at the University at Buffalo, the State University of New York.** Page 78
Erol Bars, Dr Lynn Kaczmarek
University at Buffalo, the State University of New York.
- Semi-automated process of Choline and acetate module at the Department of Nuclear Medicine at the University at Buffalo, the State University of New York.** Page 80
Erol Bars, Dr Sajjad
University at Buffalo, the State University of New York.
- Breaking in a Scansys automated synthesis box with [¹¹C]Methyl Iodide and [¹¹C]Methyl Triflate** Page 81
Jonathan W. Engle, Todd E Barnhart, Dhanabalan Murali, Nick T Vandehey, Peter Larsen, Robert J Nickles
University of Wisconsin, Madison, WI

Comparing the Results, Durability, and Production During the Evolution of C-11 targets on the RDS-111 Cyclotron Starting with the RDS111 Targets through the Progression to the Eclipse targets.

Robert C. Dennett, Greg G. Gaehle, and Robert H. Mach
Mallinckrodt Institute of Radiology, 510 S. Kingshighway, St. Louis Missouri, 63110

A RDS-111 was originally installed in the fall of 2001 at Washington University Medical School. It was installed with dual RDS111 C-11 targets with the promise of upgrading to dual eclipse C-11 targets. The original target was aluminum body with Havar target foils 0.001" thickness. The target system operated with helium cooling that also added vacuum windows to the beamline. The original targets were able to run at a beam current of 40uA and because of the helium cooling on the surface of the targets the transmission on the targets was not an issue. The reliability of the targets was very good with yields of 1550mCi with a 40μA per 40 minute bombardment. The yields and specific activity measured by radiopharmaceutical quality remained consistent with very few failures in as a result of the target.

The first upgrade to the eclipse C-11 target used an aluminum target body with a CuBe target window 0.002" thickness and a Copper hex grid to support the window on the target. This target had the ability to run at 60uA with no limitations; the improvement of the eclipse also removed the helium cooling from the target system. The C-11 yield of the target improved to 1700mCi with a 60μA per 40 minute bombardment from the RDS 111. The reliability of the targets was questionable do to an oxidation layer the developed on the back of the target window inside the target. This resulted in a green discoloration that eventually changed to a black color over time. These problems with the target window resulted in production slowly tapering off over a period of two weeks resulting in the target needing to be rebuilt frequently.

In Dec 2005 we installed a second generation Eclipse C-11 gas target which consisted of an aluminum target body with Havar target foils 0.001" thickness and a thicker copper grid from the previous target to support and cool the target window. The new gas target had the ability to run at 60 μA with a transmission limit of < 70%. To achieve this transmission, a thicker stripping foil is used during C-11 production (~ 20-25 micron). With this target the C-11 yield of the target improved to 1900 mCi@EOB for a 60 μA 40 minute bombardment. The reliability of the target improved on the production side with consistent and increased yields of the targets. The target sometimes failed prematurely due to operator error in running with transmission > 70%. Because of the significant improvements in this target the decision was made to upgrade the machine to dual eclipse. This should have allowed us the capability of running 2 C-11 eclipse targets at the same time, thereby improving yields to 3800 mCi with a dual 60μA per 40 minute bombardment. The initial RF system hampered dual production at the lower transmissions required for the new targets. This caused us to upgrade the RF to the new QEI Rf system, and this has provided us the capability to run dual C-11 gas targets. The increased yields of the C-11 from dual targets has given our original RDS-111 the ability to produce 3300 mCi with a dual 60μA 30 minute with specific activity that allows us to produce all C-11 compounds currently and previously used at Washington University in a timely manner.

Experiences Upgrading the RDS111 to an RDS Eclipse with Continuing Improvements to the Gas Targets Reliability and Production

Greg G. Gaehle, Robert C. Dennett, Robert H. Mach and Michael J. Welch
Mallinckrodt Institute of Radiology, 510 S. Kingshighway, St. Louis Missouri, 63110

A dual beam line (CTI) RDS111 was installed at Washington University In September of 2001 with the agreement to upgrade the cyclotron to an RDS Eclipse when the option was available. The RDS eclipse upgrade increases the beam current on single or simultaneously bombarded targets from 40 μ A to 60 μ A.

The benefits of upgrading to the eclipse were immediate for liquid targets F-18 Fluoride and N-13 ammonia but this was not the case for the gas targets C-11 CO₂, O-15 O₂, F-18 F₂. As a result we staged our upgrade. Initially we upgraded beam line 2 to the Eclipse and left the original RDS111 target system on beam line one until we were confident the Eclipse gas targets would work as well as expected.

The 60 μ A-40 μ A configuration for the RDS cyclotron is a good choice for flexibility and was preferred before Siemens addressed our concerns with the first generation C-11 CO₂ target Eclipse target and our demand for F-18 fluoride increased. The most recent improvements made to the C-11 CO₂ Eclipse targets have proven to be reliable, provide stable specific activity and increased yield over the RDS111 target system by 30%. The only drawback to the new targets is it needs to run at a lower transmission to prevent failure due to heat stress. At the lower transmission bombardments our original Rf system prevented us from reliably running dual C-11 target at 60 μ A. We have recently installed the new Rf system for the RDS Eclipse which has enable dual bombardments at the lower transmissions. As a result we can deliver 3300mCi of C-11 CO₂ with a dual 60uA 30minute bombardment. The specific activity as measured by the quality of our final products meets our needs and is equivalent to single target syntheses.

The Eclipse ¹⁵O₂ target is working satisfactorily, but has not improved the yield per volume of N-15 gas a primary cost concern when using this target. Thus our cost to make O-15 water is equivalent to the RDS111 target system

The Eclipse ¹⁸F₂ target works but the longevity of the targets foils is proving to be less than that of the original RDS11 targets. Improving the longevity of the foils with this gas targets is an ongoing project at Washington University.

High yield [¹¹C]- CO₂ on a commercial cyclotron enhances possibilities for clinical tracer usage.

Norling J¹, Dahlström K¹, Eriksson T¹, Nilsson R¹, Kilbourn M², Moskwa J², Smith RD³

¹GE Healthcare, Uppsala, Sweden; ²University of Michigan, Ann Arbor, USA;

³GE Healthcare, Pewaukee, USA.

High and stable production capacity of ¹¹C is the key to expansion of new clinical tracers and widespread use of ¹¹C. For this reason, GE continues its effort to optimize the performance of the PETtrace [¹¹C]- CO₂ target. The new target has the same physical dimensions as the standard target to be cyclotron compatible but a few vital changes have been done. The design is based on a different aluminum alloy with improved surface smoothness in the target chamber. By using a thicker foil and efficient helium and water-cooling it is possible to increase the filling pressure and apply higher beam current. Repeated tests show stable and high [¹¹C]- CO₂ target yield.

Method and results: In the study, nitrogen containing 1% oxygen was used as target gas, with a filling pressure of 13 bar. The target was irradiated for 30 min at 80 μA. The yield was measured by trapping [¹¹C]- CO₂ in Ascarite®.

The target shows great stability for [¹¹C]- CO₂ productions (n=26) with yields of 5.9–6.1 Ci (218–226 GBq) corrected to the time of EOB.

Increased irradiation time to 40 min at 80 μA on a single run gave 7.4 Ci (274 GBq).

Work in progress: The target is currently evaluated in daily tracer production using different methyl iodide systems (GE TRACERlab) at customer sites.

Normal and stable MeI conversion (> 37%) is shown even at this high input activity. [¹¹C]- MeI yield > 2 Ci EOS and [¹¹C]- MeI specific activity > 20 Ci/μmol have been achieved.

High and stable production of [¹¹C]- Choline and [¹¹C]- Carfentanil is also reported and will be presented in more detail.

With this new target the yield and specific activity of ¹¹C tracers has the potential to be significantly increased, as indicated by the results so far.

A flexible [^{11}C]methane target

Jacek Kozirowski¹, Peter Larsen², Holger Jensen³ and Nic Gillings³

1 Herlev Hospital, University of Copenhagen, Herlev, Denmark, 2 Scansys Laboratorieteknik, Vaerlose, Denmark, 3 Copenhagen University Hospital, Rigshospitalet, Denmark

SUMMARY/AIMS

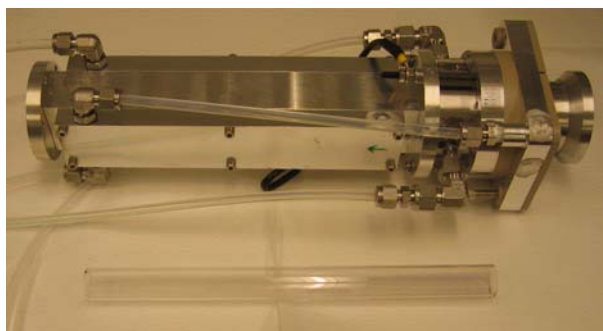
In order to improve the specific activity and lower the gas volume a new quartz lined [^{11}C]methane target has been designed and constructed. The specific activity has, so far, been improved by a factor of four and the gas volume has been reduced by a factor of four. Production rate is up to 90% of the theoretical maximum and a specific activity of 1300GBq/ μmol @ EOB has been achieved.

BACKGROUND

The original methane target is a large volume (750mL, 10bar fill pressure) conical aluminum body. The specific activity is on average $\sim 100\text{GBq}/\mu\text{mol}$ @ EOS and peaks at $200\text{GBq}/\mu\text{mol}$. The large volume (10L at NTP) makes trapping a slow process (~ 9 min). The increased demands on higher specific activity for ^{11}C -labeled neuroreceptor ligands and shorter turn over time between syntheses demanded a new improved design. Aluminum has also proven not to be the best choice for in-target methane production¹, so a change of material was also attractive.

METHODS

We wished to have a high pressure target with minimized beam-wall interactions made of an inert material. Initially we considered making a quartz bodied target (as quartz is the material of choice for many gas phase reactions, thanks to its inertness) without any other cooling but for the foils. The target would radiate the heat and the temperature would equilibrate depending on the beam current. However, in practice it seemed somewhat difficult and risky to have metal to quartz connections at high pressure ($> 40\text{bar}$) and elevated temperatures. Therefore we chose to use a quartz lined aluminum target fitted with either water (picture 1) or air cooling (picture 2), a similar design has previously been used for in-target production of H^{11}CN ².



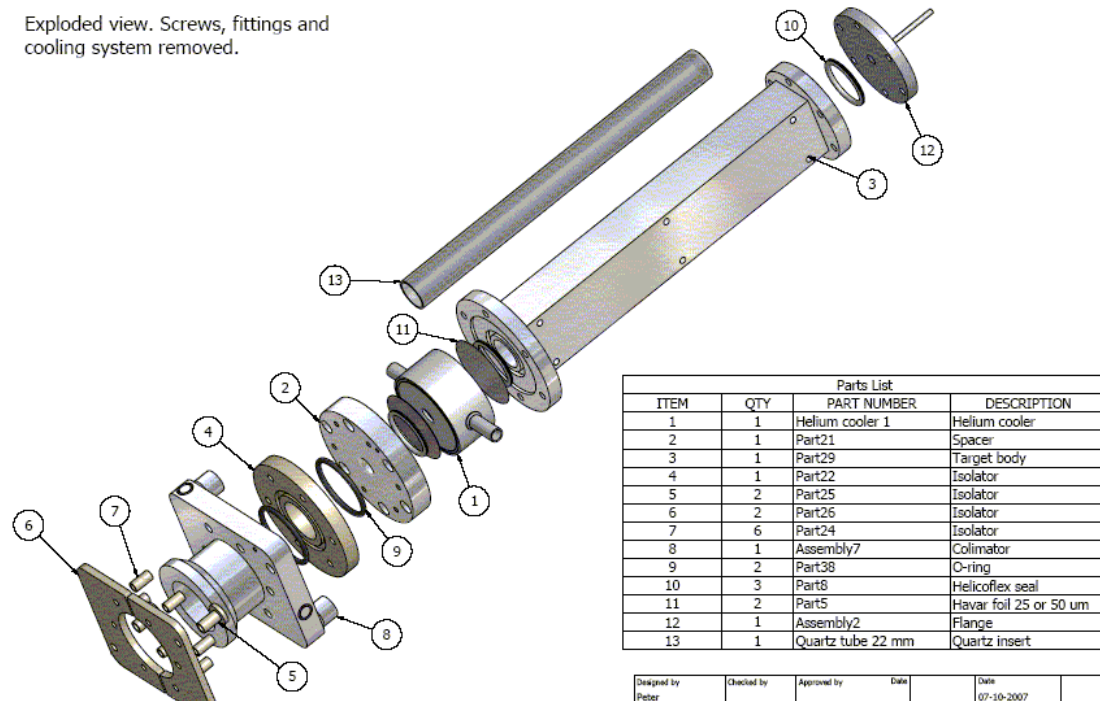
Picture 1. Target with water cooling and quartz tube (in front)



Picture 2. Target with air cooling.

The very flexible modular design allows the user to change the insert/lining just by simply removing the rear flange – this is easily done, even with the target still attached to a target exchanger. Cooling is interchangeable between water and air (passive convection).

The target consists of (picture 3) of an insulator, for the target ladder (6), collimator ($\varnothing=10\text{mm}$) (5), insulator for the collimator (4), helium cooling and foils ($25\mu\text{m}$ Havar for the vacuum and $50\mu\text{m}$ Havar for the target) sealed by Helicoflex rings (1,11), aluminum target body (3), SS rear flange (12) and a quartz tube ($L=260\text{mm}$, $\text{id}=19\text{mm}$)(13). The total volume is 75mL .



Picture 3. Target – exploded view

All irradiations were performed on a Scanditronix MC32 cyclotron run with negative ions at 17.2 MeV , giving an entrance energy of 16MeV . The target was water cooled. The target foil bursts at 60bar without irradiation, so the maximum pressure during irradiation was set to 45 bar . The target was irradiated with various fill pressures to find the maximum beam current at each (Fig 1)

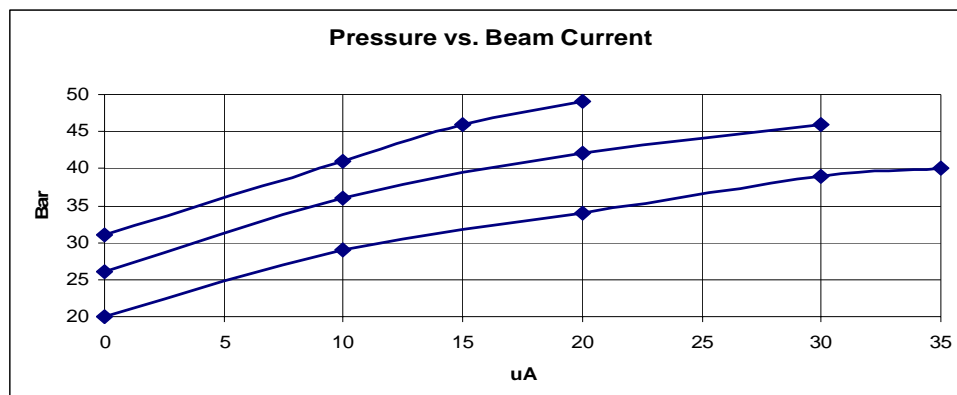


Figure 1. Pressure (bar) vs. Beam Current (μA)

Initially the target was run at $10\mu\text{A}$, for 10min at 30bar fill pressure to give a “baseline” performance. At 20 bar fill pressure the S value was $\sim 25\%$ lower at higher beam current and longer irradiation time. At 25 bar the target performed better, (table 1) but longer irradiation times decreased the yield.(as previously reported for aluminum and niobium body targets³).

Fill Pressure	Beam Current	Time	Pressure	Yield EOB	S
Bar	μA	min	Bar	GBq	GBq/ μA
30	10	10	N/A	18	6.25
30	10	10	N/A	18.5	6.42
20	10	10	N/A	16.6	5.76
20	30	10	N/A	43.5	5.03
20	30	30	N/A	90	4.69
26	30	10	45	52.5	6.08
25	25	30	42	84	5.26
25	20	10	40	34	5.90
25	20	40	40	78	5.25

Table 1. Target performance under different filling pressure and irradiation conditions.

The radioactivity yielded from the target was analyzed by radio-GC and found to only contain [¹¹C]-methane and [¹³N]-nitrogen. For the performance tests, [¹¹C]-methane was trapped in a Carbosphere cryotrap and pure [¹³N]-nitrogen was collected in a sequential gas sampling bag.

For specific activity measurements PIB and SB207145 were synthesized using a modular radiochemistry system⁴. Shortly after reassembly of the target specific activity was ~260 GBq/μmol and this has so far increased to ~1300GBq/μmol @ EOB (~370GBq/μmol @ EOS) after 6 full irradiations. The specific activity seems to be gradually increasing and we expect this trend to continue⁵.

CONCLUSION

Fitting a “normal” straight bore aluminum target with a quartz tube gives a promising methane target. The yields of [¹¹C]methane are quite acceptable and specific activities have been increased significantly compared with the old large volume target.

FUTURE

We intend to test the production of ¹¹CO₂ in the target, to try it without the quartz liner and use different energies (11 – 16,2MeV), as energy may play an important role⁶. We did not bake out the target as others have done^{2,5} so this may be considered if the specific activities do not continue to improve.

1 Radiochim. Acta, vol 88, 2000, pp 201-205, K.R. Buckley et al

2 IJARI, vol.22, 1971, pp 475-479, J.F. Lamb et al

3 NMB, vol 31, 2004, pp. 825-827, K.R Buckley et al.

4 JLCR, vol.48, 2005, pp S338, N. Gillings et al

5 10 WTTC, 2004, H.Bjork et al

6 J. Radioanal. Nucl. Chem. Letters, vol.117, 1987, M. Hanisch et al

Upgrading RDS-111 Turret Style Gas Targets: Experience with a New $^{18}\text{O}_2$ - $^{18}\text{F}_2$ Target

James P. O'Neil and Christopher A. Ramsey

Biomedical Isotope Facility
Lawrence Berkeley National Laboratory
1 Cyclotron Road, Berkeley CA 94720

In our hands, the original CTI designed gas targets for the 8-position turret are lacking in several aspects. We had previously made modifications to partially address these issues but to only limited success. Thus a new RDS-111 turret style gas target has been designed, constructed, tested and is in use for the production of [F-18]fluorine gas on the LBNL Biomedical Isotope Facility RDS-111 cyclotron. (1)

We have found that the bayonet style mounting of the nosepiece, which both seals the target entrance foil with a compression O-ring and contains the helium cooling jets, would easily un-clock and leave the irradiated foil inside the turret during target removal. Our alternative design was to attach the nosepiece with 3 screws (2-56 x 1/4"). However the fine threads in the aluminum target body had minimal clamping power and would easily strip. Originally, a clamp and O-ring were used to seal the fill/unload 1/16" tubing at the rear of the target body. While fine for more flexible PEEK tubing used for our other gas targets, this configuration would often leak with the more rigid stainless steel tubing needed for the [F-18]fluorine gas system plumbing. We replaced this system with a 10-32 thread-swage adaptor fitting that was sealed with an O-ring face seal. However the o-ring would become brittle with the F_2 gas and the fitting would leak.

It was desired to have a material such as stainless steel that would allow for more durable threads in which to clamp the nosepiece and a surface at the rear of the target to weld the swage fitting. However, the aluminum target body is desired to maintain the ability to use the Nickles' "two-shoot" production method. (2) We have therefore taken advantage of the properties of bimetallic ingots supplied by Atlas Technologies. (3) This material, which will be described in detail, is an explosion-bonded sandwich of 316 stainless steel and 6061 aluminum (FIGURE 1). A description of the explosion bonding process along with specifications of the available materials will be presented.



FIGURE 1. Bimetallic Ingots from Atlas Technologies

For the construction of the target, one bimetallic part was welded to an aluminum rod providing a stainless steel end on the aluminum target body. The assembly was machined and then welded to the 2nd ingot forming the rear of the target. An assembled target is shown in FIGURE 2.



FIGURE 2. Assembled [F-18]fluorine gas target.

As of June 2008, this target has been in full production service supplying [F-18]fluorine gas for the radiochemical synthesis of [F-18]-6-fluoro-meta-tyrosine for over 18 months. A full evaluation of the performance of this unique target will be provided.

In conclusion, a more robust target for the production of [F-18]fluorine gas in the RDS-111 turret system has been constructed. The incorporation of stainless steel on the ends of the aluminum target body has provided surfaces more amenable to durable leak free seals while maintaining aluminum as the bulk of the target body material. This target provides radioisotope in quantity and quality identical to its all aluminum counterpart while demonstrating increased reliability.

References:

- 1) J.P. O'Neil, H.F. VanBrocklin, Preparation of fluorine-18 gas from an 11 MeV cyclotron: a target system for the CTI RDS 111 cyclotron. Nuclear Instruments and Methods in Physics Research A 438 (1999) 166.
- 2) R.J. Nickles, M.E. Daube, T.J. Ruth, An $^{18}\text{O}_2$ Target for the Production of $[^{18}\text{F}]\text{F}_2$. The Journal Applied Radiation & Isotopes 35 (1984) 117.
- 3) The authors wish to thank Dick Bothell of Atlas Technologies for his generous donation of the bimetallic ingots as well as stimulating discussions and direction as per the properties of this material. This work was supported in part by the US DOE under Contract DE-AC03-76SF00098.

Improvement of the C¹¹ target at the Department of Nuclear Medicine at the University at Buffalo, the State University of New York.

Erol Bars, Dr Sajjad M., Dr Mike Haka, Steve Toonrongian.

INTRODUCTION

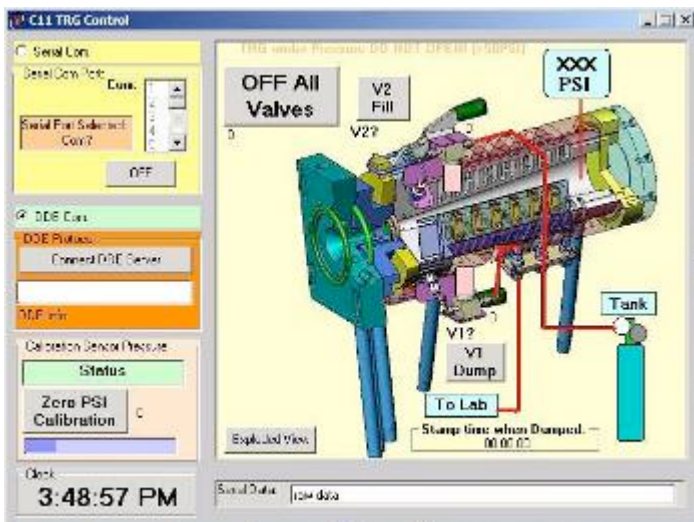
The new target design, NEMO, shows an increased C¹¹ yield when compared to Haka et. al target design. The new design offers a multi-geometrical internal volume that can be changed by replacing the back cooling flange with a new flange of various depth and volume.

The ¹⁴N(p,α)¹¹C reaction was used to synthesize Choline, HED, Raclopride, Acetate, PK, C¹¹ compounds. The multi geometrical internal volume was conceived for further yield study.

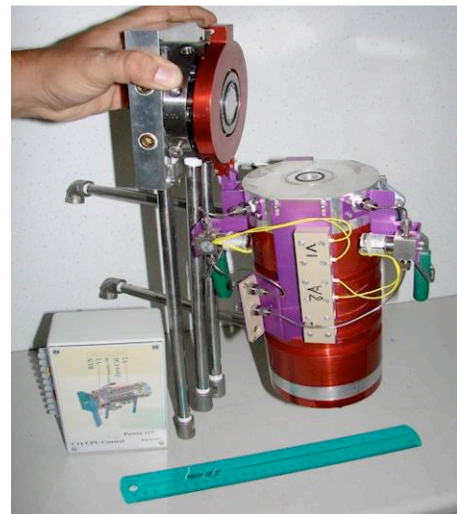
METHOD

This C¹¹ gas target, which can also be used to produce O¹⁵ from N¹⁵, is made out of aluminum 6061 grade with an internal volume of 8.5" with a long tapered bore (0.472 to 2") design. The total volume of gas used is 188 cm³. The initial loading pressure of the target is 320psi. The target isolation foil is 0.020" Al 2024 thick and 25um Al for vacuum side. The foils are cooled via Helium flow, and the target cooling and its collimator are water cooled from 6-8L/min. A quick release clamp foil holder was designed for easy access to the isolation foils, thus decreasing body exposure. The C¹¹ target was irradiated for 60 minutes at 35-40 μA. A new and advanced target controller and software program was developed to allow multiple targets and remote control operation from numerous stations through network communication. The C¹¹ was trapped in LAH solution.

C¹¹ NEMO Software



C¹¹ NEMO Target



RESULTS

Target C¹¹ NEMO Production

(Average based on > 100 runs)

Energy	Current	Time	Initial Pressure	Run Pressure	Batch in LAH
22MeV	35uA	60min	310Psi	590Psi	4.8Ci
	40uA	60min	310Psi	625Psi	>5.2Ci

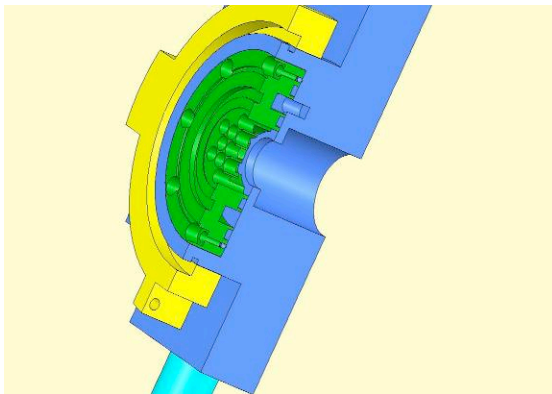
CONCLUSION:

The new target design and control system proved to be reliable. Years of effort were made to achieve optimal results.

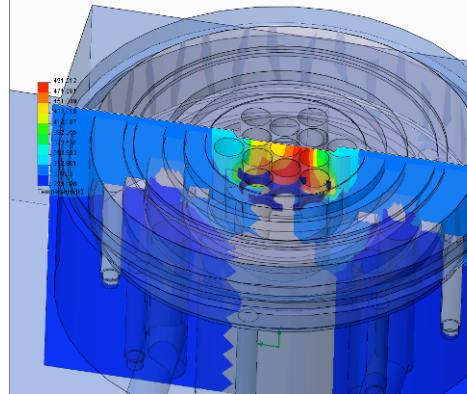
Future experiment:

A second target is under construction allowing us to maximize ¹¹C methane production with various target volume chamber inserts. We also implemented a grid isolation foil into the design to eliminate the helium cooling, allowing us to increase the beam current.

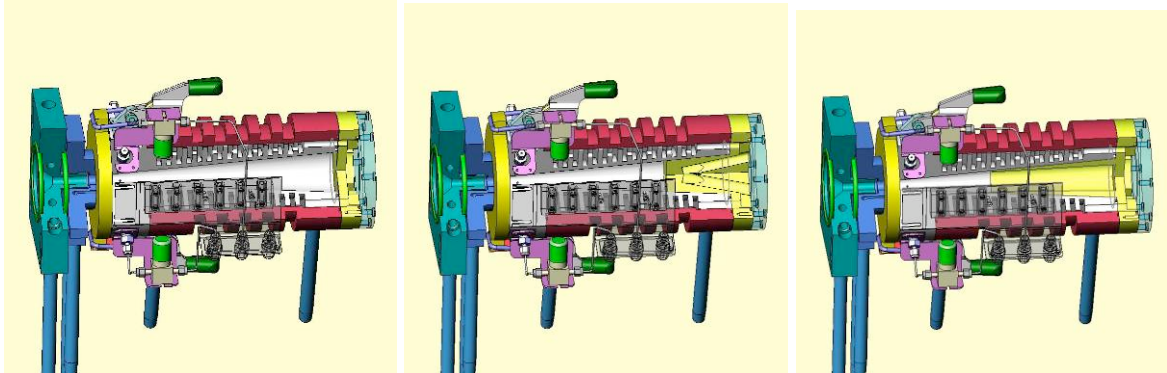
Grid Foil Holder



CosmosFlowWorks Analysis 500W



C¹¹ NEMO target various internal volume chamber configurations



Multi-kilowatt Recirculating Targets for the Production of ^{18}F

J. Michael Doster and Robert P. Newman
Department of Nuclear Engineering
North Carolina State University

North Carolina State University in conjunction with Bruce Technologies Inc. is developing recirculating water targets for the cyclotron production of high yields of ^{18}F fluoride for PET radiopharmaceuticals. Fluorine-18 is commonly produced through proton irradiation of ^{18}O enriched water by the $^{18}\text{O}(p,n)^{18}\text{F}$ reaction. Heat deposited in the target fluid by the proton beam is proportional to the ^{18}F produced, thus production is often limited by the targets ability to reject heat. For power levels above 3 kW, boiling batch targets with local cooling can become impractical due to excessive ^{18}O water volumes. A recirculating target pumps the heated fluid to an external heat exchanger where the heat is transferred to a low temperature heat sink. A typical design constraint for recirculating targets is that the target water remains below the boiling point at all times. Figure 1 shows the general layout of the recirculating target system.

A high-flow/low-volume pump and a high-capacity/low-volume heat exchanger are essential to the overall performance of the recirculating target. In this work, two different types of heat exchangers are considered. Laboratory testing was conducted on a small shell and tube heat exchanger (Figure 2) that removed nearly 6 kW of heat at flows provided by a miniature regenerative turbine pump. Laboratory testing was also conducted on a small cross flow heat exchanger (Figures 3) with measured performance of 7.4 kW and predicted peak performance approaching 10 kW.

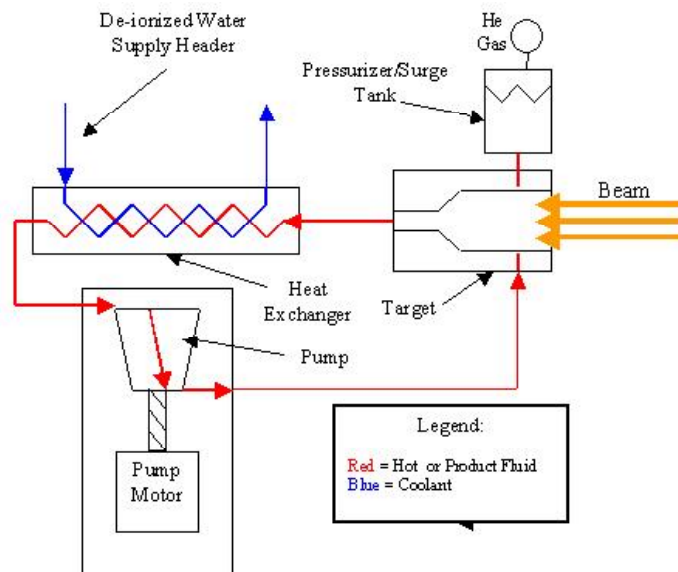


Figure 1: General layout of recirculating target system



Figure 2: Exergy LLC model 00268-2 shell and tube heat exchanger

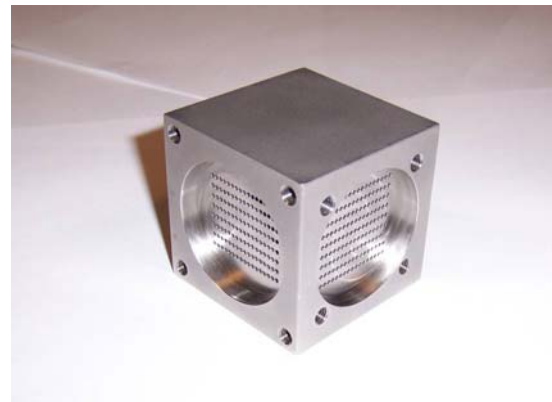
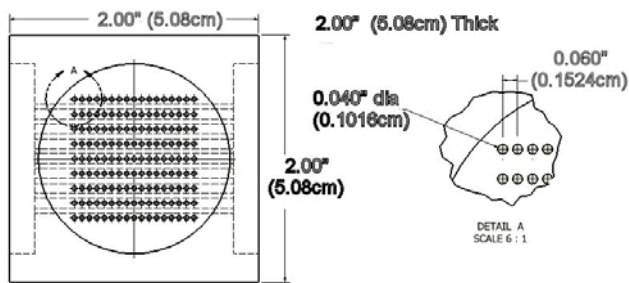


Figure 3: Prototype cross flow heat exchanger

The simulated performance of an integrated system consisting of target, pump and two tube and shell heat exchangers in series (Figure 4) indicate heat transfer rates on the order of 10 kW are feasible with existing components (Figure 5). The heat exchangers tested showed a strong dependence on the primary (product) side flow rate and their performance could be sharply increased for both designs if pump performance is increased.. This is expected as the majority of the heat transfer resistance is on the primary side. Therefore, it is essential that the pump used to drive primary side flow has sufficient capacity to operate the heat exchangers optimally. The prototype regenerative turbine pump used in this work is predicted to provide only 2 to 3 LPM in the integrated system at reasonable pump speeds. Suggested flow rates between 4 and 8 LPM are necessary to maximize performance in the heat exchangers. Future work will focus on the development of robust, low volume pumps with capacities in this range.

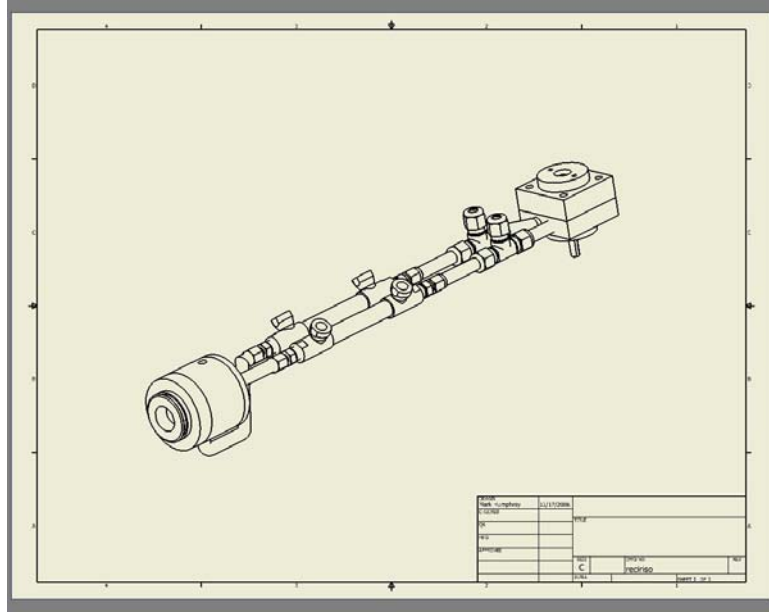


Figure 4: Integrated Recirculating Target System

TOTAL VOLUME (mL) =	22.35
Primary side flow rate (LPM) =	2.16
Heat transfer rate (kW) =	9.75

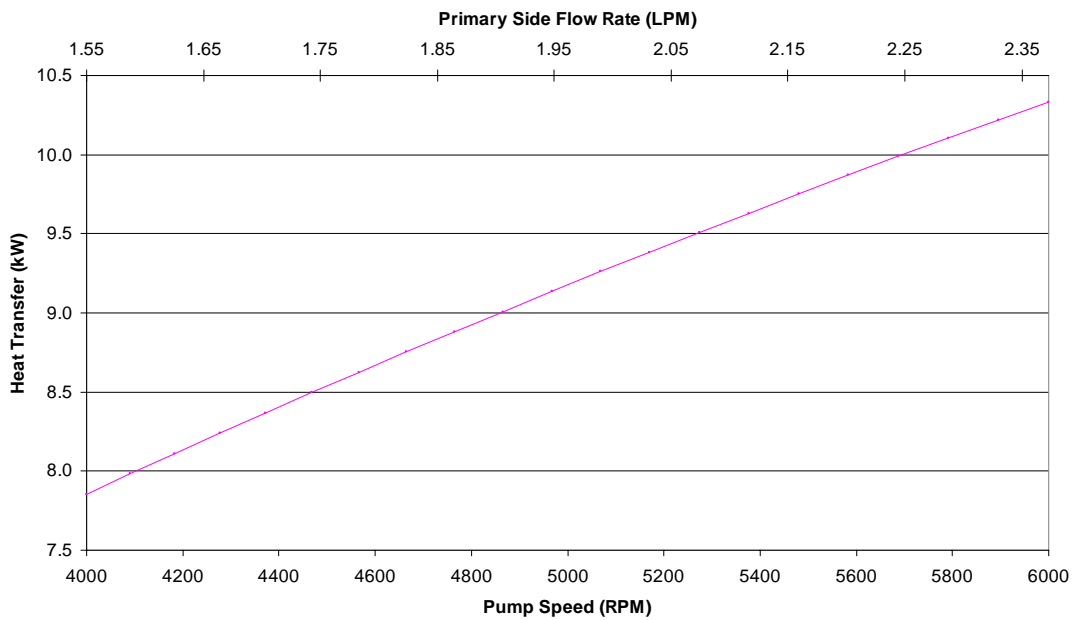


Figure 5: Simulation data for an integrated system with two Exergy model 00268-1 shell and tube heat exchangers in series

Experiences from using a PETtrace cyclotron at 130 μA (2 x 65 μA) with niobium targets producing $^{18}\text{F}^-$ / FDG

Eriksson T¹, Norling J¹, Eberl S², Husnu M³, Chicoine R³

¹ GE Healthcare, Uppsala, Sweden, ² Royal Prince Alfred Hospital, Sydney, Australia

³ Cardinal Health, Ft. Lauderdale, Florida USA

The demand for high capacity $^{18}\text{F}^-$ /FDG drives the development towards higher beam current from the cyclotron and high capacity targets. During the development tests of the niobium targets (performed at Cardinal Health, Ft. Lauderdale), they proved to have a capacity well beyond 50 μA .

This opened up for an increase of the total target current beyond the now specified 100 μA for a GE PETtrace cyclotron (corresponding to 2 x 50 μA dual beam operation). In the study referred to in this abstract, the cyclotron has been operating at a total current of 130 μA distributed on two niobium targets operating at 65 μA each. During the high current evaluation period started in April 2008 (in Sydney, Australia), no unusual behavior from the cyclotron have been reported.

At the time of abstract submittal, the cyclotron has been operating for a total of >12000 μAh on target at 2 x 65 μA (130 μA). The ion source and cyclotron are still performing very well and no changes in behavior compared to use at 100 μA have been seen except a proportionally higher ion source current. The cyclotron used for the tests was updated to “100 μA standard” and some small adjustments of the RF system were made before the high current tests were commenced.

The niobium targets show a stable performance with no indication of degradation on high currents. The $^{18}\text{F}^-$ yield shows an average saturation yield of 227 mCi/ μA on the runs made directly to a dose calibrator (n=6). This is well in accordance with the average 220 mCi/ μA (n=240) seen during the development tests of the niobium targets (direct yield measured on all these runs). During the 130 μA tests the main part of the productions has been directly transferred to the chemistry unit without an intermediate measurement of the $^{18}\text{F}^-$ activity from the target. Performing an activity balance after FDG on these productions normally account for 96% of the estimated activity based on S=227 mCi/ μA .

The saturation yield has been calculated for the complete system including targets and chemistry unit (TRACERlab MXFDG). This makes it possible to compare all FDG productions regardless of cyclotron production time and target current.

We have named this “*average system saturation yield_{FDG}*”.

The *average system saturation yield*_{FDG} representing all productions made between 100 μA and 130 μA on the niobium targets, shows 118 $\text{mCi}_{\text{FDG}}/\mu\text{A}$ (Std=9.1, n=115, $\text{FDG}_{\text{avg}}=7.8\text{Ci}$). This indicates a stable high production capacity from the target. This saturation yield takes into account target performance, time between end of bombardment and start of chemistry synthesis, chemistry unit performance and synthesis time and is not decay corrected.

The yields from higher current runs ($\geq 110 \mu\text{A}$) shows an *average system saturation yield*_{FDG} of 120 $\text{mCi}_{\text{FDG}}/\mu\text{A}$ (Std=10.2, n=55, $\text{FDG}_{\text{avg}}=8.2 \text{ Ci}$).

The yields on the highest current (130 μA) shows an *average system saturation yield*_{FDG} of 121 $\text{mCi}_{\text{FDG}}/\mu\text{A}$ (Std=7.8, n=23, $\text{FDG}_{\text{avg}}=9.1 \text{ Ci}$).

The n=x in these cases, represents number of dual productions runs.

The data on the high target currents indicates that both the target and the chemistry unit continue to perform consistently even at this high level.

Example of a high yield production:

Target current=130 μA

Irradiation time=150 min

Produced $\text{FDG}_{\text{EOS}}= 10.6 \text{ Ci}$

System saturation yield_{FDG} =133 $\text{mCi}_{\text{FDG}}/\mu\text{A}$

The results from the combination of niobium targets and the cyclotron operating at 130 μA are so far very positive. The cyclotron continues to show high reliability on the 130 μA level and FDG is produced on a high and stable level.

In order to ensure consistent reliability, this concept will be further evaluated. We do not exclude the possibility that additional upgrades might be needed for various sub systems.

High Current F-18 Water Target with Liquid Spray-Cooled Window

Alexander Zyuzin, Erik van Lier, Richard Johnson, Jay Burbee
Advanced Cyclotron Systems Inc., Richmond, BC, Canada
John Wilson
Cross Cancer Institute, Edmonton, AB, Canada

A new generation of F-18 water targets was introduced by ACSI in 2003¹ and since then installed at number of facilities.² The most commonly used 2.5 mL, 30 deg. target routinely operates at 70-80 μA , producing 5.5-6.0 Ci/hr. At maximum current ($\sim 100 \mu\text{A}$) it produces ~ 7 Ci/hr. Substantial “burn thru” is observed at currents above 90 μA . At this current the F-18 quality deteriorates causing the reduction of FDG yields. The exact reason for this is still under debate, but is presumed to be due to contaminants coming from the Havar foil. In order to maintain F-18 reactivity, a number of different approaches were considered. One of the proposed solutions that considerably improved the properties of the target window and reduced the amount of contaminants was to use a Niobium coating on the water side of the Havar foils.³ Recently ACSI has developed a new target that had larger (3.5 mL) volume and 20 deg. inclination angle. We investigated the feasibility of using a liquid spray to facilitate cooling of the target windows. A new target was tested up to 150 μA with spray-cooling and up to 130 μA without spray-cooling. Over 9 Ci of reactive F-18 was produced in one hour while operating at 135-140 μA .

Relative Cooling Efficiency Measurements

We propose to use the liquid spray (water in our initial experiment) in combination with high helium flow to improve target window cooling. This could increase target beam capacity and possibly reduce the contaminations introduced in water from the Havar foil. To test the heat removal efficiencies of different cooling methods a copper heater block with 200 W cartridge heaters and thermocouples was built. The assembly of the copper heater block to the target helium window is illustrated in Fig.1. By placing thermocouples as close as possible to the surface of the heater block, ~ 0.5 mm, we tried to simulate the temperature increase in the target window. While the absolute temperatures of the target window may be different from measured values, the relative temperature differences observed using different cooling techniques will be proportional to real temperatures of the target window.

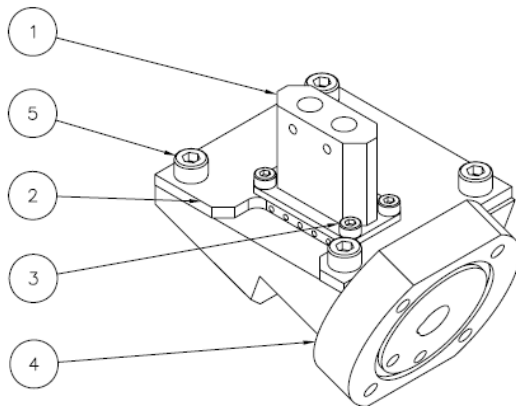


Fig.1 He window and heater block assembly

1. Heating Block
2. Insulation Plate
3. Screws
4. Helium window
5. Screws

We measured temperature increase in the heater block using a typical 85 standard liters per minute (SLPM) helium flow rate, a new helium cooling system which provides 200 SLPM helium flow and a combination of 200 SLPM helium flow with ~5 ml/min water spray. As a reference point we measured temperature increase without any cooling. The resulting temperature increase vs. time for different cooling methods is illustrated in figure 2 below. The heater block temperatures approach equilibrium after approximately four minutes of heating/cooling. Significant cooling improvements were observed when the helium flow was increased and when the water cooling spray was introduced.

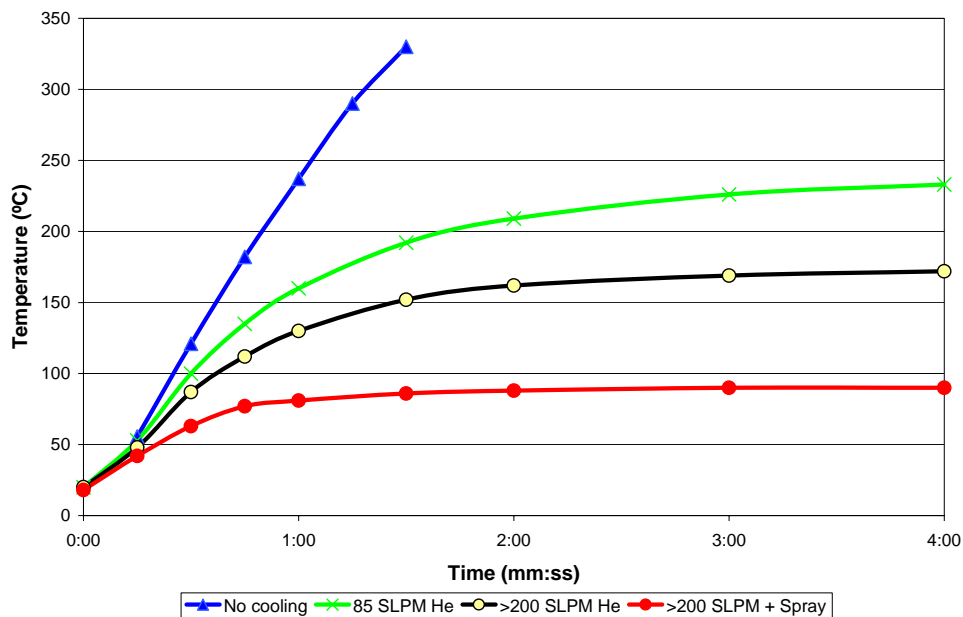


Fig. 2 Temperature vs. time for different types of window cooling

Target Testing

The target was tested up to 150 μ A. The “burn thru” was observed at ~125-130 μ A and ~140-145 μ A, respectively for Helium cooling only and Helium cooling with water spray. Enhanced cooling and larger target volume substantially reduced the operating pressure and allowed safe operation at the 150 μ A level. The relationship between pressure and current is illustrated in Fig.3 for existing targets and for the new ACSI target with 200 SLPM helium cooling with and without water spray.

A number of production runs were done using different cooling methods. Average production yields are summarized below:

Average Current	EOB Yield, mCi (60 min)
100 μ A	7000-7100
105-110 μ A	7300-7500
130-135 μ A	8700-8800
135-140 μ A	8800-9000

The saturated yield numbers are similar to those previously reported using the 2.5 mL target and varied from 220 to 230 mCi/ μ A. As the current approached the “burn thru” region, the saturated yield decreased to \sim 200 mCi/ μ A. The F-18 produced was fully retained on the QMA, even when the target was operated at 140 μ A. FDG yields were consistently better than those obtained using the 2.5 mL target at 70 μ A.

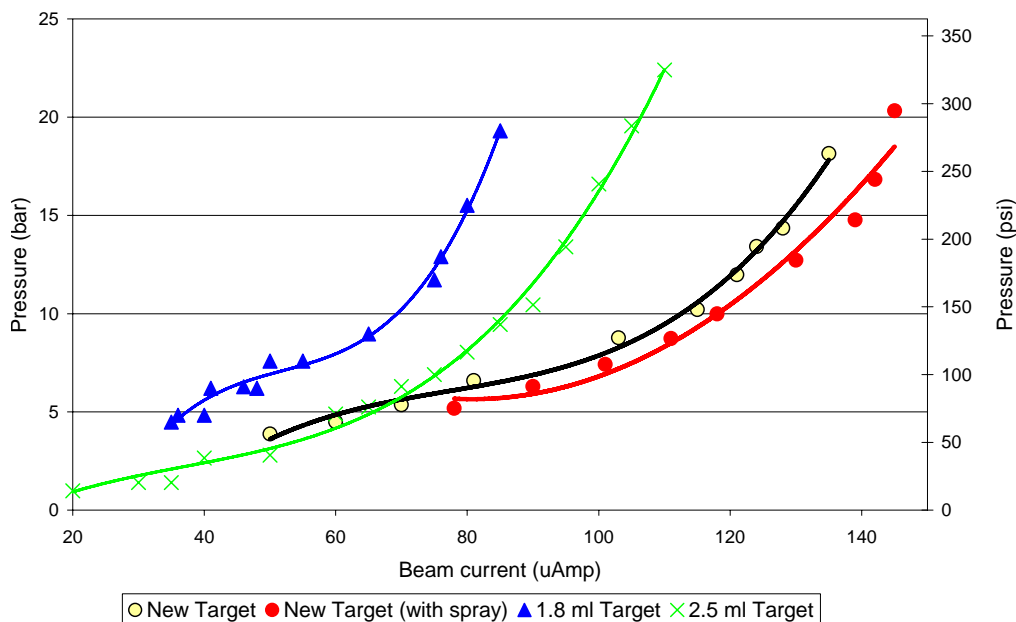


Fig. 3 Target pressure vs. beam current

A series of runs was performed to test N-13 ammonia production. The target was loaded with 4 mL of 5 mmol ethanol solution. At the end of the irradiation, the water was transferred from the target through a QMA cartridge and then through a cation exchange cartridge, where N-13 ammonia was retained. Over 2 Ci of ammonia was produced in 20 min at 100 μ A.

Future Work

- Improve the helium window cooling nozzle design to provide more efficient cooling to the curved section of the bulging foil.
- Implement an automated system that traps all active compounds during water spray cooling.
- Apply liquid spray cooling to gas targets, including a high-current Xe-124 target.

References

1. A. Zyuzin *et al.* “O-18 Water Target for High Current TR-PET Cyclotrons”, WTTC 10, Madison, WI, 2004
2. Roberto Strangis *et al.* “Reliable Fluorine-18 Production at High Beam Current”, *Cyclotrons and Their Applications 2007, 18th International Conference*, Giardini Naxos, Italy
3. John Wilson, *et al.* High Beam Current 18F-Fluoride Production and Fluoride Quality”, WTTC 11, Cambridge, UK, 2006

Deployment, Testing and Analysis of Advanced Thermosyphon Target Systems for Production of Aqueous [^{18}F]Fluoride via $^{18}\text{O}(\text{p},\text{n})^{18}\text{F}$

Matthew Stokely^{1,2,3}, Johanna Peeples¹, J. Michael Doster¹, Gerald Bida², Bruce Wieland^{1,2,3}

¹Department of Nuclear Engineering, North Carolina State University, Raleigh, NC

²Department of Nuclear Medicine, Duke University Medical Center, Durham, NC

³Bruce Technologies Inc., Chapel Hill, NC

Single phase and boiling batch water targets are the most common designs for the cyclotron production of ^{18}F via the $^{18}\text{O}(\text{p},\text{n})^{18}\text{F}$ reaction. Thermosyphon targets have design and operating characteristics which enable higher power operation than conventional boiling targets of like size. Experimental thermosyphon target systems demonstrated the feasibility of high intensity irradiation via bottom pressurized operation. An effective experimental characterization platform was developed and utilized in parallel with computational modeling efforts to further improve designs[1,2]. A control strategy was also developed to provide a simple and robust means of remote target operation. Clinical production systems were designed and deployed at two facilities.

The overwhelming majority of liquid targets used for medical isotope production are pressurized from the top of the liquid volume. Because of this fact, there exists an initial amount of non-condensable gas which mixes with the liquid and vapor during bombardment. Even a small component of non-condensable gas produces a dramatic increase in resistance to heat transfer at a condensing surface[3]. This is significant, as the condensing layer can become the limiting resistance when the target is cooled more aggressively.

In contrast, a thermosyphon target is initially filled completely and pressurized from the bottom via an external expansion volume. This maximizes the effective heat transfer area in the condensing region of the target volume by eliminating the presence of non-condensable gas. Many experimental targets of this type have been developed in previous work, of which the most aggressive designs achieved operation at power levels in excess of 3 kW[4].

Recent work has focused on scaling thermosyphon technology to suit specific cyclotron applications. Robust production systems have been developed for a TCC CS-30 at the Duke University PET Facility (DUMC) and a GE PETtrace known as the Wisconsin Medical Cyclotron(WMC). In these systems, the chamber and window materials are tantalum and Havar, respectively. The goal of these deployments was to provide target systems very closely matched in thermal capacity to the current limit of the cyclotrons.

The DUMC cyclotron has an extracted proton energy of 26 MeV and current capability of 45 μA (1170W). In the past, reflux production targets were operated at lower proton energies, which required attenuation of the particle beam. In order to achieve the maximum possible ^{18}F production, the thermosyphon target was designed to operate at full energy. Producing ^{18}F at this higher energy is both feasible and worthwhile once the radionuclidic impurities are characterized. The addition of the thermosyphon system has more than doubled the ^{18}F capacity of the facility. This target has been operated exclusively without a component failure or disassembly for cleaning since its installation in 2007.

The WMC facility typically operates two GE high yield reflux targets simultaneously via dual beam extraction. The thermosyphon target for this application was designed to tolerate beam currents approaching 100 μA (1650W), corresponding to the software limit for automated

cyclotron operation. The target was first installed in concert with a D-PACE short port collimator assembly to characterize the beam profile at the vacuum tank exit port[5]. In addition to operation at high intensity, the target has demonstrated consistent saturation yield performance for extended irradiation times (>4hr).

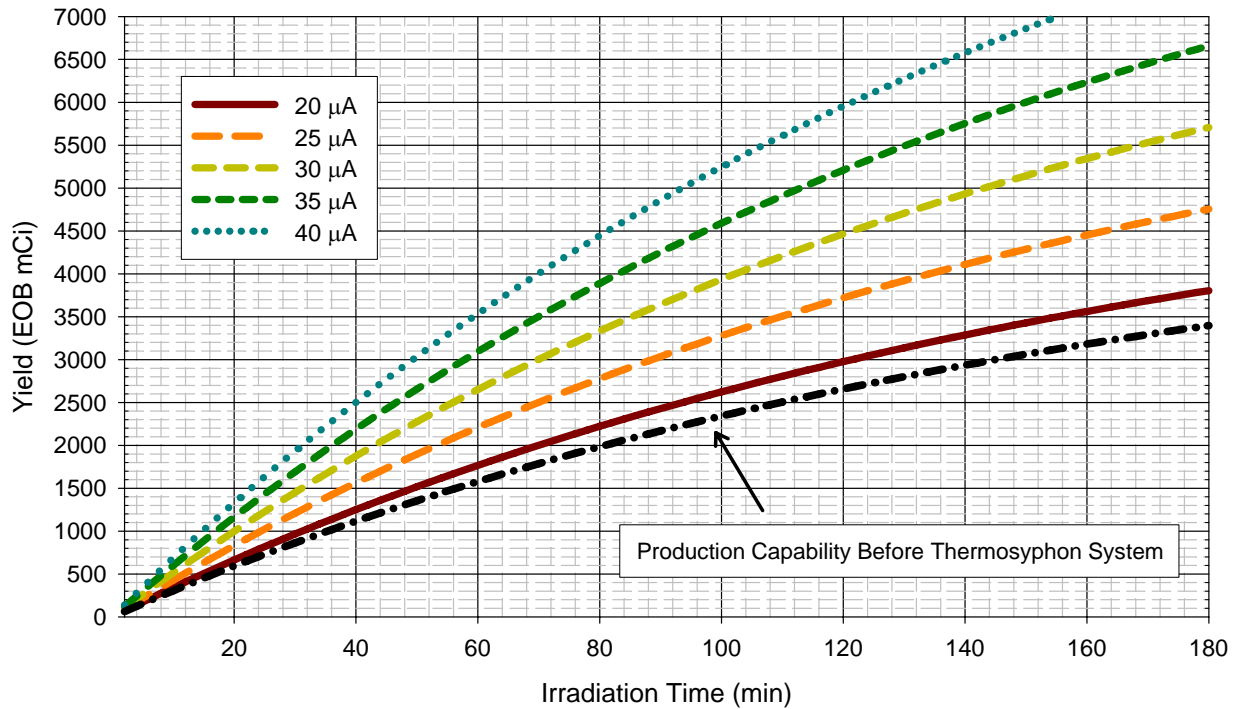


Figure 1: DUMC Thermosyphon Production Curves

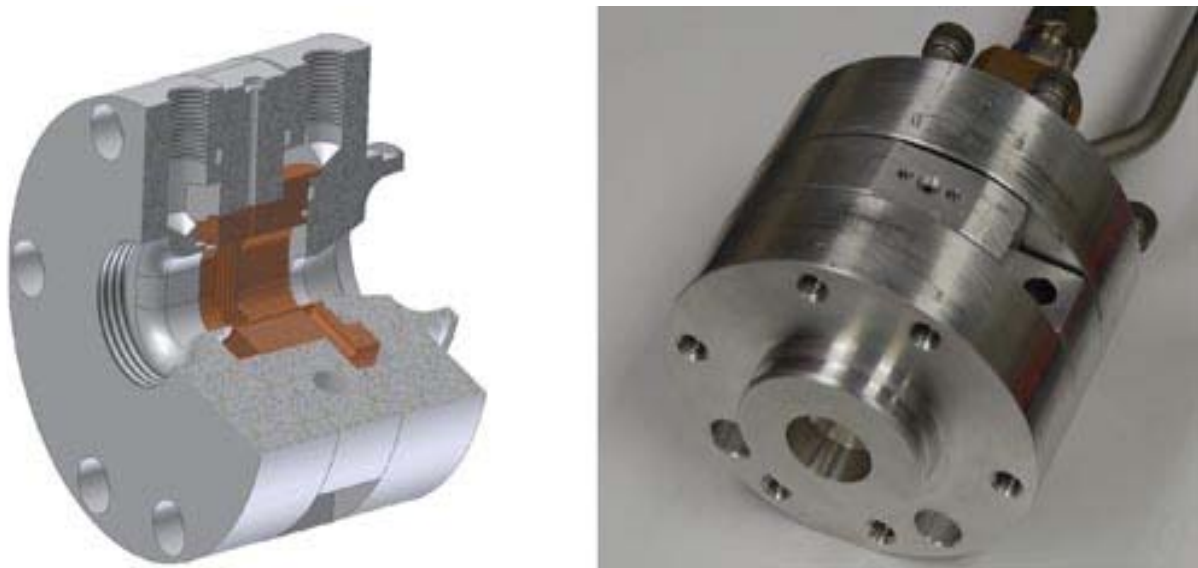


Figure 2: DUMC Thermosyphon Solid Model and Assembled Target

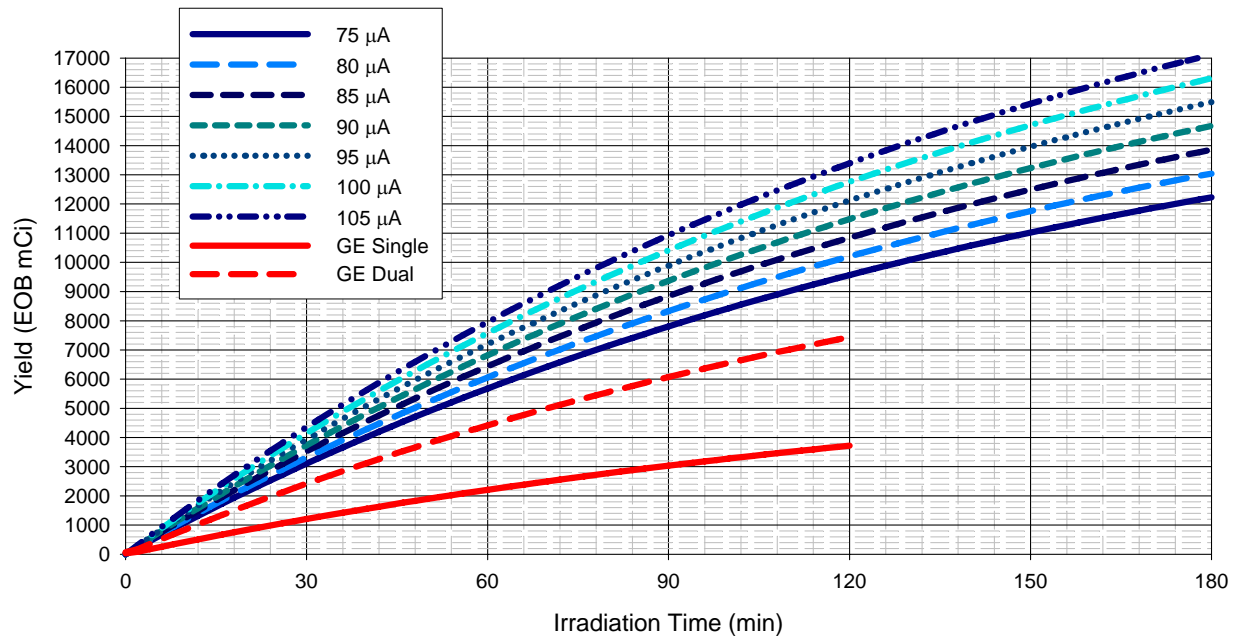


Figure 3: WMC Thermosyphon Production Curves

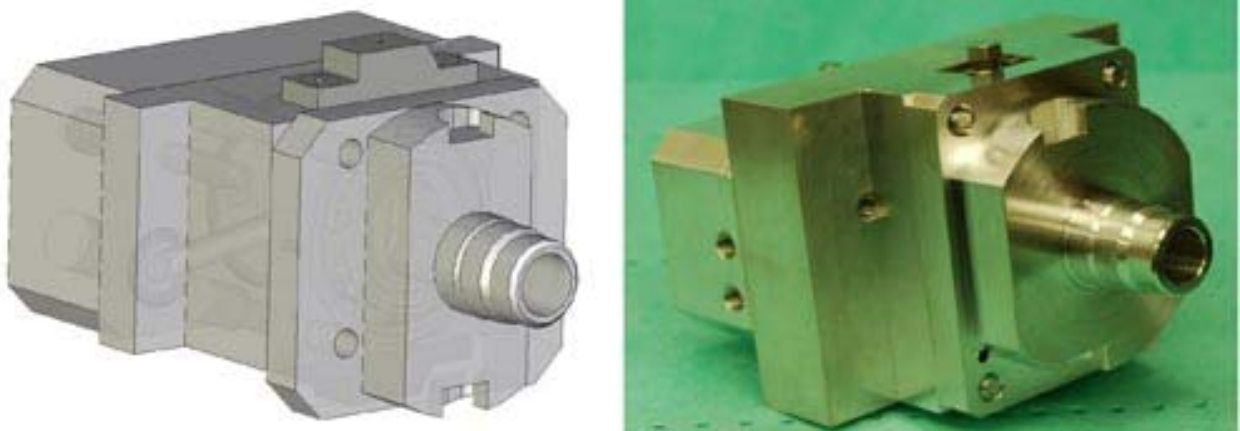


Figure 4: WMC Thermosyphon Solid Model and Assembled Target

REFERENCES

1. Stokely M.H., Deployment, Testing and Analysis of Advanced Thermosyphon Target Systems for Production of Aqueous [¹⁸F]Fluoride via ¹⁸O(p,n)¹⁸F. Doctor of Philosophy Dissertation, North Carolina State University. Raleigh, North Carolina: 2008.
2. Peeples J.L., Design and Testing of Thermosyphon Batch Targets for Production of ¹⁸F. Doctor of Philosophy Dissertation, North Carolina State University. Raleigh, North Carolina: 2008.
3. Collier J.G., Convective Boiling and Condensation. UK: McGraw Hill, 1981.
4. Stokely M.H. *et al*, "High Yield Thermosyphon Targets for Production of ¹⁸F-Fluoride," *Proceedings of the Eleventh Workshop on Targetry and Target Chemistry*. Cambridge, UK: 2006.
5. Theroux J.E. *et al*, "A 'Short Port' Beamline for Mounting Custom Targets to a PETtrace™ Cyclotron." *18th International Conference on Cyclotrons and their Applications*. Giardini Naxos, Italy: 2007.

The authors gratefully acknowledge the support of NIH SBIR Grant 5R44EB003275-03, and the collaboration of Dr. James Lamb and Gerald Rasmussen at the Wisconsin Medical Cyclotron.

Pressurized Water Target for high beam currents and multi Ci $^{18}\text{F}^-$ production

A.Cambriani, Y.Jongen, M.Degeyter, B.Lambert
Ion Beam Application SA

Introduction

The increased current output of commercially available cyclotrons requires a new approach in the design of $^{18}\text{F}^-$ static water targets. Current available targets are capable of handling limited heat loads (up to 1,5 KW). The water vaporisation along the beam strike, also called tunnelling, is the major cause of the decreased $^{18}\text{F}^-$ production yield at high power.

Target pressurisation is generally used to limit or suppress tunneling; nevertheless the maximum allowable pressure is limited to 40-60 bar due to the vacuum window foil strength (even when a support grid is used).

Materials and Methods

We are currently developing a pressurised water target which allows heavy over pressurisation (70 – 100 bar of He) of the target water in order to suppress tunneling. The system is currently being tested with 30 MeV protons, 80-160 μA beam current delivered by a IBA Cyclone 30 in Saclay. The experiments are being carried out with natural water.

The target consists of a niobium tube inserted in an aluminium body. Upper and lower caps provide the connections for water loading and unloading. An annular cooling channel is created between the tube outer wall and the aluminium body to allow deionised water to flow at 19 l/min in the annular gap. The vacuum window is made of a niobium foil.

The target filling loop is showed in Fig. 1. A double three-way valve connects the different branches of the loop in three configurations: loading, unloading, irradiation.

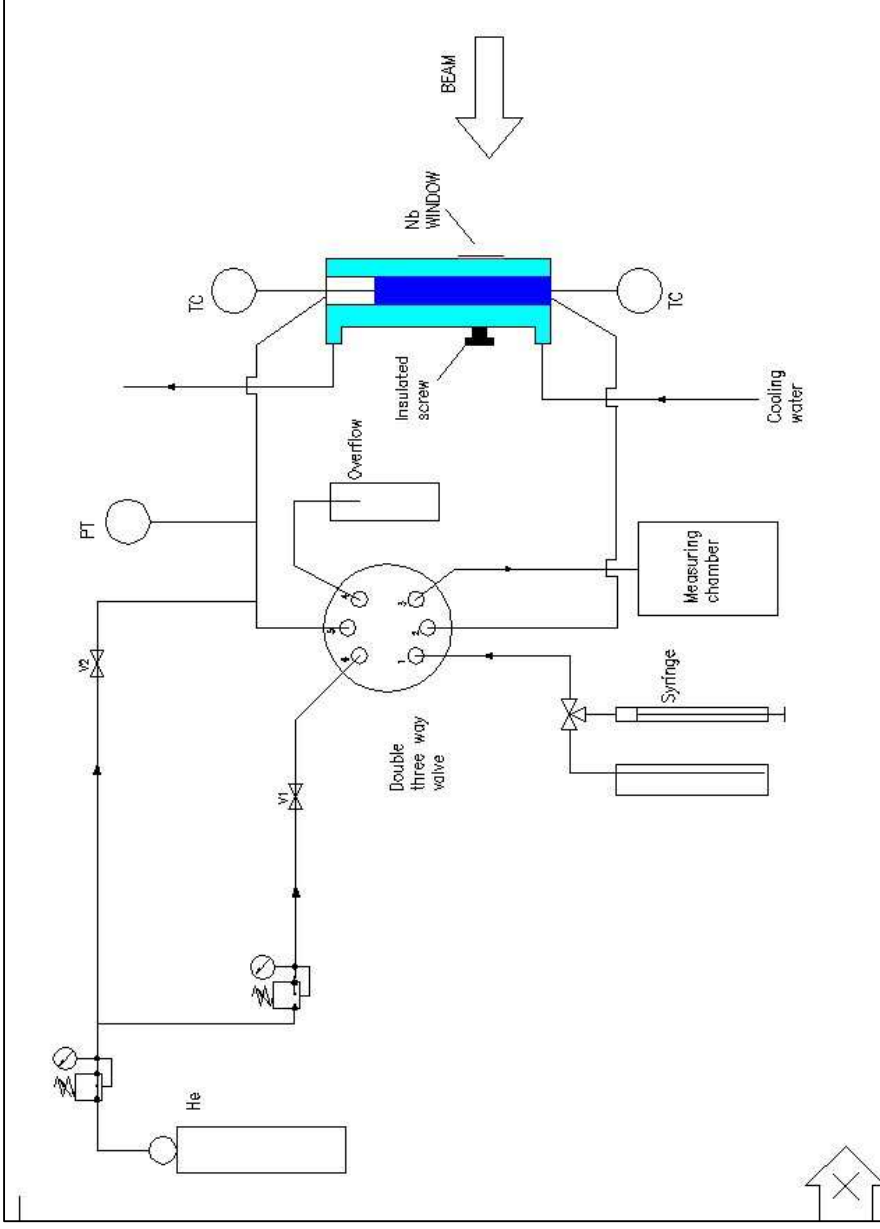


Figure 1 : Schematic representation of the filling loop

The target internal pressure is measured via a pressure transducer (PT) connected to the upper leg of the filling loop (1/16" SS tubing). The helium pressurisation is also provided on the upper leg.

The temperature inside the target is monitored via two 1,5 mm OD mineral insulated thermocouples (TC) inserted in the upper and lower region of the cylindrical volume. The lower thermocouple tip is 6 mm below the beam strike, whereas the higher thermocouple is 6 mm above (submerged in water).

The thermocouples were added because it was not possible to infer the target water temperature from the measured pressure. The system is not at saturation conditions, since the vapour is not the only gas phase contributing to the target internal pressure. During the irradiation with natural water we experienced a consistent pressure build-up which persisted for several hours after the beam shut down. This can only be explained by radiolytic gas production.

In order to monitor the evolution of tunneling, a peek insulated aluminium screw was inserted in the back of the aluminium body (opposite to the foil window). In case of tunneling the protons have sufficient energy to hit the screw. The corresponding measured current is an estimation of the magnitude of the tunneling phenomenon and of the exact time when it sets on.

The aim of these experiments is mainly the determination of the over pressure required to suppress the tunnelling phenomenon. The thermal behaviour of the system is also investigated.

The maximum allowable pressure of the niobium tube is approximately 275 bar. Once the over pressure ensures single phase conditions in the target, modelization of the thermal exchange is also simplified since we have only two regimes: natural convection inside the target and forced convection on the outer wall of the Nb tube.

It should be noted that the classic correlations for natural convection or nucleate and bulk boiling are generally derived from experimental set up featuring a hot surface in contact with the liquid. This is not the case of a charged particle beam releasing its power into the liquid phase.

The experimental results can therefore help to understand the differences and the possible corrections required to develop a suitable theoretical approach. The experimental campaign is still in a preliminary phase and the partial results are as follows.

Results and discussion

The experiments are carried on with natural water. Together with the monitoring of tunneling current and pressure evolution we also measured the $^{18}\text{F}^-$ yield. The results are extrapolated for H_2O^{18} enriched water and summarized in table 1.

During the irradiation of an empty target, the tunneling current was approximately 10 % of the beam current. This is consistent with the ratio between the foil window surface and the screw surface.

One can clearly see from the temperature and pressure values that the water in the target is subcooled, whereas the values of tunnelling current indicate that there are still protons going through. This means that the over pressure required to suppress the tunneling has not been reached yet. This is also reflected in the decreased yield at higher beam currents.

The typical pressure evolution (red curve) during an irradiation for 80 μA average beam current is shown in Fig. 2 ; similar curves are found for higher beam current. One can notice that the signal is extremely unsteady, and rapidly changing above and below its mean value. The residual pressure after beam shut down is also shown in the graph.

Table 1: Test results

Average beam current [μA]	Volume [ml]	Irradiation time [min]	He over pressure [bar]	Saturation Yield [mCi/ μA]	F^{-18} yield ^a EOB [mCi]	F^{-18} yield ^a for a 2hr-irradiation [mCi]	P_{max} [bar]	P_{res} [bar]	T_{water} [$^{\circ}\text{C}$]	Tunneling current [μA]
15	0	5	NA	NA	NA	NA	NA	NA	NA	1,4
40	6	15	0	NA	NA	NA	1,2	1	90	0,3
80	6	62	20	225,8	5916	9690	45-48	29	170	0
140	6	44	20	133,6	4752	10000	50-56	29,5	213	0,5
160	6	36	40	160,9	5268	13700	82-86	42	240	0,5
156	6	60	40	160,8	7968	13400	82-86	43	230	0,5

a: extrapolated to 100% H_2O^{18} enrichment

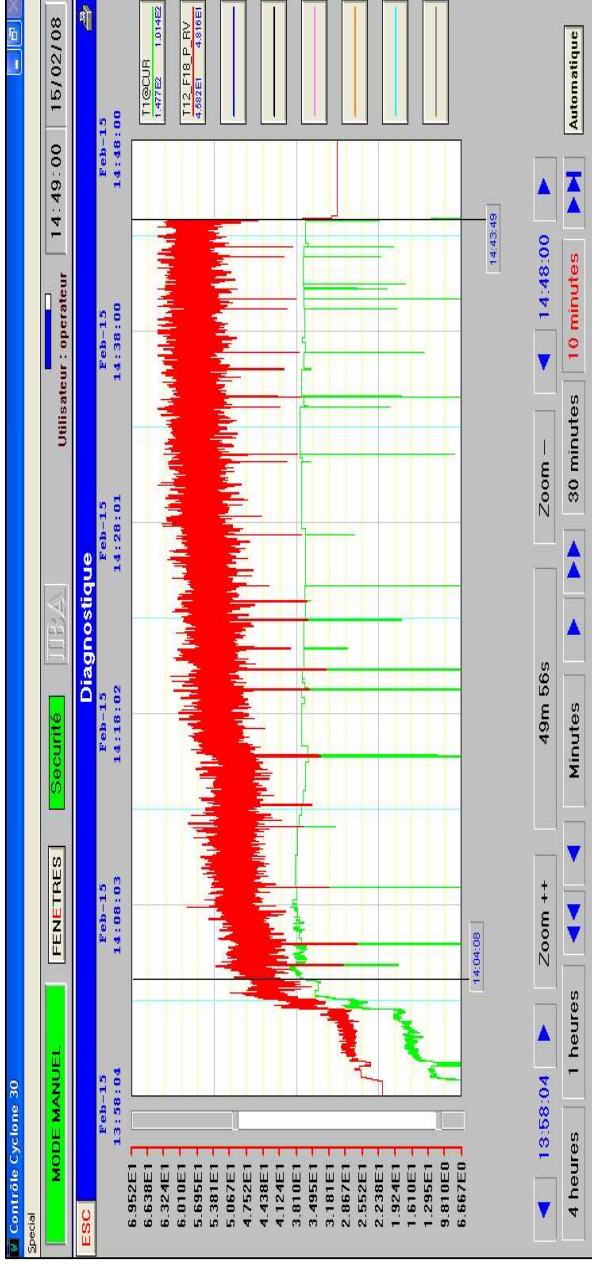


Figure 2 : Pressure evolution (red curve) for a 80 μ A beam current (green curve)

Conclusions

The experiments are still on going. At this stage we didn't reach the over pressure required to suppress tunneling but the margin to the maximum allowable pressure in the tube is still high. We plan to proceed once step at a time and increase the beam current once a complete suppression of the tunnelling has been achieved.

Abstract

SCALING UP F-18 FLUORIDE PRODUCTION IN RECIRCULATING O-18 TARGET

Kiselev M, Botov S, Sokolovski E, Lai D, Vantos T, Schreiner E, Jongen Y
IBA Molecular, Sterling, VA, USA

Conventional static liquid water targets used for manufacturing of F-18 have important limitations. Beam energy deposited into a relatively small area immediately behind the target foil overheats the foil and target material resulting in beam tunneling, reduced target output and increased maintenance effort. Furthermore, static targets must be pressurized to minimize tunneling and maintain lowest possible vapor fraction. Pressures used range from 10 to 40 bar and typically require small (8-10 mm) beam apertures and relatively thick foil (0.05 mm) or require supporting grids. Despite of all efforts static targets are incapable of handling all of the beam current produced by common commercial cyclotrons, at least two targets are needed to fully utilize beam produced. Irradiation of two targets simultaneously requires complicated extraction and sophisticated control systems which further decreases overall reliability and efficiency. Many of these problems can be avoided by use of recirculating targets¹⁻⁵ equipped with extractor system⁴.

To test and optimize recirculating target we constructed extractor station equipped with high flow rate gear pump to move target water through the loop which included the target, heat exchanger, flow meter and 100 ml expansion vessel. The system also included two pressure and temperature sensors and flow through conductivity sensor connected via bypass tube.

To extract anionic radioactive products with no interruption of main loop flow the secondary loop made of 1/16 inch OD PEEK tube was connected to main loop. Dynamic pressure drop in main loop was sufficient to drive water through the secondary loop at flow rate of 10-20 ml/min. Two high pressure 6-port valves open and close the secondary loop.

During irradiation the secondary loop was normally closed. Depending on target used and size of tubes connecting target to pump and heat exchanger the flow rate in main loop was 400-1200 ml/min, corresponding to pressure drop of 5-2 bar between pump outlet and expansion vessel. To maintain optimal pump performance it was necessary to pressure expansion vessel by means of venting through an adjustable backpressure regulator.

Produced radioactive isotopes were extracted on Waters QMA SepPak cartridge by diverting approximately 10-20 ml/min flow rate through the secondary loop for 5-20 min. Two Alltech Maxi clean cartridges (SCX and SAX, 600 mg each) were used in series with anion exchange cartridge to control conductivity. Without these cartridges repeated extractions would have been impossible because of contamination of water with salts washed off QMA⁴. Extracted isotopes were then eluted using pneumatically actuated fixed volume syringe pump with 1 ml of 0.3-1.0 M KHCO₃ solution.

After elution the QMA cartridge was rinsed with 1 ml of water and dried for 2 minutes in flow of helium while eluted isotopes was delivered into remote hot cell for measurement. Efficiency of extraction was estimated by comparison of two consecutive extractions, it was found that on an average 73% of F-18 was extracted in the first portion.

To optimize target design, two different flow through targets were constructed: variable depth target with double foil (Rev A) and simplified fixed depth target with single foil (Rev B).

Variable depth target had 12 mm ID beam aperture with 0.025 mm vacuum havar foil. Helium cooling space was separated from target material by second 0.05 mm havar foil. Target depth (from foil to the back) was adjustable from 5 to 35 mm by moving threaded insert. Target water was supplied to target cavity from a gear pump pump at the center of inner cavity, it passed through threaded target insert and is directed through 2.35 mm orifice toward the target foil. 0.025 mm havar foil was used in all experiments except the first one, when 0.05 mm foil was used. It was found that 0.05 mm foil develops a heat spot, similar to that observed in a conventional static target. While 0.025 mm foil never changed its appearance even after 12 hours under beam in excess of 100 uA.

Using Rev A target a series of 2-hour irradiations at 100 uA with flow rate of 400-500 ml/min were carried out with target depth set to 10, 8 and 6 mm respectively, and target insert was examined after each irradiation. No damage was observed with 10 mm depth, at 8 mm a heat spot developed while at 6 mm the insert was significantly damaged. It was found that helium cooling was not necessary to cool target foil. After vacuum foil was removed and helium cooling space sealed and evacuated, the target was irradiated for total over 12 hours with no apparent damage to target foil.

Based on these findings, target Rev B was optimized and simplified. Helium cooling cavity and foil were removed. Target water cavity depth was 10 mm, foil thickness 0.025 mm, aperture diam. 16 mm. O-18 water is supplied through 2mm diam. hole in the center, and removed through 6 mm diam. hole on the top side. Double seals were used between vacuum and water. Target loop was loaded with 100 ml of 1% O-18 water for test runs. Target water temperature at the outlet of the target was 70-76C. Water temperature after heat exchanger was 50-55C with typical temperature variation of about 20C. Thus, 70% of beam energy is being removed by target water flow.

Scale up production runs with duration of 4-8 hours were conducted using 85-90% enriched water at 130-150 uA beam current and flow rate of 700-800 ml/min in Rev B target, demonstrating target yield similar to that achieved in static targets.

CONCLUSIONS:

Flow through target and extraction system were optimized. 10 mm deep target with 0.025 mm thick foil did not require helium cooling and is stable for over 50 hours under beam in excess of 140 uA without visible foil damage. The results indicate that recirculating target can be used for large-scale production of F-18 using one target per cyclotron and may allow to increase production of F-18 while reducing consumed O-18 water material. It can also increase productivity by eliminating unnecessary idle periods for re-filling the target.

REFERNCES:

1. Morelle et al, Proc. 3rd WTTC, Vancouver, B.C., pp. 50-51, 1986
2. Iwata et al, Appl. Rad. Isot. V.38, No 11, p. 979-984, 1987
3. Linder et al J. Appl Rad Isot, V24, pp. 124-126, 1973
4. Kiselev et al. US Pat 6,567,492 May 20, 2003
5. Wieland et al, US Pat 7,200,198 April 3, 2007 and other references therein

Development and Validation of Computer Models for Design of Batch Boiling Targets for Production of ^{18}F

Johanna Peebles, Matthew Stokely, Michael Doster

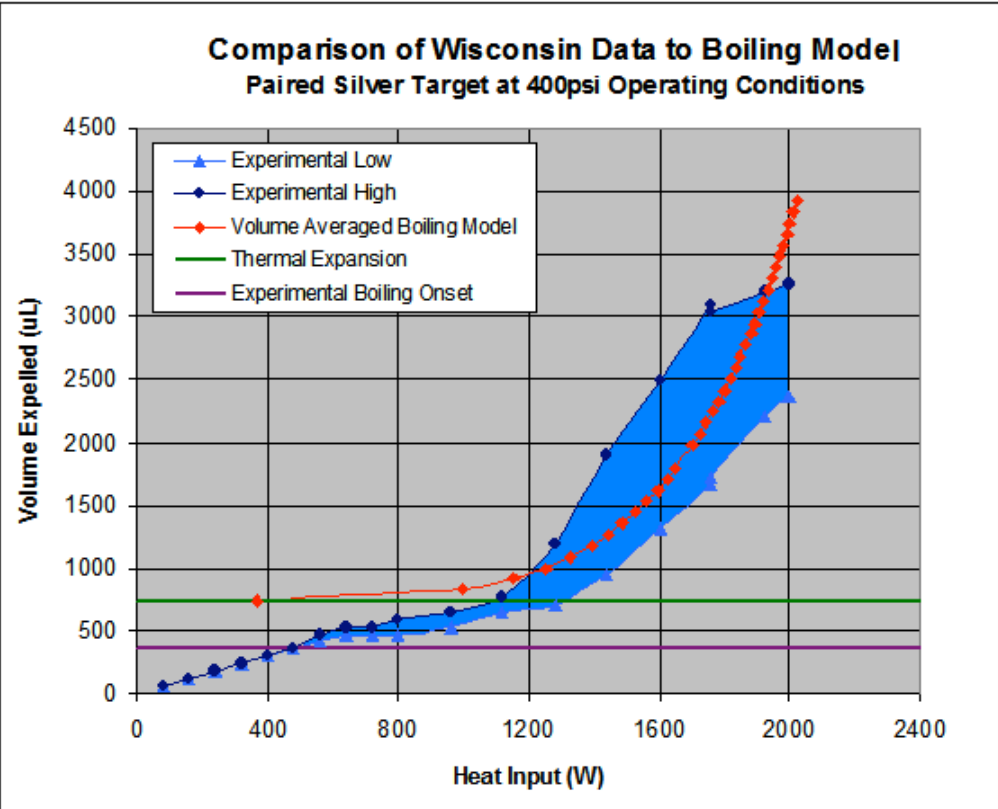
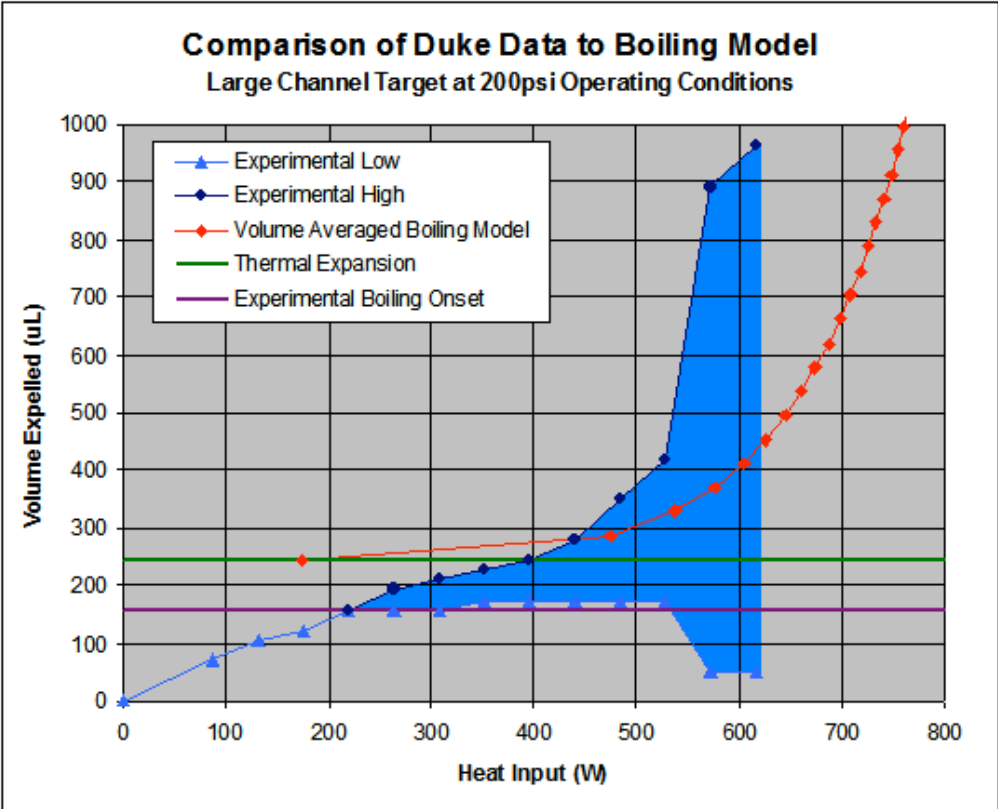
North Carolina State University

Batch boiling water targets are commonly used to produce ^{18}F through the $^{18}\text{O}(p,n)^{18}\text{F}$ reaction by proton bombardment of ^{18}O -enriched water. Historically, design of batch boiling targets has been purely empirical, which required a significant amount of trial and error, long lead times and no guarantee of an optimal design. A fundamental approach to target design from a modeling perspective has been developed, and this approach has been implemented to design new targets with enhanced production capabilities. For range-thick targets, ^{18}F production is directly proportional to beam current. Accordingly, target production can be increased by optimizing the heat rejection capabilities of the target, and target performance considerations can be essentially reduced to a heat transfer problem. Computer models were developed which describe heat transfer in a boiling target using basic engineering principles. These models were developed to predict target thermal performance and have been validated with experimental test data from the Duke University Medical Cyclotron and the Wisconsin Medical Cyclotron. These models allow researchers to predict the effects of changing target geometry and materials in the absence of, or with limited, expensive and time-consuming experiments.

Heat conduction and convection in a batch boiling target can be modeled using known temperatures and standard heat transfer coefficients. Correlations for boiling and condensing heat transfer coefficients, submerged jets, and coolant flow in channels are widely available in literature. A FORTRAN code was developed to evaluate heat transfer coefficients based on boiling conditions in the target chamber, target pressurization, and coolant flow rates. COMSOL Multiphysics, a program which uses finite element techniques to solve partial differential equations to simulate physical phenomena, was used to solve the heat conduction problem in the target body using the provided heat transfer coefficients and known boundary conditions.

These methods have been applied to thermosyphon targets, but are directly applicable to Reflux targets and batch boiling targets in general. The computer model was validated using four thermosyphon targets, which all featured circular cooling channels, jet cooling on the back of the target, and deep target chambers with race-track shaped or circular cross-sections. The general modeling technique, however, can easily be applied for alternate target chamber shapes and sizes and for finned targets with coolant flow in grooves. The model can also easily be applied for serial coolant flow or parallel flow through multiple cooling systems.

Good agreement between model predictions of average target void as a function of beam current and observed experimental data was observed for four targets which featured different target body materials, chamber dimensions, and coolant geometries. Two of the targets were designed for and operated at the Duke University CS-30 cyclotron and two at the Wisconsin Medical Cyclotron. Observed target behavior and model predictions suggest bulk boiling in the target chamber without formation of a distinct vapor region.



Ionic contaminants in irradiated [¹⁸O]water generated with Havar and Havar-Nb foils

J.S. Wilson¹, M.A. Avila-Rodriguez^{1,3}, S.A. McQuarrie¹

¹Edmonton PET Centre, 11560 University Ave., Edmonton, AB, T6G-1Z2 CANADA

³Turku PET Centre, Kiinamyllynkatu 4-8, Turku, 20520 FINLAND

Introduction: Ionic contaminants generated during [¹⁸O]water bombardment to produce of [¹⁸F]fluoride can reduce the reactivity of fluoride for nucleophilic substitution reactions. Target entrance foils are the principle source of metallic ionic contaminants found in irradiated water samples and a foil has been prepared in which a layer of chemically inert niobium has been sputtered onto the Havar surface to reduce the metal ion contamination.

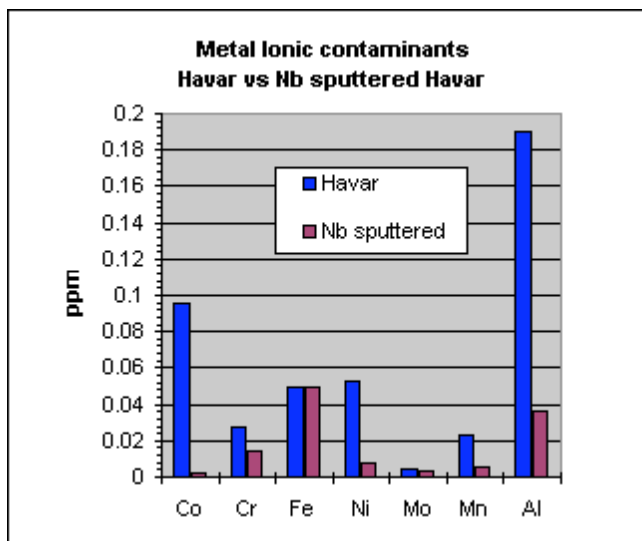
Aims: To quantify the ionic contaminants which arise from water samples irradiated in a niobium target with Havar vs niobium sputtered Havar as entrance foils and to evaluate the selective adsorption and elution of the ions from QMA anion exchange cartridges in commonly used activated forms.

Methods: The thickness of the Nb film sputtered on the Havar foil was on the order of 188 ± 20 nm while the thickness of the Havar foils was $38 \mu\text{m}$ ($1.5\text{E}-3$ inch). Irradiations were performed with 17.5 MeV protons at currents from 50 to 100 μA lasting for 1-2.5 hours. Radionuclidic contaminants were determined via gamma spectroscopy while cold ionic impurities were determined with ICP-MS. Sep-Pak QMA light cartridges from Waters were tested in the non-activated, bicarbonate, carbonate forms as well in the carbonate form following hydrogen peroxide vapor sterilization. Chromafix 30-PS-HCO₃ from Macherey-Nagel in the bicarbonate form were also analyzed.

Results: A marked decrease in metal ions was observed when using the Nb sputtered foil versus the straight Havar. Contaminants arising from Havar can be observed owing to the microporosity of the niobium layer. Much higher levels of ionic impurities were generated from new entrance foils of either type which decreased rapidly after 3-4 irradiations on a fresh entrance foil to reach a constant value for subsequent irradiations with the same integrated current. Constant Fe levels may be due to stainless steel contact in both. One water sample irradiated (60 μAh) with Havar-Nb foil showed a concentration of Nb of 0.036 ppm.

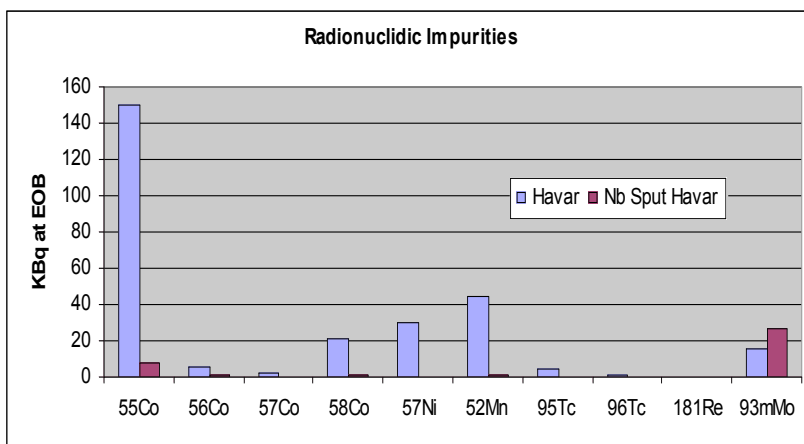
Cold Ionic Impurities in ppm

	Havar new	Havar 3rd irrad	Nb Havar new	Nb Havar 3rd irrad
Co	1.42	0.0953	0.0533	0.002
Cr	0.0624	0.0278	0.0251	0.014
Fe	0.2	0.05	0.05	0.05
Ni	0.375	0.0522	0.0354	0.0078
Mo	0.01	0.004	0.007	0.003
Mn	0.11	0.023	0.01	0.005
Al	1.25	0.19	0.385	0.036
Sb	0.0063	0.0002	0.001	0.0009
Ba	0.021	0.002	0.009	0.001
Cu	0.096	0.003	0.01	0.004
Pb	0.333	0.0001	0.012	0.001
Tl	0.00055	0.0001	0.00474	0.00058
V	0.0009	0.0002	0.0001	0.0005
Ca	0.8	0.3	1	0.3
Na	7.7	2	4.1	3.3
K	2.2	0.6	0.6	0.6



Radionuclidic Contaminants from Elements of Havar

Product	t _{1/2}	Reaction
⁵⁵ Co	17.5 h	⁵⁸ Ni(p,α)
⁵⁶ Co	77 d	⁵⁶ Fe(p,n)
⁵⁷ Co	272 d	⁵⁷ Fe(p,n)
		⁶⁰ Ni(p,α)
		⁵⁸ Ni(p,2p)
⁵⁸ Co	71 d	⁵⁸ Fe(p,n)
⁵⁷ Ni	35.6 h	⁵⁸ Ni(p,pn)
⁵¹ Cr	27.7 d	⁵² Cr(p,pn)
⁵² Mn	5.6 d	⁵² Cr(p,n)
⁹⁵ Tc	20 h	⁹⁵ Mo(p,n)
⁹⁶ Tc	4.3 d	⁹⁶ Mo(p,n)
¹⁸¹ Re	19.9 h	¹⁸² W(p,2n)
^{93m} Mo	6.85 h	⁹³ Nb(p,n)



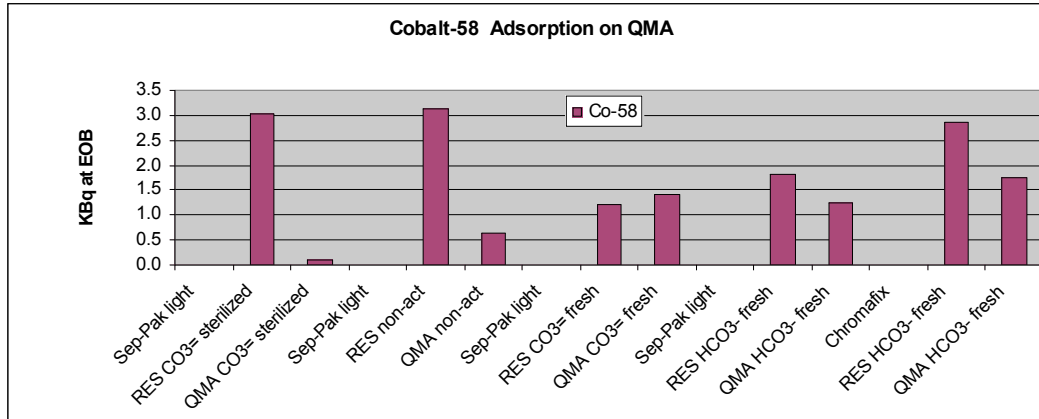
Isotopes of Co as well as ⁵⁷Ni and ⁵²Mn were the predominant radionuclidic impurities from irradiations done with a Havar foil. These isotopes arise from proton activation elemental nickel, iron and chromium which are major constituents of the material. Elemental ⁵⁹Co produces only very long lived radionuclidic by-products (⁵⁹Ni = 7.6e4 yr) which would not be observed in this study. The level of ^{93m}Mo was increased with the use of the Nb sputtered foil as there is a contribution from both the target body and the foil.

Total of radionuclidic contaminants are in amounts of ppt and therefore of little chemical consequence when looking at ¹⁸F at levels of 50-80 ppb. .

QMA elution and ion distribution

The major radionuclidic impurities of Havar were monitored in samples passed on to QMA cartridges and the residual water and cartridge were gamma counted. The QMA cartridge is a very good post irradiation purification media for fluoride as most ions go through with the residual water and wash and are not retained (⁵⁷Ni, ⁵²Mn etc.) whereas ^{93m}Mo was completely adsorbed on the resin. Cobalt adsorption however, was dependent on the activation state of the QMA resin. Elution of the retained cobalt has been found to be dependent on the ionic and solvent concentration and is under further study.

In a single study looking specifically for iron, it was observed that the irradiated sample had levels below detection however the eluant solution and the eluted fluoride both showed the presence of iron in amounts in the same magnitude as the F-18. The level of trace ions in the eluant solution must be monitored closely as these will ultimately go through the QMA into the eluted F-18 cocktail.



RES = Residual water passed through QMA QMA = cartridge
 Sterilized = subjected to H₂O₂ vapor sterilization non-act = non activated QMA (from package)
 Fresh = freshly activated

Conclusions: Metal ionic impurities in water samples irradiated with the Havar-Nb foils were much lower than the samples irradiated with an unmodified Havar foil. Cold ionic contaminants are found in ppm and high ppb levels and are significant as typical amounts of ¹⁸F fluoride are at levels of 10-80 ppb. Radionuclidic contaminants are in the ppt levels and are chemically of little relevance but can serve as a surrogate markers of cold ionic contaminants. There is potential for QMA resin cartridges to be used as purification media as opposed to a simple trap and release cartridges.

COMPARISON BETWEEN DIFFERENT TEMPERATURE MEASUREMENT METHODS FOR A SOLID TARGETRY IRRADIATION SYSTEM

S. Chan, D. Cryer, R.I. Price & RAPID GROUP

*Department of Medical Technology and Physics, Sir Charles Gairdner Hospital
Perth, Western Australia*

INTRODUCTION:

The production of longer lived isotopes such as ^{124}I [$T_{1/2} = 4.18 \text{ d}$] and ^{64}Cu [$T_{1/2} = 12.85 \text{ h}$] requires a semi-automated solid targetry system. The production yield of any radioisotopes is directly dependent on target current impinging on the target material. This is limited by the cooling efficiency of the target material in the target holder and the O-ring material used to secure the cooling mechanism.

Simulations of the thermal characteristics of the target material under specific cooling configurations were calculated using SolidWorks (COSMOSFloWorks). In order to validate the model, thermocouples were inserted into a platinum disc used for the production of ^{124}I . Comparisons were made between the experimental and theoretical results in relation to the location of the thermocouples.

The initial experiment shows a poor correlation between experimental and theoretical temperatures for the center of the target. This is due to the placement and thickness of the thermocouple used for this experiment. As a subsequent of the initial experiment a second disc with a different physical construction was used in order to better determine the temperature of the bulk material.

AIM:

Validate the SolidWorks model by comparing the theoretical and experimental results. Compare the results for the two platinum discs with different physical construction.

METHOD:

The thermal characteristic of the solid targetry system was modelled using COSMOSFloWorks. COSMOS uses a finite element method to solve partial differential equations at individual nodes within the model. The overall effect determines flow characteristics and heat exchange between the coolant and the target material.

The beam is modelled by applying a surface heat source of variable wattage on a platinum target ($\Phi = 25\text{mm}$, $t = 2\text{mm}$). The beam is assumed to be completely homogeneous with the same diameter as the 12mm collimator. Chilled water is applied to the back face of the target disc at a measured flow rate of 28L/min at 18 °C. The model was tested over various target currents from 0.5 μA (9W) to 30 μA (540W) together with the measured flow rate stated above.

The model was verified experimentally by irradiating two platinum discs with 2 type-K thermocouples inserted inside. The thermocouples are inserted from the rim of the platinum disc and the shafts runs from the circumference to their respective locations. The first thermocouple is located at the geometric center, while the second is at the 8mm radius to measure the temperature near the O-ring seal.

The first disc has a circular platinum mesh pressed into the irradiated face of the disc substrate. This is used for the deposition of target material such as TeO_2 for the production of ^{124}I . The two thermocouples has a thickness of 1.5mm in diameter, thus the center thermocouple protrudes between the platinum mesh and the substrate.

The second platinum disc is a blank substrate with no mesh on the irradiated face. The 2 type-K thermocouples are thinner with a diameter of approximately 0.5mm.

The measured temperatures for the two thermocouples were recorded for both platinum discs at various target currents (20 sample points ranging from 0.5 μ A to 30.75 μ A). The measured target currents obtained experimentally were used as a parameter for the simulations. The theoretical temperatures were calculated for both platinum discs for each corresponding thermocouple locations. The results are then compared with the experimental results.

RESULTS:

The temperature measured at the 8mm radius for the two platinum discs shows a strong correlation with between the theoretical and experimental results. With target currents ranging from 0.5 μ A to 30 μ A the temperature is 20°C to 65°C, respectively. The linear regression between the theoretical and experimental results is very close to the line of identity. For the platinum disc without mesh the equation is:

$$\text{Theoretical} = 0.95 * \text{Experimental} + 2.43 \quad (R^2 = 0.98)$$

With mesh the equation is:

$$\text{Theoretical} = 1.13 * \text{Experimental} + 3.26 \quad (R^2 = 0.99)$$

The platinum disc with the mesh on the irradiated face produced the greatest discrepancy between theoretical and experimental results for the temperature at the center. With a target current of 30.7 μ A (540W) the theoretical model calculates a maximum target temperature of 154°C, measured experimentally this is 340°C. For the same target current the temperature measured at the center for the blank platinum disc was only 173°C.

The discrepancy is due to the mounting of the thermocouple at the center of the two platinum discs. With the first platinum disc the thermocouple is mounted in between the platinum mesh and the substrate, this exposes the thermocouple directly to the incident beam. Also the thickness of the thermocouple contributes to the measured temperatures via thermal conduction along the sensor's shaft. This effectively measures the line temperature for the radius of the incident beam rather than the point at its center location.

The results for the second platinum disc with thinner thermocouples and no mesh gave a better temperature reading at the center of the target. The linear regression shows a strong correlation between the theoretical and experimental results, this is close to the line of identity.

For the platinum disc without mesh the equation is:

$$\text{Theoretical} = 0.82 * \text{Experimental} + 2.76 \quad (R^2 = 0.99)$$

In comparison, with mesh is:

$$\text{Theoretical} = 0.43 * \text{Experimental} + 4.61 \quad (R^2 = 0.96)$$

DISCUSSION & CONCLUSIONS:

Since the melting point of the target material is much higher than that of the O-ring, our concern is the integrity of the O-ring at different target currents. At 30 μ A the maximum recorded temperature near the O-ring seal is 65°C, this is 140°C below its operating limit. The strong relationship between the theoretical and experimental results validates the temperature model at the 8mm

radius. This provides the ability to check the temperature at the O-ring seal for different target current and cooling configurations.

The discrepancy at the center location between the theoretical and experimental results was minimised by using a blank substrate and thinner thermocouples. This produced a truer temperature representation of the bulk material, which correspond well to the calculated center point value produced by the model. The experiment shows an approximate 20% error between the theoretical and experimental results. In comparison the disc with the platinum mesh has an average error of approximately 57%.

The successful validation of the temperature model will allow us to predict the temperature effects of any target material for a given production criteria. Further variations to experiment such as investigating the hydrodynamic effects of changing the distance of the impinging water jet to the target, and the introduction of a rough target surface for the cooling side can be modelled in COSMOSFloWork. It is anticipated the modifications will theoretically derive an increase in the cooling efficiency of the target material, therefore increasing the ability to irradiate at a higher target current.

REFERENCES:

¹Elex Commerce (2002) *COSTIS operating Manual*, Belgrade Yugoslavia.

JJ. Comor, (2003) *Nuclear Instruments and Methods in Physics Section A*, **521**:161-170.

J. Cornelius, (2006) Eleventh International Workshop on Targetry and Target Chemistry, **11**:18-19.

A ROTATING TARGET FOR THE IRRADIATION OF RA-226

Dr. M. Harfensteller¹; Dr. J. Moreno²; Dr. R. Henkelmann²; Dr. M. Mentler³; Dr. E. Huenges³; Dr. V. Bechtold¹; Prof. Dr. A. Tuerler²; Dr. E. Kabai²; Dipl.-Ing. A. Eursch⁴;

¹ Actinium Pharmaceuticals, API

² Institute of Radiochemistry, Technische Universität München

³ Institute E17, Technische Universität München

⁴ Institute for Machine Tools and Industrial Management, Technische Universität München

The alpha-emitter Ac-225($t_{1/2}=10d$) is a promising isotope for the cancer treatment in the alpha-immuno-therapy (APIT). One production method for this isotope is the irradiation of long-lived Ra-226($T_{1/2}=1600a$) with protons in a cyclotron via the $(p, 2n)$ reaction. The alpha-emitter Ra-226 decays to the isotope Rn-222 ($T_{1/2}=3,8d$) which is a noble gas. The challenge is to design and evaluate a target which safely houses Ra-226 and the daughters for high beam currents and long irradiation times. The unique design and the automated preparation of this radium target are discussed.

The target consists of a target cup which includes the function of a beam window and provides the housing for the target material. The target cup material is aluminum. As target material dried radium nitrate is used. The target cup is designed to enclose more than 100 mg of radium nitrate. The thickness of the target window is optimized to degrade the beam energy of the TUM cyclotron with app. 21 MeV to obtain a high production yield. The target cup is closed hermetically with a target cover to prevent any release of the target material and the radon.

To reduce contamination risks the radium nitrate is dissolved in an aqueous solution for the target preparation. This solution is dispensed in the target cup and dried subsequently. The radon emitting radium salt is closed hermetically by the target cover. After the automated preparation, the radium content of the target is measured by α -spectrometry.

To distribute the thermal load of the beam with currents up to 100 μA , the target is rotating with 1000 rpm and water cooled from the backside.

The reproducibility of the automated target preparation process with up to 100 mg of radium is demonstrated thus enabling several successful irradiations. In each run more than 2 GBq Ac-225 were obtained with a very high radioisotopic and chemical purity.

Production of ^{64}Cu on the CC18/9 Cyclotron at TPC, a work in progress

M.A. Avila-Rodriguez^{1,2}, J. Rajander^{2,3}, S. Johansson^{2,3}, P.O. Eriksson^{2,3}, T. Wickström³,
S. Vauhkala^{1,2}, E. Kokkomäki^{1,2}, J. Schlesinger^{1,2}, O. Solin^{1,2}

¹Turku PET Centre, University of Turku, Kiinamylynkatu 4-8, 20520 Turku, Finland

²Centre of Excellence on Molecular Imaging in Cardiology and Metabolic Research

³Accelerator Laboratory, Åbo Akademi University, Porthaninkatu 3, 20500 Turku, Finland

Introduction: a targetry system for the irradiation of solid targets has been installed on one of the external beam lines of the CC18/9 cyclotron (Efremov Scientific Research Institute of Electrophysical Apparatus, St. Petersburg, Russia) at Turku PET Centre (TPC) new laboratory. The aim of this project is to develop metallic radionuclide production, with emphasis in ^{64}Cu , as feedstock for the labeling of high specific activity radiotracers for PET-based molecular imaging.

Target: the target holder, designed and machined in aluminum, consist of two pieces holding a gold disk (24 mm ϕ \times 1 mm thick) which serves as backing for the electrodeposition of isotopically enriched substrates. The front piece of the target holder has a thickness of 0.5 mm at the entrance of the proton beam and serves the dual role of vacuum seal and energy degrader. This piece is held in place by the vacuum of the beam line and is water cooled during the bombardment. The back piece of the target holder is a cooling water chamber on which the gold disk, with the plated target material, is mounted for the irradiation. Both pieces of the target holder are tightened pneumatically providing a water seal to the back of the disk. After allowing a 2-3 hours post-irradiation cooling time, the back piece of the target holder is retracted allowing the disk to drop into a lead container.

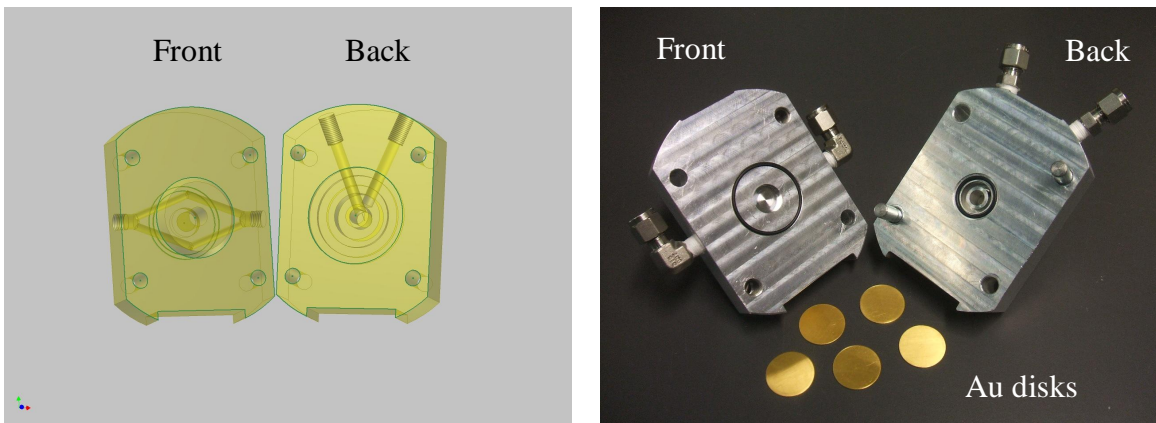


Fig. 1. Schematic drawings showing the cooling water channels and picture of the target holder.

Post-irradiation processing: a radiochemical separation system was designed for the processing of the irradiated targets. It consists of a holder for the dissolution of the target material, a liquid chromatography column packed with ion exchange resin, pneumatically operated syringes to dispense the different solvents onto the separation column, a hot-block housing a v-vial to evaporate to dryness the eluted fraction containing the radioactivity, and miniature radiation detectors (Geiger-Muller) to monitor the different steps of the processing. The dissolution holder consists of a pneumatically operated Teflon insert, on top of a hot-block, that exposes only the electrodeposited substrate. After the dissolution, the acidic solution containing the target material and radioactive product is remotely transferred onto the separation column. To achieve a better separation profile only gravity is allowed to work during the elution process. The post-irradiation processing apparatus, located in a shielded mini-cell, is schematically displayed and remotely operated from a touchscreen.

Production of ^{64}Cu : This metallic PET-nuclide will be produced via the $^{64}\text{Ni}(p,n)$ reaction with the enriched target substrate electrodeposited on Au backing. After degradation of the nominal energy of the cyclotron, the effective energy of the proton beam impinging on the plated ^{64}Ni is planned to be $\sim 14\text{-}15$ MeV. Radiochemical separation of radiocopper from the nickel target material is performed by the well-known chromatography of the chlorocomplexes using an anion exchange column with AG1-X8

resin. The production rate for a thin target ($14 \rightarrow 9$ MeV) is expected to be on the order of $10 \text{ mCi}/\mu\text{Ah}$. Preliminary productions runs are planned for late June, 2008.

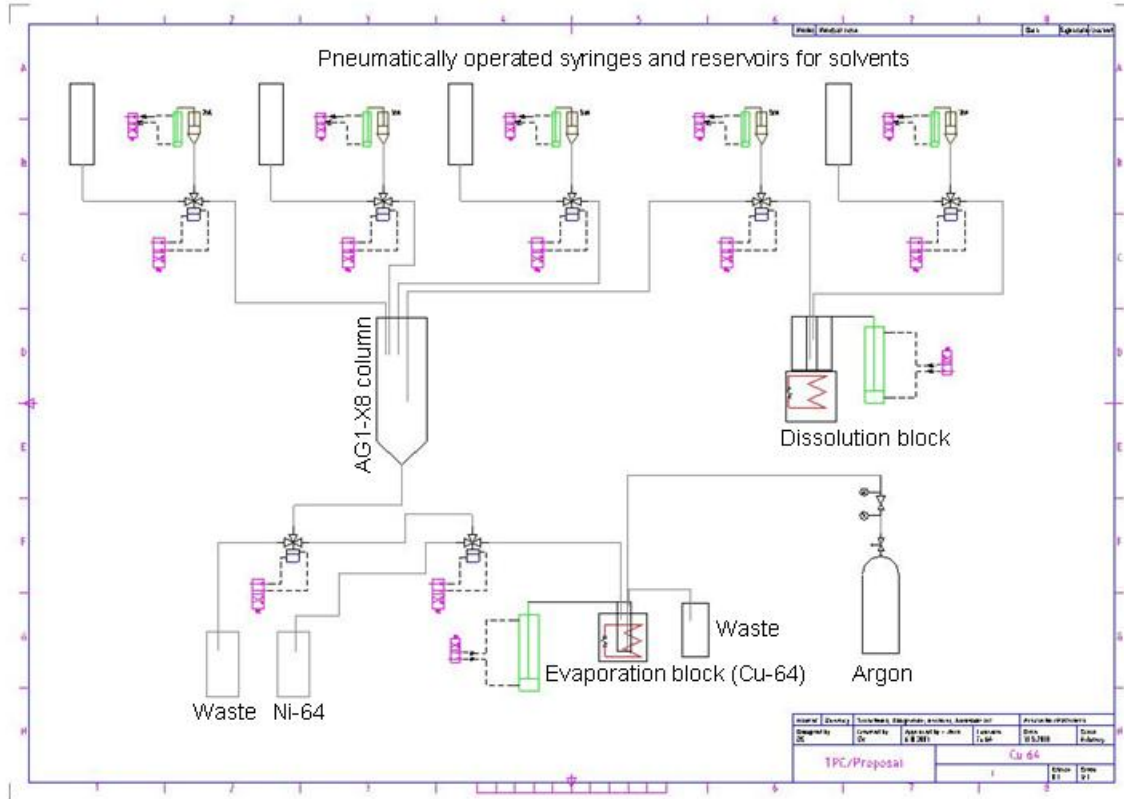


Fig. 2. Schematic diagram of the separation system.

DESIGN AND CONSTRUCTION OF A COMPACT SEMI AUTOMATED SOLID TARGET IRRADIATION SYSTEM FOR THE PRODUCTION OF ^{124}I , ^{64}Cu PLUS VARIOUS SOLID-TARGETRY BASED RADIOISOTOPES, USING AN 18/9 MeV IBA CYCLOTRON.

D.CRYER, S. CHAN, R.I.PRICE & RAPID GROUP.

*Department of Medical Technology and Physics, Sir Charles Gairdner Hospital, Perth,
Western Australia*

INTRODUCTION: Since commissioning of the IBA 18/9 Mev medical proton cyclotron at Sir Charles Gairdner Hospital, the facility has produced radio-pharmaceutical products using both the liquid and gas targets. The need to produce longer lived isotopes such as ^{124}I [$T_{1/2}=4.18\text{d}$] and ^{64}Cu [$T_{1/2}=12.85\text{ h}$] has initiated the construction of a semi-automated solid targetry system.

AIM: To design and construct a reliable system able to produce solid-targetry based radioisotopes. The apparatus must be easy to load and unload with minimal human contact. The irradiated disk must also withstand high irradiation currents.

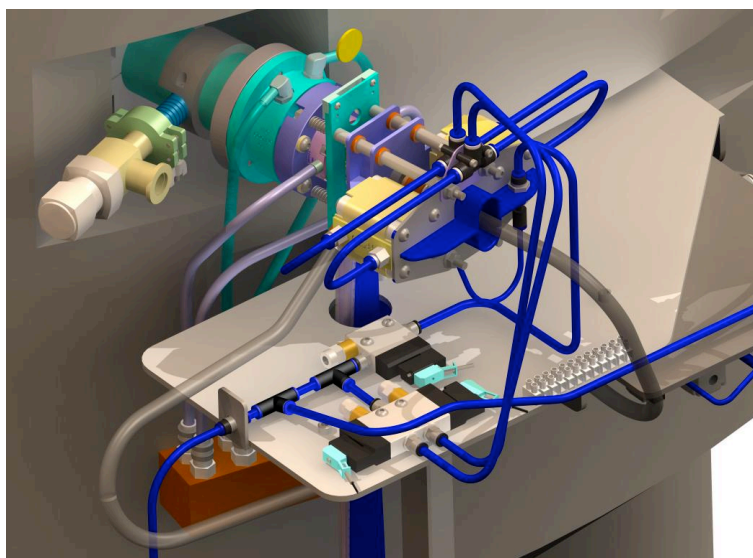


Fig.1. Solidworks drawing of solid target system attached to IBA Cyclotron

METHOD: The initial design was inspired by a commercially available solid targetry system [1]. Due to the design of the exit ports located on the 18mMev IBA cyclotron, a 300mm-beam line was manufactured and installed. There is an additional exit port on the beam line; this is for pulling the vacuum down prior to opening the port to the cyclotron. Attached to this is the solid target system, this unit is mainly constructed from aluminium rather than stainless steel, to reduce radiation exposures whilst servicing and handling the unit. All parts for the solid target unit are machined in house.

The target disc is 25mm in diameter with a thickness of 2mm. The graphite collimator restricts the beam to a maximum diameter of 10mm, thus improving the homogeneity of the beam irradiating the target. To accommodate different target areas the graphite collimator is interchangeable. A reduced collimator size ensures the beam remains perpendicular to the target surface, assisting with the alignment of the non-

focused beam. The graphite collimator has also been designed so that a beam degrader can be incorporated. The degrader will be used to reduce the beam energy level to 14.7mev, for the production of ^{64}Cu . The target rear surface is cooled with a water jet and the front surface by He gas flow. A havar window separates the He-filled space from the vacuum of the beam line. A specially designed window spacer sits between the target and window. Designed to distribute an even flow of cooling gas, over the face of the target and vacuum window. The target and collimator are cooled by chilled water in a closed system that circulates via a heat exchanger. The temperature is maintained at 18°C with a supply flow rate to the cooling jet of 28L/min.

A Siemens programmable logic controller (PLC) is used to activate the various valves for the correct operation. The target is secured in the guiding rail using a pneumatic piston. To prepare for an irradiation, the pneumatic rams seal the cooling mechanisms on both sides of the target. The water cooling circuit is active once the target disk is secured and the cooling jet is in place. The water supply to targetry system is bypassed pre and post irradiation. To unload the target water is purged from the system using compressed air. The pneumatic rams release the target from the cooling mechanism, and the disk falls into a transport container.

Work has been done in developing a purpose built transport container Fig.3. The idea being to minimise contact with the active disk whilst retrieving and extracting the various solid based radioisotopes.

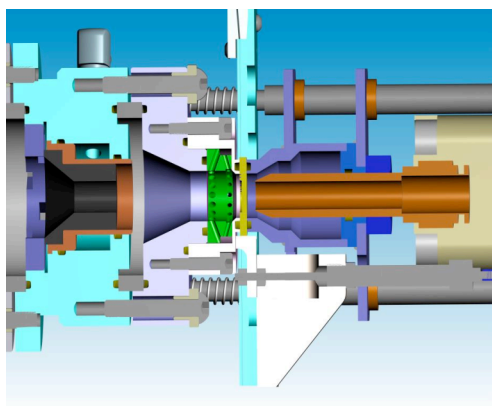


Fig.2. Cross section of solid target



Fig.3. Solid disk transporter

RESULTS: Target disks have been successfully loaded and unloaded and tested at various target currents. To validate the system and to determine the maximum current achievable, a platinum disc with 2 thermocouples of a diameter of 1.6mm, one mounted at the centre and the other at the 8mm radius, was irradiated. Since the melting point of the target material is much higher than the o-rings (205°C), our concern is the integrity of the o-rings at different target currents. At target current of 30 μA the temperature near the o-ring seals was approximately 60°C. This is 145°C below the operating limit. The temperature measured at the centre is 340 °C.

Irradiation of Mo and TeO₂ target have produced test quantities of ^{96}Tc and ^{124}I respectively [2,3]. These test productions have demonstrated the viability of the solid targetry system

DISCUSSION & CONCLUSIONS: We have successfully developed a solid targetry system to be used with an IBA 18MeV medical cyclotron. Future development is in progress to remotely extract the irradiated disk from the bunker incorporating designs to minimise radiation exposure. To optimise the water-cooling for higher beam currents. A second platinum disk is to be made using 0.5mm thermocouples rather than 1.6mm. The theory being this should give more accurate results, due to less surface area of the thermocouple and more depth to protect it from the effects of the beam. Concurrent developments include investigations into the preparation of target materials on disk substrate. The sublimation of the target material from the irradiated disk and the development of a positron detector.

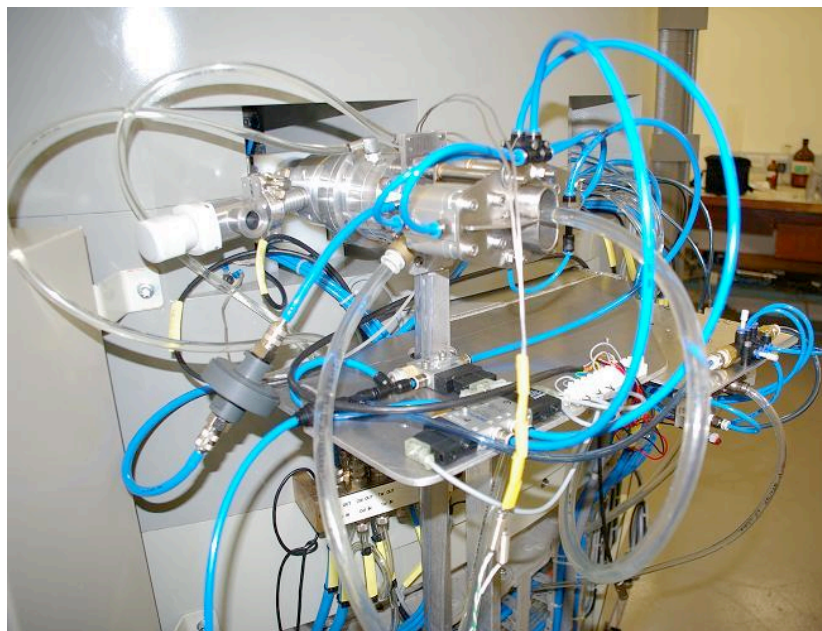


Fig.3. Picture of complete working system

REFERENCES:

- ¹Elex Commerce (2002) *COSTIS operating Manual*, Belgrade Yugoslavia.
- ²RA. Fox, (2001) *Australas Phys Eng Sci Med*, **24**:153-159.
- ³SM. Qaim (2003) *Appl Radiat & Isot*, **58**:59-78.

Thermal Modeling of an ^{124}I Solid Cyclotron Target

K. Gagnon^{1*}, M.A. Avila-Rodriguez³, and S.A. McQuarrie²

¹ Department of Physics, University of Alberta, Edmonton, Canada

² Faculty of Medicine and Dentistry, University of Alberta, Edmonton, Canada

³ Turku PET Centre, Turku, Finland

* Corresponding author: 11560 University Ave, Edmonton, AB, Canada T6G 1Z2, kgagnon@phys.ualberta.ca

Aim: With an increased interest in producing non-traditional PET isotopes, caution must be employed to minimize the exposure received by personnel upon the recovery of cyclotron irradiated solid target materials. To this end, a solid target design has been proposed whereby the target's water cooling is indirectly coupled to the target material support plate through means of a cooling finger. Through use of a remote air-actuated mechanism, this design allows for the shielded release of the target material/support plate without the need for breaking either the vacuum or water seal. As possible imperfections in the contact of the cooling finger and support plate bring concerns regarding the thermal stability of the target with the potential for volatilization of the ^{124}I product or enriched $[^{124}\text{Te}]\text{Al}_2\text{Te}_3$ substrate, the goal of this study is to investigate the cooling performance of the proposed target design.

Methods: COMSOL Multiphysics[®] version 3.3 was used to model the thermal performance of the target resulting from incomplete contact of an aluminum cooling finger and platinum support plate. With the geometry of the setup defined in Figure 1, the thickness, extent, and position of the simulated region(s) of incomplete contact were varied and taken as being either air or thermal compound. As the optimal proton beam energy degradation for minimizing the contamination of ^{123}I through the $^{124}\text{Te}(p,2n)$ reaction pathway is given as $13 \rightarrow 9$ MeV [1], the incident beam power density was taken as 1.5×10^6 W/m² (corresponding to 20 μA of 13 MeV protons). The steady-state general heat transfer application of the heat transfer module [2] was used to model the conductive and convective heat transfer while the flow of the cooling water was modeled using the momentum balance k - ε turbulence application of the chemical engineering module [3]. Although boundary conditions and heat transfer coefficients were primarily selected as defined by the COMSOL Multiphysics[®] environment, the heat transfer coefficient for the water-aluminum interface was independently defined using the Dittus-Boelter heat transfer correlation [4] for a flow velocity of 2 m/s.

Results and Conclusions: Results of modeling a region of incomplete contact as an air gap showed that the extent of the air gap along the cold finger/support plate interface has a larger effect on the temperature distribution than the thickness of the air gap. Although thermal compound was found to decrease the maximum temperature of the target plate, results suggest that cooling without the thermal compound may possibly prove adequate given reasonable contact between the two interfaces. Further introduction of helium cooling on the top surface of the target into the model, along with experiments using thermal compound are essential for ensuring that ^{124}I yields are not compromised as a result of volatilization.

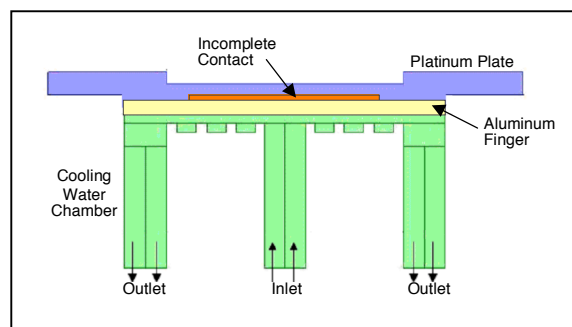


Figure 1: Geometry of this study showing the four essential subdomains of the model.

[1] B. Scholten, *et al.*, Excitation functions of $^{124}\text{Te}(p,xn)^{124,123}\text{I}$ reactions from 6 to 31 MeV with special reference to the production of ^{124}I at a small cyclotron, *Appl. Rad. Isot.*, **46**, 255-259 (2005)

[2] COMSOL Multiphysics, *Heat Transfer Module User's Guide*, Version 3.2, Comsol (2005)

[3] COMSOL Multiphysics, *Chemical Engineering Module User's Guide*, Version 3.2, Comsol (2005)

[4] F. McQuiston, *Heating, ventilating and air conditioning: analysis and design*, 4th Edition, Wiley, New York (1994)

Multi Purpose Solid Target System for a MC 17 Scanditronix Cyclotron Pneumatic Manoeuvrable for Low Personnel Doses

Jonathan Siikanen¹, Tomas Ohlsson² and Anders Sandell²

¹University of Lund, Department of Medical Radiation Physics, ²Lund University Hospital, Sweden

Aim

New labelling techniques for metal radionuclides (1) have been developed meanwhile target systems for metal radionuclide production are poorly developed for MC 17 Scanditronix cyclotron with a wide beam. This project's goal was to design a flexible target system for different solid materials in the form of foils, bricks or sputtered targets. The goal is to design a target system that benefits from the full beam capacity and energy of MC 17 Scanditronix (50 μ A and 17 MeV protons). Furthermore the system needs to be remotely manoeuvrable to avoid unnecessary personnel dose.

The trend of more micro PET dedicated for small animals opens the field for non-conventional radionuclides for pre clinical studies. The introduction of positron emitting isotopes with longer half life (in the proximity of days) allows immuno-PET, i.e. the combination of PET and monoclonal antibodies (mAbS). An interesting metallic PET radionuclide is ⁸⁹Zr (2, 3, 4, 5, 6, 7) ($E_{\beta\text{max}}=897$ KeV, $I_{\beta+}=0,227$) with a 3.27 day half life which makes it compatible with immuno-PET and also possible to distribute over large distances from the production site.

Methods

The target system is designed for a Scanditronix MC 17 with a 40 mm wide and 10 mm high entrance window for an approximately 35 mm wide and 5 mm high beam. The target foil is water cooled directly to gain cooling efficiency. The mounting and dismounting of the target material onto the cyclotron's beam extraction position is controlled by a pneumatic cylinder and a vacuum technique.

The target consists of an alumina hood which is mounted with stays to a pneumatic cylinder and an alumina frame which is attached to the cylinder's piston. Before irradiation a foil is mounted to the frame by applying vacuum to the cooling water line. The vacuum makes the frame act as a vacuum cleaner and thereby attaches the foil. The foil is then pushed against the 40x10 mm beam entrance hole in the hood with the cylinder piston. Between the foil and the frame an O-ring is used to seal the cooling water cavity. Before irradiation starts the vacuum is cut and the line is switched to a water line. During irradiation the cylinder is always activated to pressure the foil against the wall. After irradiation the water line is switched to a vacuum line, the cylinder is activated the opposite way and the foil can be dropped directly to a lead container by cutting the vacuum line.

A simple prototype was constructed for testing of water flow, water pressure and force needed to get a tight system. The cooling water cavity behind target material is 40 mm wide, 10 mm high and 1.5 mm deep (0.6 ml). Target foils must have the same dimensions as the outer frame dimensions (50x20 mm) leaving an frame size of 5 mm for the tightening with an O-ring (2.4 mm O.D) in an O-ring track.

The water flow was calculated to 3 l/min. The small 1.5 mm depth led to a water pressure of approximately 3 bars. The prototype indicated a tight system at 25 kg pressure so a pneumatic cylinder with 50 kg capacity was used. The crucial point with this target design is the tightening between foil, O-ring and the frame. In a first attempt, testing with alumina bricks and irradiation of yttrium foils was investigated.

Results

Production results and target testing will be presented at the conference.

References

1. Verel, I., et al., *⁸⁹Zr immuno-PET: comprehensive procedures for the production of ⁸⁹Zr-labeled monoclonal antibodies*. J Nucl Med, 2003. **44**(8): p. 1271-81.
2. Kalman Shure, M.D., *Radiations from Zr-89* Physical Review, 1951. **82**(1): p. 122-122.
3. Saha G.B., Porile N.T and Yafee L. Sa"(p, xn) and (p, pxn) Reactions of Yttrium-89 with 5-85-MeV Protons" Phys. Rev 1966, **144** p 144
4. Mustafa, M. G., et al. "Measurements and a direct-reaction-plus-Hauser-Feshbach analysis of ⁸⁹Y(p,n)⁸⁹Zr, ⁸⁹Y(p,2n)⁸⁸Zr, and ⁸⁹Y(p,pn)⁸⁸Y reactions up to 40 MeV." Physical review (1988).
5. Dejesus O.T, Nickles R.J, *Production and Purification of ⁸⁹Zr, a Potential PET Antibody Label*. Appl. Radiat. Isot., 1990. **41**(8): p. 789-790.
6. J. Zweit, S.D., H.L. Sharma, *Production of No-carrier added Zirconium-89 for Positron Emission Tomography*. Appl. Radiat. Isot., 1991. **42**(2): p. 199-201.
7. Wilma E. Meijs, J.D.M.H., Hiddie J. Haisma, et al. *issn Production of Highly Pure No-carrier Added ⁸⁹Zr for the Labelling of Antibodies with a Positron Emitter*. Appl. Radiat. Isot., 1994. **45**(12): p. 1143-1147.

Corresponding author: Jonathan.Siikanen@med.lu.se

Investigation of Failure Mechanisms in Niobium-Encapsulated Gallium Targets for the Production of Germanium-68 Radioisotope

Hong T. Bach, Thomas N. Claytor, Michael A. Connors, James F. Hunter, Francois M. Nortier, Donna M. Smith, and Frank O. Valdez
MS C914, Los Alamos National Laboratory, Los Alamos, NM 87545

John W. Lenz
John W. Lenz & Associates, 412 Muskingum Road, Waxahachie, TX 751653

Chuck Moddrell and Paul A. Smith
P.A. Smith Concepts & Designs, 1475 Central Ave. Suite 250, Los Alamos, NM 875443

An analysis of the Nb-encapsulated Ga target failures at Los Alamos National Laboratory Isotope Production Facility since 2005 reveals no underlying cause for target failures. Targets have failed from different lots of Nb and Ga starting materials, at different irradiation current levels, during different irradiation periods (both short and long), and at different levels of beam cycling. We hypothesize that the target failure mechanism is a complex process controlled by a variety of factors. A few of these are listed below:

- Microstructure and defects in the Nb window or weld joints due to material or fabrication deficiencies.
- Liquid Ga embrittlement of the Nb window due to Ga diffusion into the Nb grain boundaries, corrosion by Ga, or formation of Ga-Nb alloy.
- Residual stress in the Nb window or welds.
- Work hardening of the Nb window due to mechanical pulsation and thermal cycling.
- Internal over pressure due to trapped gas expansion or boiling of Ga.
- Erosion of the Nb window due to mechanical interaction with the pulsed beam and turbulent cooling water.
- Radiation damage to the Nb window.

Our data show that the predominant failure mode is the formation of pinholes or cracks on the Nb windows. Understanding this failure mode is the first step toward improving the Nb capsule integrity. Payoffs include improvements in system reliability and radioisotope production rate, thus increase in financial benefits, decreased clean-up cost, and reduced risks of exposing maintenance personnel to radioactive contaminated cooling water and equipment. The goals of this study are to understand the failure mechanism of the Nb-encapsulated Ga targets and to develop suitable materials or fabrication techniques to improve target capsule integrity and reduce target failure rate.

Firstly, the microstructure of material is usually a key factor in its technological applications as it determines a wide variety of properties including mechanical strength, toughness, corrosion resistance and hardness. Furthermore, structural changes may take place during prolonged exposure to irradiation and high temperature. Therefore, an understanding of the structural integrity of targets before, during, and after irradiation is crucial. However, structural analysis of a failed target which has a very high radioactive

contamination level and dose rate is difficult and costly. In-situ monitoring or assessment of targets during irradiation with beams is costly to be implemented. Therefore, knowledge of the structural integrity of a target before irradiation plays an important role in that when a breach occurs, the location of the breach can be compared with the initial data to determine if there is a structural integrity issue in play.

Our initial study indicates a non-uniform Ga/Nb wetting, grain size/structure variation and some inclusions in Nb metals, and also the presence of voids in the Ga material. To obtain this information we used ultrasonic imaging and digital radiography techniques, each of which defined a different property of the target. Knowledge of initial target structural integrity will allow us to locate the failure location and this would potentially define the failure mechanism, which would then aid in defining additional studies and/or fabrication corrections. The most recent failed target data show a correlation of the breach location with the Ga wetting and voids/defects in the Nb rear window.

Additionally, thermal cycling as a result of beam trips may cause thermally induced stress given the low melting and freezing point of Ga. The questions we are looking to answer are: Is the degree of Ga/Nb wetting increasing with temperature? At what temperature will Ga start to form an alloy with this Nb? Are there any cracks or pinholes developed during aging by thermal cycling? What Nb grain size/structure are undesirable from the standpoint of thermal cycling? Understanding of the temperature and thermal cycling effects in combination with structural integrity of the target would give additional insight into the mechanism for failure and would indicate if there exists a fundamental problem with this target material and/or the fabrication scheme. We used digital radiography to detect and monitor voids in Ga during heating (~ 35°C) and cooling (ice temperature). Real-time data indicated that most of the voids in Ga had migrated to the top during heating and disappeared during cooling. Re-heating of the target to 35°C did not bring the voids in Ga back. Experiment for thermal cycling this target to higher temperatures is under way.

Finally, irradiation conditions can affect structural integrity of the target. Currently we do not have the capability to perform in-situ monitoring or assessment of targets when they are in beam. Instead, we occasionally pull targets during an irradiation and visually examine them. The visual examination is only qualitative and in some failed targets the breach size and location are not detectable. The capability of non-destructive assay of targets during irradiation would provide information on structural changes that occur as a result of irradiation. The ability to pull targets during irradiation and perform non-destructive analysis on them not only would allow for the determination of irradiation effects on structure integrity, but might also allow us to indentify the nature, location and size of flaws/micro cracks before they become critical, reducing the potential losses due to a catastrophic failure: loss of target material and beam time, and unplanned shutdown and maintenance. This technology could be applied to other targets resulting in considerable costs savings both in downtime and clean-up.

Efficient Separation of ^{64}Cu from ^{67}Ga Waste Product with Solvent Extraction and Chromatography : Co-production of ^{64}Cu and ^{67}Ga

K.S. Chun, H. Park and J.H.Kim

Department of Radiopharmaceutical, Korea Institute of Radiological and Medical Sciences(KIRAMS), 215-4, Gongneung-Dong, Nowon-Gu, Seoul, Korea, 139-706

AIMS: ^{64}Cu is one of the most useful and versatile radio-copper radionuclide in the nuclear medicine owing to its multiple decay scheme, which involve electron capture (41%), β^- (40%) and β^+ (19%) decays, and has an intermediate half-life for radiopharmaceutical synthesis of many compounds^[1]. These properties make its radiopharmaceuticals useful for PET imaging of tumors and targeted radiotherapy labeled on small compounds and monoclonal antibody^{[2][3]}. Several production methods using $^{64}\text{Ni}(p,n)^{64}\text{Cu}$, $^{64}\text{Ni}(d,2n)^{64}\text{Cu}$, and $^{68}\text{Zn}(p,\alpha n)^{64}\text{Cu}$ ^[4] have been reported. Among them, $^{68}\text{Zn}(p,\alpha n)^{64}\text{Cu}$ nuclear reaction is the most economical although its production yield is lower than other reaction because ^{64}Cu can be separated from ^{67}Ga waste product by solvent extraction using 0.01% dithizone in $\text{CCl}_4\text{-HCl}$ and anion exchange resin(AG1-x8) supplied by BioRad.

METHODS: All reagents used for production were of analytical grade. Enriched ^{68}Zn (isotopic purity 98%) was purchased from Isoflex, Russia. ^{67}Ga waste product was collected from ^{68}Zn recovery system eluting 2N HCl on anion resin column. The gamma-ray spectrum and the radioactivity of radioisotopes in ^{67}Ga waste product was obtained with HPGe detector coupled with MCA(ORTEC EG&G) and calculated with the comparison of NIST reference source. For solvent extraction of ^{64}Cu from ^{67}Ga waste product, pH was adjusted to 3 with c-NaOH and DM water was added to adjust to the normality of ^{67}Ga waste to 2N. Solvent extraction was performed twice with 0.01% dithizone in CCl_4 . ^{64}Cu separated with organic phase was back extracted to aqueous phase with 7N HCl and anion resin(AG1-x8) was applied for purification of final ^{64}Cu solution.

RESULTS and CONCLUSION: The radionuclides in ^{67}Ga waste product obtained from ^{68}Zn recovery system were ^{64}Cu , ^{67}Cu , ^{67}Ga , ^{57}Ni , $^{55,57}\text{Co}$ and the radioactivities of ^{64}Cu and ^{67}Cu were 1,200mCi and 6mCi at EOB, respectively. The total processing time and the separation yield of Cu nuclides from Ga product waste with solvent extraction

using 0.01% dithizone in CCl₄ and anion resin(AG1-x8) were about 2hrs and higher than 90%, respectively.

[1] P. J. Blower, J. S. Lewis, and J. Zweit, Copper Radionuclides and Radiopharmaceuticals in Nuclear Medicine, Nucl. Med. Bio. Vol. 23, p.957, 1996

[2] S.V. Smith, Molecular Imaging with Copper-64, J. Inorganic Biochemistry, vol. 98, p.1874, 2004

[3] W. Cai, K. Chen, L. He, Q. Cao, A. Koong, and X. Chen, Quantitative PET of EGFR Expression in Xenograft-bearing Mice Using ⁶⁴Cu-labeled Cetuximab, a Chimeric anti-EGFR Monoclonal Antibody, Eur J Nucl Med Mol Imaging vol.34, p.850, 2007

[4] S. V. Smith, D. J. Waters and N. D. Bartolo, Separation of ⁶⁴Cu from ⁶⁷Ga Waste Products Using Anion Exchange and Low Acid Aqueous/Organic Mixtures, Radiochimica Acta Vol. 75, p. 65, 1996

Development of Tandem Targets for a Vertical Beam Target Station

G. F. Steyn¹, C. Vermeulen¹, E. Isaacs¹, S. DeWindt¹, D. Saal¹, H. P. Burger², C. van Rooyen², F. C. de Beer³, H. Knox⁴ and J. Isobe⁵

¹ iThemba LABS, P. O. Box 722, Somerset West 7129, South Africa

² National Laser Centre, CSIR, P. O. Box 395, Pretoria, 0001, South Africa

³ Nuclear Technology Division, Necsa, P. O. Box 582, Pretoria, 0001, South Africa

⁴ EB Welding CC, Pelindaba, P. O. Box 582, Pretoria, 0001, South Africa

⁵ MDS Nordion, 4004 Esbrook Mall, Vancouver, BC, Canada V6T 2A3

Aims

Two kinds of tandem targetry are currently in routine use on the Vertical Beam Target Station (VBTS) at iThemba LABS. A Mg/Ga tandem target was developed for the simultaneous production of ²²Na/⁶⁸Ge and a Rb/Ga tandem target for the simultaneous production of ⁸²Sr/⁶⁸Ge. These targets have to withstand prolonged bombardments with a beam of 66 MeV protons and a beam current of 250 μ A. The integrity of targets under these harsh bombardment conditions is essential, therefore methods of non-destructive evaluation of target capsules were investigated.

Methods

All target materials are natural (*i.e.* not enriched). The Mg and Ga are encapsulated in Nb and the Rb in stainless steel. Both Ga and Rb are metals with a low melting point, near room temperature (Ga: 29.8°C; Rb 38.9°C) thus they are always in a liquid state during bombardment. In contrast, the encapsulation metals have relatively high melting points (Nb: 2468 °C; SS: nominally 1375 °C for the grade used) to effectively contain the target material and to provide a barrier between the target material and the fast-flowing cooling water. Ga and Rb have other favourable properties for targetry: In contrast to their melting points, their boiling points are relatively high (Ga: 2403 °C; Rb: 686 °C). Their volume changes during solid to liquid phase transitions are minimal (Ga: -1.094%; Rb: +1.038%), thus the capsules can be filled completely without risk of stress-induced failure, a well-known phenomenon when using salts of these metals as target materials. Since the heat transfer between the liquid metal target material and capsule walls is excellent, these targets are expected to withstand prolonged bombardments with high intensity proton beams.

In the case of Mg, encapsulation with an inert metal is essential (even though Mg has a relatively high melting point of 648.8 °C) as open Mg at elevated temperatures reacts with the cooling water and loses mass.

Figure 1 shows a photograph of the tandem targets as one would see them when removed from their respective target holders. The beam is stopped in the second target. With a 66 MeV proton beam of 250 μ A intensity, 16.5 kW is deposited in only a few cubic cm of material and the available surface to cool from is very limited. Water cooling is provided in a 4π geometry in the form of 1 mm thick layers flowing over the major outer surfaces of the capsules, with a linear velocity of 30 to 35 m/s. The relatively high flow rate, at a pressure of 10 bar, is required to obtain a sufficient forced convection heat-transfer coefficient and to suppress surface boiling. (Note that the formation of a steam layer on a target surface can lead to the heat flux becoming critical, leading to sudden and catastrophic target failure.)

Figure 2 shows the relevant excitation functions (taken from EXFOR compilations) and production energy windows. Not all the energy from the beam is available for radionuclide production as the target-holder entrance window, capsule walls and cooling water all constitute “dead” layers. A smaller energy window for ⁶⁸Ge production in the Rb/Ga target was selected in order to maximize the ⁸²Sr yield.

The individual components of the capsules are pressed from sheet metal (of 0.5 mm thickness) and/or machined at iThemba LABS. The welding of the capsules for the Rb targets is done by the National Laser

Centre (NLC) of the CSIR in Pretoria [1], using state-of-the-art Nd:YAG-laser based welding equipment in combination with an advanced robotic positioning system. Note that a very high demand is placed on the integrity of the welded joints, which should be defect-free and of a uniform weld bead geometry. That quality was only achieved once the CSIR was consulted. Empty capsules are shipped to MDS Nordion in Vancouver, Canada, for filling with the Rb metal, then shipped back to iThemba LABS, ready for bombardment. Note that these capsules are provided with Swagelok fittings (having screw-on caps) through which the highly reactive Rb metal is injected in an inert argon atmosphere.

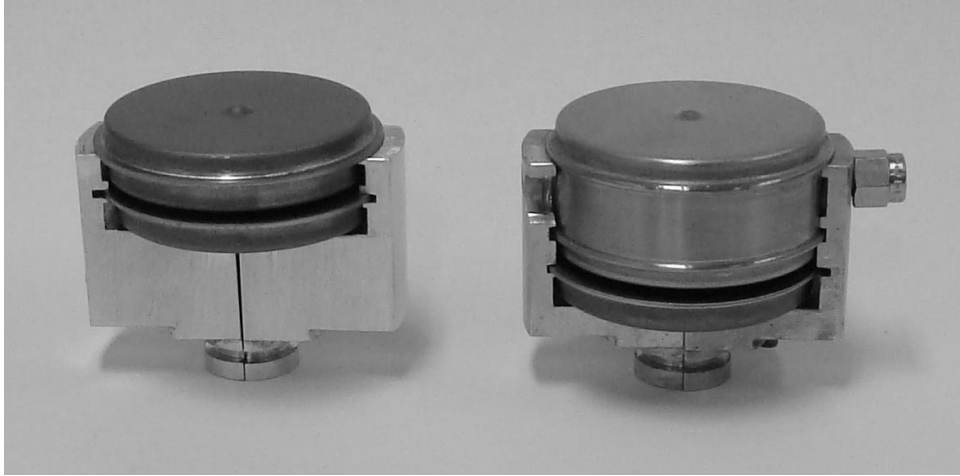


Figure 1: LEFT: Encapsulated Mg/Ga targets for the simultaneous production of $^{22}\text{Na}/^{68}\text{Ge}$ in the VBTS. RIGHT: Encapsulated Rb/Ga targets for the simultaneous production of $^{82}\text{Sr}/^{68}\text{Ge}$ in the VBTS. Note that these “inner assemblies” have been removed from their respective target holders. The beam direction is vertical and downwards. The inner diameter of the capsules is 40 mm.

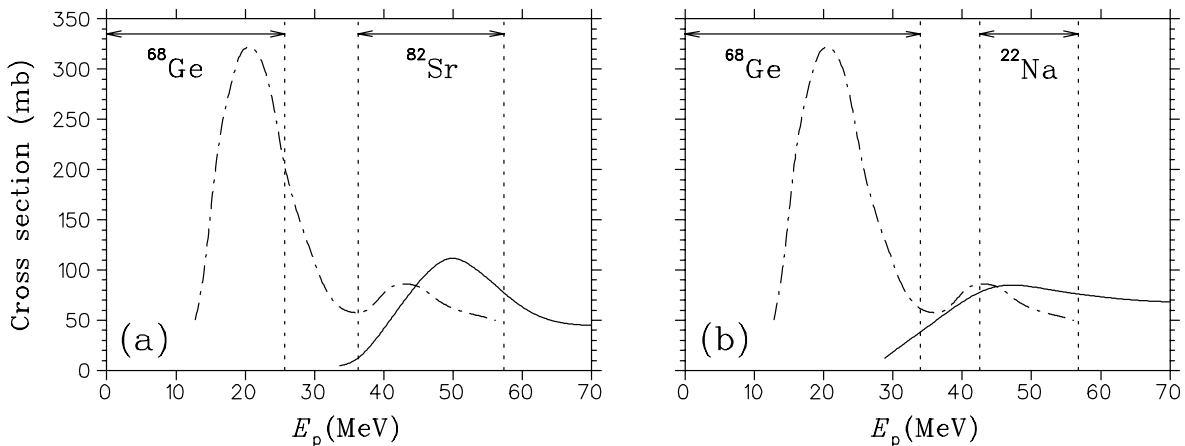


Figure 2: Excitation functions (a) for the production of ^{68}Ge and ^{82}Sr and (b) for the production of ^{68}Ge and ^{22}Na . The production energy windows as implemented for VBTS targetry are indicated by the arrows.

For the manufacture of the capsules for the Mg and Ga targets, other requirements make electron-beam (EB) welding the technology of choice: These capsules are not provided with Swagelok fittings as the target material cannot be introduced at a later stage into “empty” capsules. Instead, the target material is sealed into the capsule at the time it is welded together. Since EB welding is done in vacuum, air from the atmosphere is effectively removed from the capsule. This is important, as trapped air can expand when targets reach elevated temperatures during bombardment, which can lead to pressure-induced capsule rupture. The EB welding of capsules for iThemba LABS is done by EB Welding CC, Pelindaba.

Both x-ray and neutron radiography techniques have been investigated for purposes of non-destructive evaluation of the integrity of welded joints on target capsules. While not much success was obtained with x-ray radiography, neutron radiography shows tremendous promise. Figure 3 shows a few results from an evaluation done by means of 3D thermal neutron computed tomography on an empty Rb target capsule, performed by the South African Radiography (SANRAD) facility [2] at the SAFARI-I nuclear reactor, Necsa, Pelindaba. By obtaining images of an object using neutron transmission from many angles, an image can be reconstructed from its various projections. Figure 1 (a) shows such a reconstruction, while (b) and (c) shows various cuts made in the frontal and axial directions, respectively. Slices in the axial, frontal and sagittal directions are shown in (d), (e) and (f), respectively. In this particular study, 247 frontal, 538 axial and 468 sagittal slices were generated, making it possible to investigate the welded seams extensively. In practice, these images can be enlarged to fill an entire computer screen.

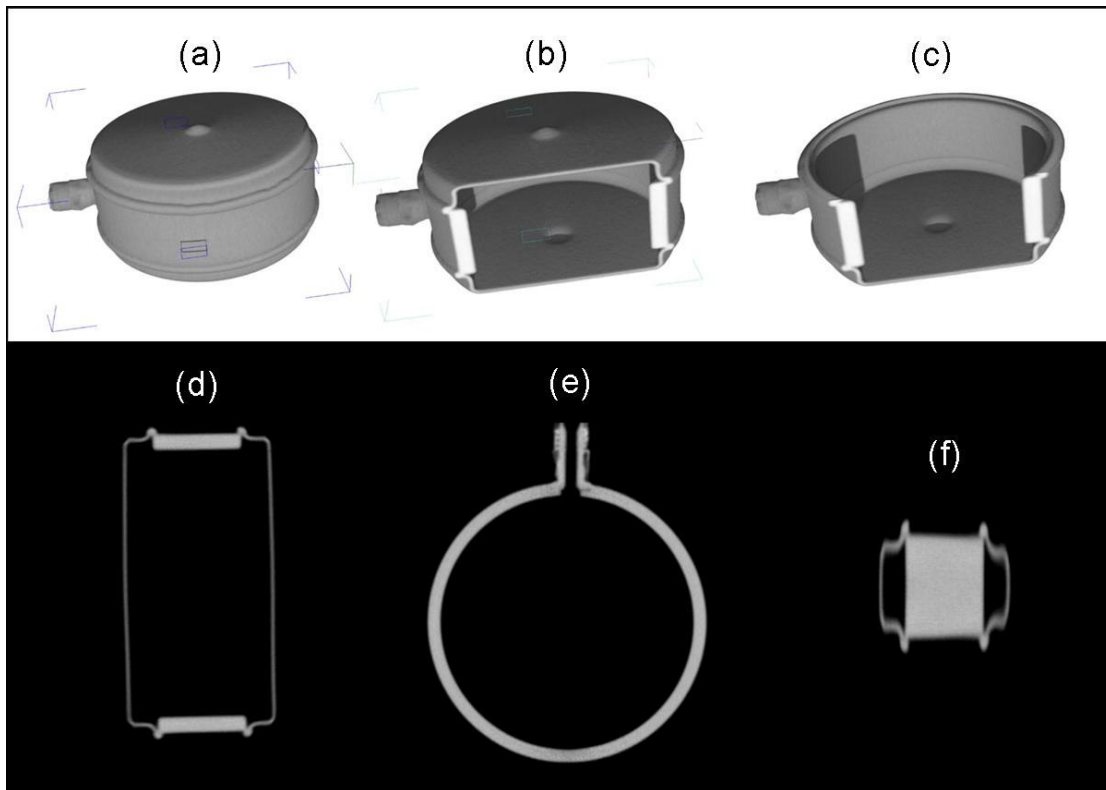


Figure 3: Full reconstructed image (a) and with selected cuts (b and c) of a target capsule, obtained by thermal neutron tomography. Axial, frontal and sagittal cuts are shown in (d), (e) and (f), respectively.

Results and Conclusion

Production rates of nominally 9.3 MBq/ μ Ah (^{82}Sr) and 1.1 MBq/ μ Ah (^{68}Ge) are obtained with the Rb/Ga target, while the values for the Mg/Ga target are 2.9 kBq/ μ Ah (^{22}Na) and 1.7 MBq/ μ Ah (^{68}Ge), respectively. Successful bombardments up to a cumulative charge of 40 000 μ Ah have already been performed.

References

- [1] African Fusion (Ed. J. Warwick), the official magazine of the South African Institute of Welding, Crown Publications, February 2008 edition, p. 31. Available from URL: <http://www.crown.co.za/africanfusion.html>.
- [2] F. C. de Beer. *Nucl. Instrum. and Meth. A* **542** (2005) 1.

A Simple Method for Measuring the Beam Profile of Charged Particle Accelerators

M.A. Avila-Rodriguez, J.S. Wilson, S.A. McQuarrie

Edmonton PET Centre, 11560 University Ave., Edmonton, AB, T6G-1Z2, CANADA

Introduction: Cyclotron production of non-standard PET nuclides such as radiometals and radiohalogens usually involve the irradiation of expensive, isotopically enriched, solid substrates. Accurate assessment of the beam profile to match the target material with the shape of the proton beam is desirable in order to keep the amount of the expensive substrate as low as possible. Other applications where the measurement of the beam profile would be useful are following maintenance service to the cyclotron, change of the stripper foil, beam/target alignment procedures, measurement of beam intensity distribution for modeling and simulations, etc. Beam profiles are commonly measured by an autoradiography technique using either radiographic film or digital radiography with a storage phosphor imaging system. But these techniques require expensive equipment or film development systems that are not available in most cyclotron facilities. The classical “paper burn” technique is useful in beam/target alignment procedures, but is not quantitative. Gafchromic EBT films (International Specialty Products, Wayne, NJ, USA) are colorless, grainless and transparent before exposure to radiation and can be handled and prepared in room light. During exposure the film develops an instantaneous blue color without requiring latent chemical, optical, or thermal development or amplification. The color intensity is a function of the exposure with higher exposures resulting in a progressively darker blue color.

Objectives: Explore the feasibility of using radiochromic films (RCF) as a simple and inexpensive tool to measure and qualitatively and quantitatively analyze the beam profile of charged particle accelerators.

Methods: A thick Cu foil was irradiated with 17.5 MeV protons using a water-cooled 30° slanted target. After allowing one-hour post-irradiation cooling time a piece of RCF

was placed in direct contact to the foil in order to get an autoradiographic image of the proton beam strike. The color development of the RCF was instantaneous when exposed to the irradiated foils and the exposure was stopped when the beam strike was visible on the film (50-70% of the maximum color intensity developed by the film). The exposed RCF were digitalized using a conventional flatbed scanner (256 grey levels, 8-bit, 600 dpi, TIFF format) and analyzed using the software DoseLab version 4.00, which can be freely downloaded at <http://doselab.sourceforge.net/index.html>.

Results: Five minutes of proton irradiation on a thick Cu foil produced ^{65}Zn , ^{62}Zn and ^{63}Zn in approximate ratios of 1:10:10⁵ (EOB), respectively. The RCF illustrated the proton beam strike area when exposed for 30 sec, 30 min, and 60 h; after allowing a post-irradiation cooling time of 1 h (mostly ^{63}Zn activity), 10 h (mostly ^{62}Zn) and 100 h (mostly ^{65}Zn), respectively. The copper plate can be reused allowing 3-4 days of cooling time between irradiations. The graphical user interface of DoseLab facilitates the quantitative analysis of the digitalized images. Spatial calibrations (pixels to distance), beam intensity distributions, isodose curves and iterative profiles are only a few of the applications that can be performed with this software (Fig. 1).

The use of DoseLab is useful when a detailed quantitative analysis of the beam profile is needed or when the 2D distribution of the beam intensity is required. For example, this data can be used as an input source function to simulate, model and optimize the heat transfer process in solid targets, which has aided in the development of our cyclotron targets. The use of RCF for beam/target alignment purposes can be performed by means of a simple visual analysis. The price of an 8"×10" sheet of Gafchromic EBT film is on the order of \$20 CAD, which is enough to get at least 50 beam profiles. In this study only a thick foil of Cu was used, but many other materials could be used with this purpose. These materials include, but are not restricted to, Ti, V, Fe, Cr, Ni, Zn, Y, Zr, Mo, Ru and Ag. Even thin foils (~25 μm) of Cu and Nb irradiated in stack proved to be adequate to get the beam profile. This technique can also be extended to other accelerated particles by choosing the appropriate target material.

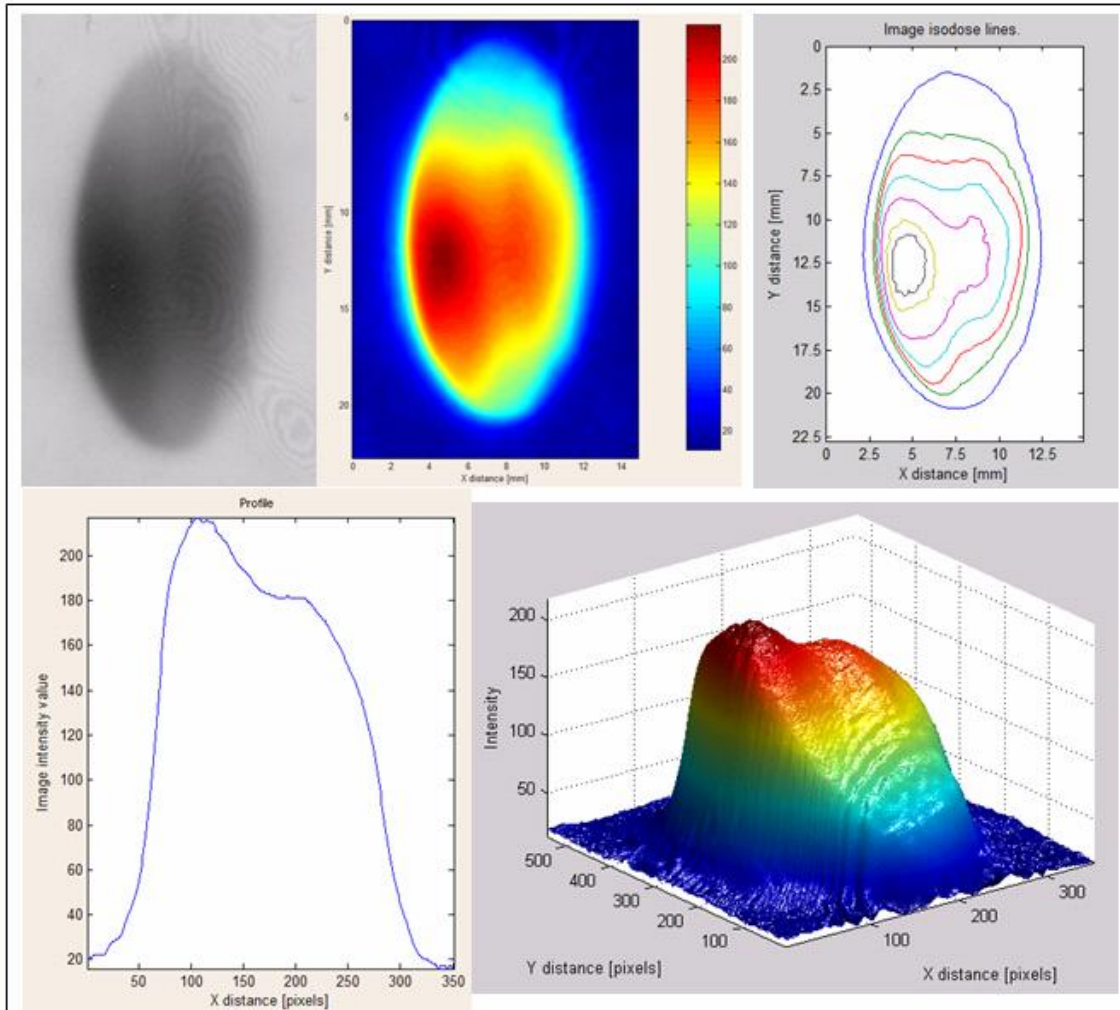


Fig. 1. Beam profile showing a split proton beam due to a damaged stripper foil. This figure shows the scanned image of the RCF (upper left), the correspondent intensity distribution (upper center and bottom right), isodose lines (upper right), and the beam profile along the x-axis (bottom left).

Conclusions: The simplicity, cost effectiveness and high spatial resolution of this method makes RCF very attractive as an accurate tool to perform qualitative and quantitative (intensity distribution) analyzes of the beam profile of charged particle accelerators.

Proton Beam Monitoring via (p,xn) Reactions in Niobium

M.A. Avila-Rodriguez^{1,3}, J.S. Wilson¹, S.A. McQuarrie¹, M.J. Schueller², J.O. Lill³, J. Rajander³, O. Solin³

¹Edmonton PET Centre, 11560 University Ave., Edmonton, AB, T6G-1Z2 CANADA

²Brookhaven National Laboratory, Upton, NY, 11973 USA

³Turku PET Centre, Kiinamyllynkatu 4-8, Turku, 20520 FINLAND

Introduction: Although excitation functions for the $^{93}\text{Nb}(p,xn)$ nuclear processes have been previously measured, there is poor agreement between the existing literature values which are rather old or published only in graphical form. Proton irradiation of Nb in the energy range of biomedical cyclotrons ($10 < E_p < 19$ MeV) produces ^{93m}Mo ($t_{1/2}=6.85$ h), ^{92m}Nb (10.2 h) and ^{89}Zr (78 h), which could be used as monitor reactions if accurate cross section data for these reactions is available.

Objectives: to measure the excitation function of proton induced reactions on Nb nuclei to evaluate their potential as monitor reactions of proton beams in an energy range up to 18 MeV.

Methods: Excitation functions were measured by the standard stacked foil technique using the activation method. A total of five stacks consisting of 4-7 Nb foils, separated by Al foils for energy degradation, were irradiated at different extraction energies (13.7-17.8 MeV) on the TR19/9 cyclotron at the Edmonton PET Centre (EPC). The incident energy and intensity of the proton beam was verified by using a Cu monitor foil in the front of each stack. To test the potential use of the measured excitation functions as monitor reactions, activity ratios of the different activation products were measured at Brookhaven National Laboratory (BNL) on a TR19/9 cyclotron. Irradiations were performed at five different incident energies from 12-19 MeV, as indicated by the extraction-radius to energy relationship. A comparison between Cu and Nb monitor foils was performed at Turku PET Centre (TPC) on the CC18/9 cyclotron. In this case, a stack containing one Nb foil in-between two Cu foils was irradiated and the effective energy of the proton beam at the center of each foil was determined. In all cases the activity of the

different activation products in the foils were assessed by γ -spectroscopy using calibrated HPGe detectors at the respective facilities participating in this study.

Results: Figure 1 shows the excitation functions of the different reactions including literature values. An energy shift of ~ 1.5 MeV in the maximum value of the excitation function was found between the data measured in this work and Levkovskij (1991). The data of Kiselev and Faizrahmanova (1974) showed a considerable discrepancy across a wide range of cross section values. Activity ratios of the different radionuclides produced by 10 min of proton bombardment on Nb are plotted in Fig. 2. This figure includes the activity ratios measured at BNL and TPC, which are in remarkably good agreement with the cross section data measured at EPC. Tables 1 and 2 show a summary of the results for the experiments performed at BNL and TPC. The excellent agreement between the Cu and Nb monitor foils used at TPC validate the use of Nb as monitor foil.

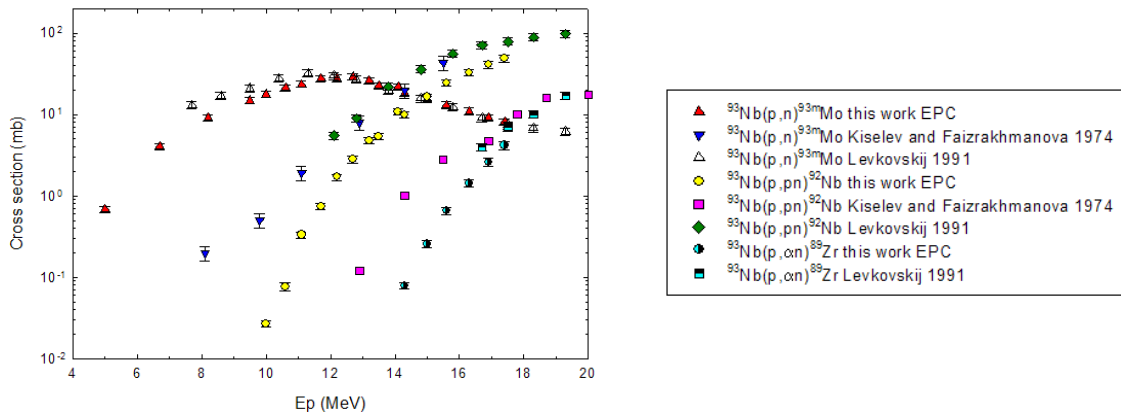


Fig. 1. Excitation functions for the proton induced reactions on Nb nuclei.

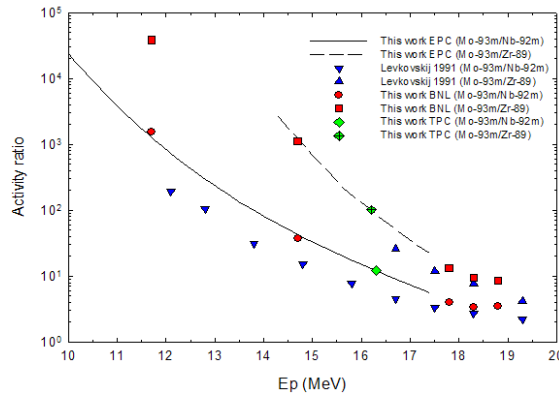


Fig. 2. Activity ratios (10 min of bombardment) of the different proton activated products on Nb.

Table 1. Determination of the mean incident proton energy using Nb as monitor foil.

Mean nominal energy (MeV)	Activity ratios measured at BNL		Determined E (MeV) using EPC data as standard	
	$^{93m}\text{Mo}/^{92m}\text{Nb}$	$^{93m}\text{Mo}/^{89}\text{Zr}$	$^{93m}\text{Mo}/^{92m}\text{Nb}$	$^{93m}\text{Mo}/^{89}\text{Zr}$
11.7	1536.7	38492	11.6±0.2	ND
14.7	36.77	1114.0	14.9±0.02	14.8±0.02
17.8	4.023	13.119	18.0±0.03*	17.8±0.03*
18.3	3.380	9.619	ND	ND
18.8	3.527	8.544	ND	ND

*Determined using linear extrapolation. ND: not determined.

Table 2. Determination of the mean incident proton energy using Cu and Nb as monitor foils.

	Activity ratios measured at TPC			Determined E_0^* (MeV)
	$^{62}\text{Zn}/^{65}\text{Zn}$	$^{93m}\text{Mo}/^{92m}\text{Nb}$	$^{93m}\text{Mo}/^{89}\text{Zr}$	
Front Cu foil	404.4			17.1±0.1
Middle Nb foil		12.22	101.83	16.9±0.1
Back Cu foil	198.5			17.0±0.1

*After energy degradation correction.

Conclusions: The cross section data obtained in this study for the different proton induced reactions in Nb nuclei have been successfully tested and validated for its use as monitor reactions for proton energy measurements in the range from 10 to 18 MeV.

References

B.G.Kiselev and N.R.Faizrahmanova, Reaction cross sections of (p,n), (p,pn) and (p,alpha+n) on 93-Nb, In: 24.Conf.on Nucl.Spectr.and Nucl.Struct.,Kharkov 1974, p.356.

V.N. Levkovskij, Cross-section of medium mass nuclide activation (A=40-100) by medium energy protons and alpha particles (E=10-50 MeV), Inter-Vesi, Moscow 1991.

Decommissioning the Birmingham Nuffield cyclotron

D.B. Mackay¹, N. Berovic², D. Parker²

¹*University of Edinburgh, QMRI, 47 Little France Cres., Edinburgh EH16 4TJ*

²*University of Birmingham, Edgbaston, Birmingham, B15 2TT, UK.*

History

Construction of the Birmingham Nuffield cyclotron started in 1939. It was a 60 inch Lawrence design and was a multi-particle fixed energy machine from 10MeV protons to 40MeV alphas. In the early years it was used as an experimental uranium isotope mass separator by Oliphant. The cyclotron was rebuilt after the war and first beam was produced in approx 1948. The cyclotron had hand-beaten copper dees, plane pole faces and air-cooled main coils. The dees and resonators were mounted on a trolley and could be pulled back out of the magnet.

It ran round the clock for most of its life. From the late 1960's it was a major source of radio-isotopes for The Radiochemical Centre, Amersham. The irradiations were carried out on a variety of internal targets. Sputtering from some of the targets caused contamination of the inside of the cyclotron. In particular the irradiation of magnesium targets and silver targets used in production runs. The cyclotron was finally switched off in 1999. The dose rate of the most active target remnants was still >10mSv/hr in 2002.

Inventory of nuclides

An inventory of the nuclides was produced in 2002 after an extensive programme of measurement using a Ge detector calibrated at multiple energies across the range of interest. An inventory was required as part of the process for obtaining approval for disposing of the active parts of the machine. The complete cyclotron, except for the magnet was sent for disposal to a low level storage facility in Sellafield approx 3 years after final switch-off. The 18,000kg of material fitted into one container provided by BNFL. The total activity in the container was 7GBq.

Results of activity measurement.

The magnet and main coils remain in situ in a secured area designated as 'Accumulation for decay'. The site has been licensed by the Environmental Agency (EA) for storage of waste until it decays. The annual cost of inspection is approx. £1000. The neutrons produced by the cyclotron have scattered through the bulk of the magnet steel and the surrounding vault walls. The total activity of Co-60 was 5GBq in 200 tonnes of magnet steel. This activity is continually monitored to satisfy the requirements of the EA. In February 2008, a repeat measurement was made of Co-60 activity and the results for the distribution of specific activity are shown in figure 1.

The positions of the internal target and deflector are indicated on the figure and the circle shows the pole piece location.

Samples of steel were taken from the median plane at the edges of the yoke. An additional sample was taken from the edge of the pole piece under the internal target position. The highest activities were recovered from the positions nearest the internal target (88 Bq/g) and deflector (47Bq/g). This source does not produce an unacceptably high radiation dose rate in its vicinity because the Co-

⁶⁰Co is distributed throughout the yoke so that there is significant self-shielding. It will require 40 years decay to reach a level of 0.4Bq/g. The storage area is subject to regular EA inspections.

Results a) Magnet steel.

RESULTS FOR Co-60 ACTIVITY OF MAGNET YOKE OF THE NUFFIELD CYCLOTRON ON 08/02/2008

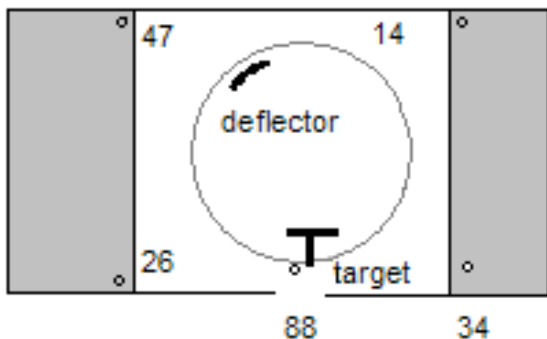
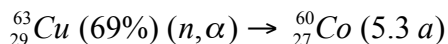


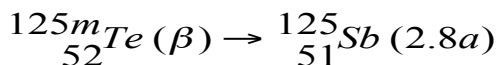
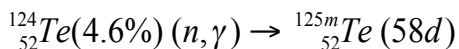
Figure1. Schematic plan of main magnet

Results b) Copper main coil winding.

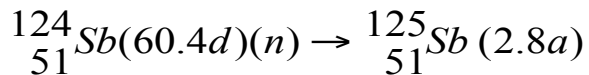
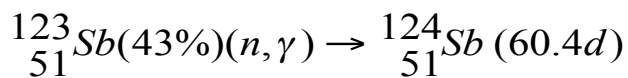
The main activity is due to ⁶⁰Co. It is interesting to note that the neutron irradiation of copper has resulted in significant production of ⁶⁰Co in the windings of the main magnet. As recently as February 2008, the specific activity of the copper due to ⁶⁰Co was 0.21 Bq/g. The reaction responsible for this activity starts from ⁶³Cu (69% abundance) and the ⁶⁰Co is produced by the reaction



The sample contains traces of other activity. ¹²⁵Sb is an interesting case as it is present with a specific activity of 0.1 Bq/g. We surmise that its origin may be either due to impurity of ¹²⁴Te (abundance 4.6%) which would by (n, γ) reaction produce ^{125m}Te (58d). ^{125m}Te in turn decays into ¹²⁵Sb by beta decay.



Another production route may be via ¹²³Sb (43% abundance) and an (n, γ) reaction into ¹²⁴Sb. If neutrons scattered several times while getting to the coils, they will be slowed down to energies between 4 and 100eV where antimony has several resonances that reach values in excess of 1000 barns. ¹²⁴Sb has a 60.4 day half-life so over its lifetime it captures neutrons to make ¹²⁵Sb.



The windings would be ready for disposal in approx 2 years from the present when the sum of all activities will have dropped below 0.4Bq/g

Results. c) Concrete from block wall.

Nuclide	Activity Bq/g	Half-life (years)
Eu-152	0.024	12.5
Eu-154	0.008	16
Co-60	0.018	5.7

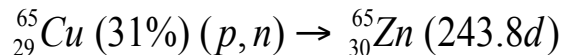
The two europium isotopes have long half-lives so it is just as well that the content is so small, otherwise disposal would present problems.

Guidelines for disposal.

The UK Environmental Agency (EA) will only accept applications to dispose of waste in which the nuclides have been identified and quantified.

BNFL Sellafield will only accept waste that has EA approval and complies with statutory regulations.

Parts of the cyclotron such as the dees had high specific activity due to Zn-65 produced in the reaction.



They were treated as an intrinsic part of the machine and their high activity was averaged over the bulk of the less active material. This procedure cannot be applied to items that are not integral parts of the cyclotron eg radioactive sources.

Conclusions and lessons to be learned.

Keep neutron flux down – high efficiency processes, beam losses low.

Use external not internal targets. Self-shielding using magnet yoke may not be trouble-free.

Locate shielding as close to targets as possible.

Neutron activation of copper, causing accumulation of Co-60 needs to be considered.

Adopt use of sacrificial layers in vaults to simplify decommissioning.

Use materials in construction that are low in impurities that give rise to high activities due to neutron activation.

The University of Birmingham has also disposed of an AVF cyclotron (radial ridge) adapted from the 1939 Cambridge cyclotron design.

These two machines were replaced with a Scanditronix MC40. It is currently used for the production of Rb-81 for medical diagnostics, production of radio-isotopes for PET in engineering and also radio-biology research.

Optimization of the Pulsar 7- a 7MeV linear accelerator

Gimshi Eyal^a, Dr. Alex Tsechanski^a, Dr. Eli Shalom^b

a-The faculty of engineering sciences department of nuclear engineering Ben-Gurion university

b-Isotopia Molecular Imaging, Research & Development department

Abstract

Isotopia M.I (Molecular Imaging) is company which manufactures isotopes for nuclear imaging, located in Israel. The company had recently purchased the AccSys PULSAR -7; a 7MeV mobile Linear Accelerator stationed in Petach-Tikva, Israel. It is a radiofrequency linear proton (H^+) system for PET (Positron Emission Tomography) radionuclide production. The PULSAR® -7 is capable of producing nucleophilic fluorine-18, carbon-11, oxygen-15 and nitrogen-13, but in our system the isotope currently produced is fluorine-18.

The purpose of this project is to increase the yield of the radioisotopes produced since it only provides 70% of its potential.

In order to achieve this goal the first action taken was studying the accelerators components; these are arranged in a straight-linear, elongate fashion and progress through the system from the low energy end to the high energy end. The components are: a H^+ Duoplasmatron Ion Source, a Low Energy Beam Transport (LEBT) system, a Radio Frequency Quadrupole (RFQ) first stage accelerator, a Drift Tube Linac (DTL) second stage accelerator, a High Energy Beam Transport (HEBT), and the Shielded PET radionuclide target system and structure.

The second stage was learning the accelerator operation and maintenance methods in order to ensure the stable and reproducible operation and production of the desired product.

The third stage was analyzing and optimization of the different systems during and after the system operation. This was done using a PC-based control system which records different parameters as the accelerator operates. The purpose of the analysis is to observe the function of each of the components apart in order to receive a better production yield.

For the first evaluation of the Pulsar's production, a total of 60 consecutive runs were observed and analyzed. The results which were gathered in a tabulated manner consisted of the Beam current, which is the average charge per unit time deposited in the target, the bombardment time is the actual time the beam ran for the production of fluorine-18. The yield was calculated via a sensor, located in the ^{18}F reactor inside the synthesis module. For the performance calculations

we used a quantity which allows comparison of all data for consistency of operation as shown in **Table 1**, production rate. Derived from the production of radioactivity:

production rate (mCi/i A)	Sat ¹⁸ F at EOB (mCi)	F18 (mCi)	Saturation (1-e ^{-λt})	Average Current (i A)	Beam time (min)	Run Number	Target
25.76	1947.46	613	0.31	75.6	60	1	1
32.04	2319.47	750	0.32	72.4	62	2	1
31.09	2319.47	750	0.32	74.6	62	3	1
21.26	1515.67	900	0.59	71.3	143	4	1
14.05	1039.80	450	0.43	74	90	5	1
23.67	1708.87	670	0.39	72.2	79	6	1
23.53	1656.63	440	0.27	70.4	49	7	1
13.20	999.77	319	0.32	75.75	61	8	1
30.62	2446.23	770	0.31	79.9	60	9	1
12.19	940.22	300	0.32	77.1	61	10	1

$$A = n\sigma I(1 - e^{-\lambda t})$$

Table 1

A - production of radioactivity, n - number of target nuclei, σ - the reaction cross section.
I - the beam current, λ - the decay constant, t - the length of bombardment.

The production rate is the saturation yield divided by the beam current:

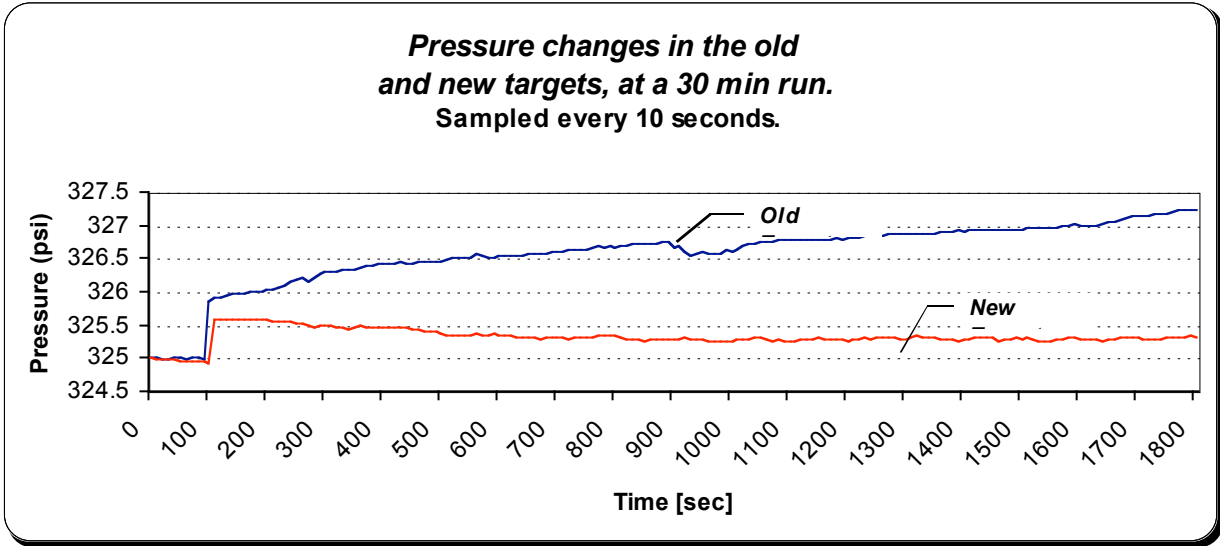
$$\text{Saturation activity} = \frac{\text{Actual yield}}{\text{Saturation factor}} \Rightarrow n\sigma I = \frac{A}{(1 - e^{-\lambda t})}$$

$$\text{Production rate} = \frac{\text{Saturation activity} \left[\frac{mCi}{\mu A} \right]}{\text{Beam current} \left[\frac{\mu A}{\mu A} \right]}$$

The overall average production rate and beam current were used to evaluate a theoretical production curve of ¹⁸F.

The action taken for the improvement was a better cooled target. The new target which was prepared at AccSys laboratories was shipped to Israel. It was mounted on the target system and the data was obtained in the same manner as the old target.

The immediate results showed in **Scheme 1** a better pressure holding target, as the pressure in the target was stable instead of arising. Further data was obtained after 40 consecutive runs using the same analysis methods as for the old target.

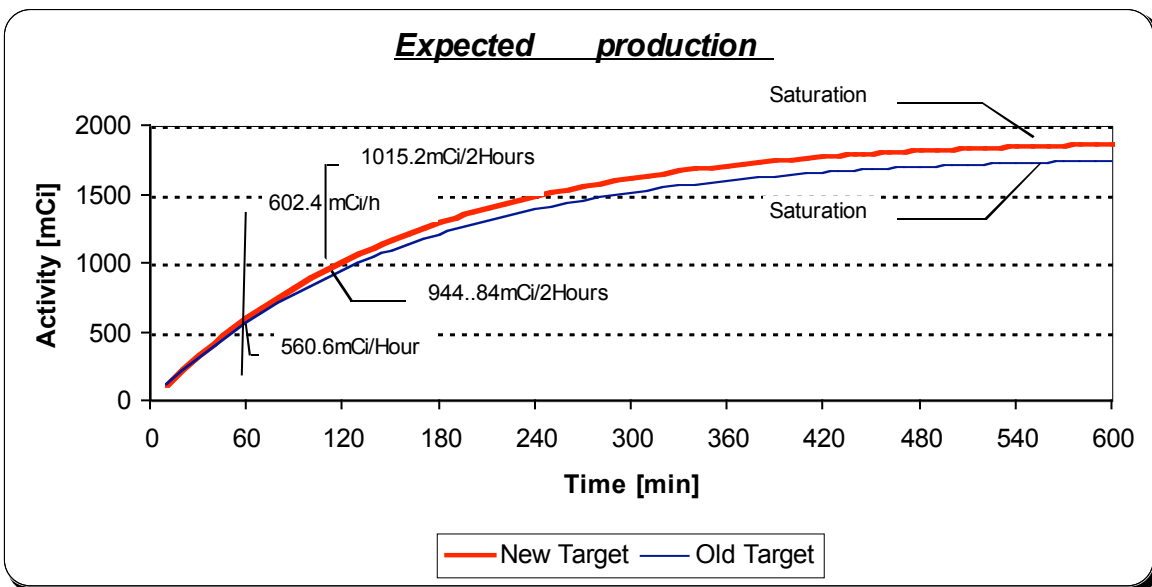


Scheme 1

The production yield was raised in 7% as it shown in **scheme 2**. We think that a better cooling system on the target reduce the possibility of air bubbles created from the beam on the enriched water target $H_2^{18}O$.

Further work still has to be done in order to increase the yield and efficiency of the Pulsar. Some actions which are recommended to be tested could be the alignment of the beam, changing the target cooling system and using thicker target window (a larger cross section at 5 MeV than 6 MeV). Increasing the pressure on the target by changing the grid will decrease the possibility of creating air bubbles.

Keywords: Proton, Linear accelerator, Duoplasmatron, RFQ, DTL, fluorine-18.



Raclopride synthesis conducted on a microfluidic chip

S. Haroun, T. J. Ruth and Paul C.H. Li

Department of Chemistry, Simon Fraser University, Burnaby, BC, V5A1S6, Canada

The use of microreactor chips, which can increase the reaction efficiency and reduce the operation costs of conventional chemical experiments, has become a very popular option over the recent decade. In this research we explore the synthesis of an unlabeled probe, raclopride, which is used for medical Positron Emission Tomography (PET) scans. Reaction conditions including temperature and time for this synthesis were optimized. Through this the efficiency of the synthesis process was improved by reducing side products. Furthermore, through the manipulation of gas-liquid and liquid-liquid interactions in various microreactor chips an efficient mixing technique for the reactants was determined. The reactant fluids' viscosities were carefully considered when determining the flow rate of the liquid reactants; whereas the flow rate of the gas-liquid reactants was considered in order to control the surface area of mixing. These findings will be discussed along with the next phase of the project where the radiolabeled probe is synthesized.

Synthera: A versatile platform for Nucleophilic Substitution Labeling Reactions

Alexander Schmitz, Ph.D. and Richard Freifelder, Ph.D.

Dept. of Radiology, University of Pennsylvania

Introduction:

In the clinical environment, FDG accounts for the vast majority of clinical PET (Positron Emission Tomography) radio-pharmaceuticals. However, when one considers the research side of PET the pallet of options open to the researcher is much, much broader than FDG. ^{11}C compounds are of great interest to researchers today in spite of its somewhat short, 20 minute, half-life. Methyl iodide, methyl acetate, methyl triflate, and hydrogen cyanide are common starting forms for labeling ^{11}C compounds. ^{18}F compounds, both as F^- and F_2 are also of interest and can be advantageous to work with because of the longer 109.8 minute half-life.

Regulatory involvement is making flexibility in the radio-pharmacy production area harder and harder. This is especially true for radio-labeled compounds for human use and there have been a number of groups that have approached human use compounding using different methodologies. Home made synthesis units are still quite often used because they can be put together in a flexible manner and on a quick time scale. Some radiochemistry groups dedicate a single synthesis unit to a single compound (often in a single hot cell). Those units can still be home made or can be quite compact (i.e. micro-fluidic devices such as offered by Advion) There are also a number of commercial units now available that claim the ability to manufacture multiple compounds with only modest changes in the kits and chemicals (Bioscan, IBA-Molecular, GE, etc.). Finally, modular chemistry units that provide complete flexibility are now available (Eckert and Zeigler).

At the University of Pennsylvania we have concentrated some of our efforts on one specific platform, Synthera from IBA-Molecular, for ^{18}F nucleophilic substitution compounds. In collaboration with IBA-Molecular we have been using the Synthera synthesis unit for a number of ^{18}F compounds with very positive results. This solution was chosen for a number of reasons. The Synthera format is quite small easily fitting into a small, mini-hot cell. It is a single or "1-pot" system using pre-sterilized cassettes and pre-packaged reagent kits for FDG synthesis. By simply changing a few chemicals and running a different control script, the platform allows us to manufacture a range of pharmaceuticals in a very controlled and reproducible setting. So far we have produced 3 compounds with the unit in the past 6 months of work. We describe that work here.

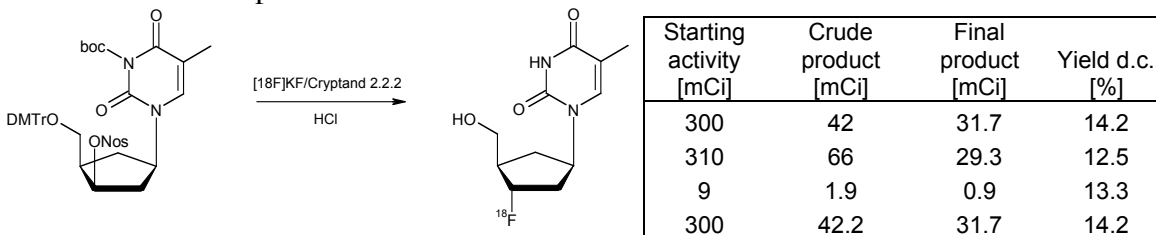
FLT Synthesis:

In contrast to FDG which measures cellular metabolism, fluorothymidine (3'-Deoxy-3'-[^{18}F]fluorothymidine, [^{18}F]FLT) has been reported to measure cellular proliferation and thus is important in measuring growth of cancer cells. Recent clinical studies have also shown it to be a promising tumor therapy response marker for lung and other kind of cancers.

The majority of publications report two different precursors, 5'-O-(4,4'-dimethoxytriphenylmethyl)-2,3'-anhydrothymidine (anhydro-precursor) and (5'-O-DMTr-2'-deoxy-3'-O-nosyl- β -D-threo-pentofuranosyl)-3-N-BOC-thymine (lyxo-precursor). We focused on the latter due to the fact that manually conducted syntheses

with the lyxo-precursor yielded more product than the previously used anhydro-precursor. Typical yields of the manual FLT synthesis are 5-8% (decay corrected) on average.

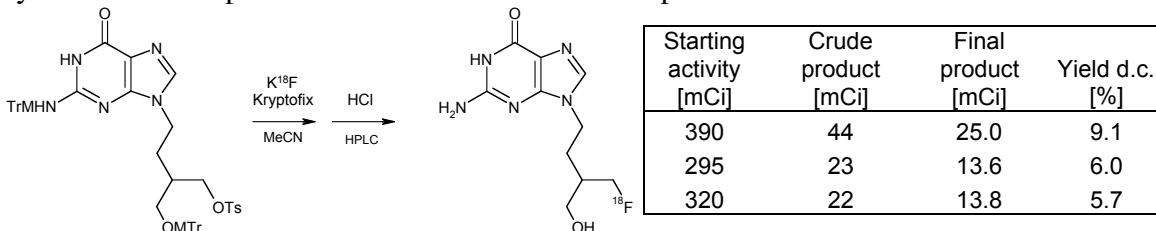
After adapting the manual synthesis to the Synthra synthesis module, scripting the method, which was based on the available FDG method and testing reaction conditions, the FLT method was finalized. This automated synthesis includes delivery of the ^{18}F -target contents into the Synthra box, elution of the trapped $^{18}\text{F}^-$ from the QMA cartridge, removal of all solvents and drying in the reaction vial. Then the dissolved (dry acetonitrile) precursor is added to the dried reaction vessel to perform the labeling step. Work up consists of hydrolysis with HCl, neutralization with a sodium hydroxide solution. The mixture is then passed through an Alumina-N cartridge to remove unreacted $^{18}\text{F}^-$. The crude product is then injected into semi-prep HPLC (Phenomenex C₁₈ Luna, water/EtOH 9:1) for final purification. Overall yield was higher than utilizing the manual synthesis method and specifics of the procedure will be discussed. The chart below shows the experimental results.



FHBG Synthesis:

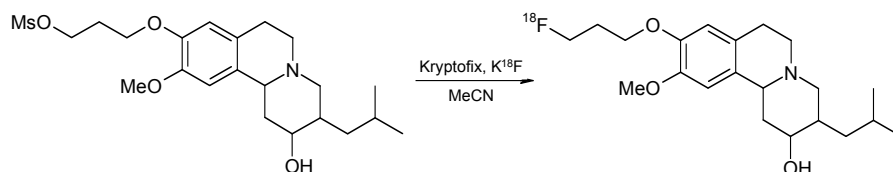
9-(4-[^{18}F]-Fluoro-3-hydroxymethylbutyl)-guanine (^{18}F -FHBG) is an imaging agent for gene therapy using PET. It can be used to measure the magnitude, location and timing of expression of the transgene.

To synthesize ^{18}F -FHBG we used monomethoxytrityl-9-[4-(tosyl)-3-monomethoxytrityl-methylbutyl]-guanine (Tos-FHBG). Typically the manual synthesis yields about 3-5% (decay corrected) ^{18}F -FHBG on average. The synthesis could easily be transferred to the Synthra synthesis unit due to its similarity to the previously conducted FLT synthesis. Aside from the different precursor, this synthesis was designed to be identical to that of ^{18}F -FLT to achieve maximum flexibility of the synthesis unit. Labeling conditions and work-up step are identical to that of the FLT-synthesis and utilize the same Alumina N cartridge and semi-prep HPLC column and solvent. The overall yields were slightly higher than that of the previously done manual syntheses. Conditions of synthesis will be presented and the results of the experiments are:



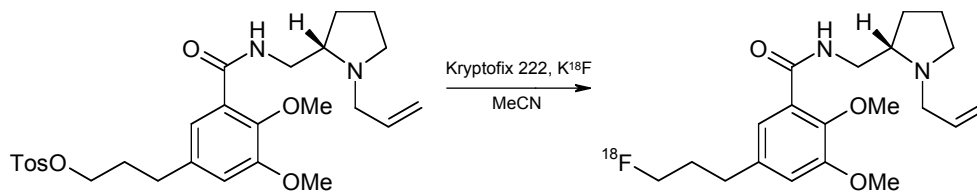
FP-DTBZ:

Dihydrotrabenazine (DTBZ) derivatives, here [^{18}F]-9-Fluoropropyl-9-desmethyl-DTBZ (FP-DTBZ), image the vesicular monoamine transporter 2 in the brain and have demonstrated its usefulness in conjunction with the diagnosis and monitoring of Parkinson's disease and Huntington's disease. ^{18}F -labeled DTBZ can be synthesized via nucleophilic substitution of corresponding mesylate compounds. Currently we use (+/-)-2-Hydroxy-3-isobutyl-9-(3-methanesulfonyloxypropoxy)-10-methoxy-1,2,3,4,6,7 hexahydro-11bH-benzo[a]-quinolizine as precursor in a manual synthesis method to yield the desired ^{18}F labeled compound. Adapting the synthesis to our Synthera module is promising due to the lack of substrates and hydrolysis reagents being added to the reaction. Work up and final purification will be done by semi-prep HPLC and trapping and elution with a Sep-Pak C_{18} cartridge. First synthesis results with Synthera have achieved a 6.5% yield compared to a 5.7% yield by hand synthesis. Experiments will continue.



Fallypride:

^{18}F -Fallypride is a well-known dopamine D2/D3 antagonist and is currently being used as dopamine D2/D3 receptor imaging agent. This has enabled human and non-human brain PET studies using ^{18}F -Fallypride. Radio-synthesis of ^{18}F -Fallypride comprises the nucleophilic substitution of the corresponding tosylate precursor and purification via semi-prep HPLC and C_{18} -Sep-Pak cartridge. The reaction does not require additional substrates beyond the labeling agents and will be adapted to the Synthera box according to the success with our FP-DTBZ experiments.



Summary

Even when the yield is not significantly higher than that of a manual synthesis method, the ability to use pre-sterilized, pre-measured parts and reagents cannot be underestimated. Currently we are able to switch between compounds daily but another advantage of the Synthera unit is its ability to eject the cartridges, which hold the bulk of the remaining activity that does not go to waste. This means that multiple runs per day are easily accomplished. This flexibility allows us to manufacture compounds by nucleophilic substitution simply and easily and allows us to manage beam on target time advantageously. For a center with both an active clinical and research program this is crucial. For the FDA, the Synthera unit fulfills necessary regulatory requirements.

Relatively Inexpensive Platform for Building Automated Chemistry Modules to Synthesize C-11 and F-18 Radiopharmaceuticals

Greg G. Gaehle, Chris Bognar, Jeff Willits, and Robert H. Mach
Mallinckrodt Institute of Radiology, 510 S. Kingshighway, St. Louis Missouri, 63110

Introduction:

While preferred, the cost of commercially available automated chemistry modules can be cost prohibitive in the beginning stages of research. In many cases justifying the cost of a system in excess of \$100,000 to synthesize a radiopharmaceutical potentially 50 times is a barrier that prevents the research from being accomplished or leads to excessive doses to the radiochemist as they synthesize the needed radiopharmaceuticals in a manual remote fashion.

To address this problem, we have developed a relatively inexpensive platform that can be customized to synthesize a large array of radiopharmaceuticals. While we have used this platform to build dedicated systems, we have also demonstrated that a platform is flexible enough to make a variety of radiopharmaceuticals with a single system. Currently, we have used the platform to build dedicated system to synthesize 6-[F-18] fluorodopa (1), 1-[11C] D-Glucose (2, 3), C-11 -6-OH-BTA-1 (PIB) (4, 5), C-11 Palmitate (6). To demonstrate the flexibility of the platform we synthesized C-11 Acetate (7) using the module now dedicated 6-[F-18] fluorodopa. The cost to build a system with HPLC purification is \$12,000US with another \$4,000 needed to complete testing.

Method:

The Chemistry platform is operated using Arcus digital and analog I/O modules connected to a PC through a USB port and controlled by a Visual Basic program. The digital module has 8 digital inputs and outputs, while the analog module provides 8 analog inputs and 2 analog outputs. In theory up to 256 modules can be used providing substantial scalability to the chemistry platform.

The Visual Basic program was designed to prompt the user through the cleaning and setup of the chemistry module, requiring user acknowledgement after each step. All of the steps can be recorded to a production file. The program then proceeds linearly through each step of the synthesis and records the module's action. The interface between the PC running the Arcus modules and the chemistry module components is accomplished through 16 channel isolated field racks. The field rack accept Opto22 modules that can provide a wide range of voltages, both AC and DC, to a large variety of valves, heaters or any other imaginable component that needs power. The same field rack can also accommodate Opto22 input module, to acquire closure signals as feed back from the modules operation. Analog signals from radiation detectors and other device can be accepted directly by the Arcus analog I/O module as long as the signal falls in the range of ± 5 Vdc.

We use 120Vac, 5Vdc, 12Vdc and 24Vdc to power all of the chemistry modules. We chose small din rail mounted power supplies from Omron or Sola to provide 5Vdc, 12Vdc and 24Vdc. This power configuration provides a great deal of flexibility in choosing components used in constructing the chemistry module.

The housing for our most recent modules was chosen based on ease of manufacturing and resistance to the chemical reaction they are performing. For 6-[F-18] fluorodopa and 1-[11C] D-Glucose Delrin® was chosen due to low cost strength and splash resistance to acid.

Valve choice was made based on successful use in the past. We have successfully used valves from NResearch Incorporated, colepalmer, Valco Instruments and Parker Hannifin Corporation.

The bodies of the reactors used with these modules are machined for under \$300US. We currently have reactors for 2ml V-vial, 15ml conical vessel and a 10ml conical vessel. The temperature of all the reactors are controlled with temperature controllers (CAL controls) that can be monitored and controlled with the PC via RS232. The reactor is heated with heat

cartridges (Tempco) and cooled with vortex coolers (Exair). The current temperature range of chemistry platform reactor is 0C to 150C.

Conclusion:

The syntheses performed on our chemistry modules are fully automated while giving the chemist the ability to control, acknowledge and record steps that assures control of drug purity. This minimizes the burden of validating the automation.

The following includes yields of radiopharmaceuticals currently being produce with this chemistry platform. The average yield of 6-[F-18] fluorodopa using this chemistry platform is 20% having a radiochemical purity exceeding 95% and a specific activity greater than 1000mCi/mmol. The average decay corrected yield from $^{11}\text{CO}_2$ of 1-[11C] D-Glucose produced using platform is 7% with radiochemical purity greater than 98%. Using the methoxymethyl protected phenol (MOM) as a precursor we synthesize C-11 PIB with decay corrected yield of 25% from C-11 methyl iodide having a specific activity of 1000-5000Ci/mmol. The yields of C-11 palmitate range from 20 to 40% with a radiochemical purity greater than 95%.

All of the radiosyntheses performed on these modules meet all RDRC and or USP requirements for drug purity. Utilization of these inexpensive modules greatly enhances the flexibility of our production facility to supply numerous radiopharmaceuticals on an as-needed basis, dependent on the demand schedule of other PET tracers at our institution.

References:

1. Moerlein SM, Verrant JA, Bellamy JA, Perlmutter JS, Welch MJ. Optimized clinical production of the PET tracer 6-[F-18]fluorodopa. *Int. Pharm. Abstr.* 1999; 36: 2269.
2. Dence, Carmen S., Powers William J., and Welch Michael J., Improved Synthesis of 1-[11C]D-Glucose. *Appl. Radiat. Isot.* Vol 44, 1993; 971-980.
3. Bender, D and Gee, AD, Solid Phase-Supported Reaction of N.C.A. H11CN with Arabinose: a simplified Automated Synthesis of D-[1-11C] Glucose. *J Label Compd Radiopharm* 1998;XLI:287-300
4. Alan A. Wilson , Armando Garcia1, Alexandra Chestakova, Hank Kung and Sylvain Houle, A rapid one-step radiosynthesis of the *b*-amyloid imaging radiotracer N-methyl-[11C]2- (40-methylaminophenyl)-6-hydroxybenzothiazole ([11C]-6-OH-BTA-1), *J Label Compd Radiopharm* 2004; 47: 679–682
5. Chester A. Mathis, Yanming Wang, Daniel P. Holt, Guo-Feng Huang, Manik L. Debnath, and William E. Klunk, Synthesis and Evaluation of 11C-Labeled 6-Substituted 2-Arylbenzothiazoles as Amyloid Imaging Agents,
6. Welch M.J., Dence C.S. Marshall D.R. and Kilbourn M.R., 1983, *J. Lab. Comp. Radioph.* 20, 1087-1095
7. Robotic preparation of Sodium Acetate C 11 Injection for use in clinical PET *Nuclear Medicine and Biology, Volume 29, Issue 5, July 2002, Pages 613-621*
Stephen M. Moerlein, Gregory G. Gaehle, Michael J. Welch

COMMERCIAL PRODUCTION OF FDG IN FOUR CYCLOTRON FACILITIES SERVING FORTY PET CENTERS

Ayfer Soylu, Harun Küçükmidil

MONROL NUCLEAR PRODUCTS INDUSTRY AND TRADE INC., TURKEY

MONROL Nuclear Company was founded in 1995 in TURKEY for the production and import of radiopharmaceuticals. We are producing Mo-99/Tc-99m generators and kits and preparing Iodine 131 solution/capsules and Thallous-201 Chloride from bulk solutions. We are serving about 150 Nuclear Medicine centers in Turkey and in other countries. All MONROL facilities are performing their production according to GMP and radiation safety rules and are audited by the Turkish Atomic Energy Authority and the Ministry of Health. More than 100 personnel are working in MONROL.

F-18 Fluorodeoxyglucose (FDG) is produced in all four production facilities and distributed to 40 centers all over the country. More than 35,000 FDG doses were dispensed by MONROL in 2007. This is approximately 10 % of the FDG doses used in Europe. The company operates five cyclotrons at four locations: Two IBA Cyclone 18/9 (18 MeV), two Siemens RDS Eclipse (11 MeV) and one GE PET Trace (16.5 MeV). The chemical synthesis modules used for FDG production are: two CPCU (CTI) modules, one EXPLORA (CTI) module, two FX-FDG (GE) modules and one SYNTHERA (IBA) module.

There are also some research activities carried out in MONROL which include : “Improved high current liquid and gas targets for cyclotron produced radionuclides”- Coordinated Research Project supported by the International Atomic Energy Agency , “Production of F-18 labeled Fluorothymidine” , “Recovery and quality control of cyclotron irradiated O-18 water” , “Prevention of radiolysis in FDG productions with high radioactivity” and “Design and manufacture of home-made Tantalum and Niobium targets”.

Future programs include: production of F-18 radiopharmaceuticals other than FDG and initiation of the production of O-15 and N-13 radiopharmaceuticals. We are planning to establish three more cyclotron facilities in different regions of Turkey to achieve nationwide supply of PET radiopharmaceuticals. Building a cyclotron in Romania is among the projects initiated. The company also made several agreements to run cyclotrons built in the Middle East region for 10 year periods.

Performance of a preloaded cassette based synthesis module for F-18 FDG production.

Paul E. Christian, H. Eric Smith, Brandon S. Buckway, John Gibby, Melissa L. Brooks, Kathryn A. Morton, John M. Hoffman, Huntsman Cancer Institute, University of Utah, Salt Lake City, Utah

¹⁸F-FDG production using automated synthesis modules occasionally suffers from variations in percent yield. Low yields and failed batches have plagued production due to variations in preparation of reagents, system cleaning, valve and tubing failures, etc. A new system using small volume, preloaded reagents and columns on a disposable cassette has recently become available. Our study evaluated the performance of this new module relative to percent labeling of FDG, accuracy of radiation detectors, and robustness. Twenty batches were produced using 30.3-250GBq in order to evaluate the FDG percent yield over a wide range of activity. USP quality control tests were performed on three qualification runs (average 246GBq) immediately after production and again at 12 hours post production. Measurements from onboard pin radiation detectors were validated by comparing the dose calibrator readings of F-18 activity delivered from the cyclotron to the detector readings after the activity was quickly transferred to the synthesis module. In addition, a comparison of the final product activity was performed utilizing detector readings of the final product syringe and readings from a dose calibrator to which the product was completely transferred. Results: The average percent decay corrected yield from the 20 test runs was 87.6 with standard deviation of 5.6% and range 74-93%. Comparison of the onboard radiation detectors to dose calibrator measurements had a correlation of 0.994 with slope of 0.994 and 0.992 and 1.01 respectively for the input and output detectors on the synthesis module. The qualification batches passed required quality control tests immediately after production and 12 hours post production with respective radiochemical purity averaging 99.3% (99.3-99.4%) and 96.95% (95.9-97.9%). Summary: The new FDG module has demonstrated highly reproducible FDG yield (>80%). Onboard radiation detectors were accurate in determining the activity produced, and the system appears to be robust in high activity production runs.

A proportional counter for blood radioactivity measurements

H. T. Sipilä¹, A. Roivainen¹, J. Johansson¹ and S-J. Heselius²

¹ Turku PET Centre, Turku University Central Hospital, PO Box 52, FI-20500 Turku, Finland

² Turku PET Centre, Accelerator Laboratory, Porthaninkatu 3, FI-20500 Turku, Finland

INTRODUCTION

Pharmacokinetic analyses of PET data require the exact determination of the input function, i.e. the determination of radioactivity concentrations in blood and plasma. Silicon diodes have been used for measuring time-activity curves during PET imaging in rodents [1]. Conventional BGO detectors are also widely used for blood activity measurements in human studies (Allog Ab, Sweden). The purpose of the present study was to evaluate the usefulness of a proportional counter for routine on-line analyses of blood samples obtained during PET studies of rodents. The detector system was tested for ¹⁵O measurements. Oxygen-15 has a rather high positron energy of 1.7 MeV. The sensitivity of a gas filled detector is very low for 511 keV photons but charged particles like positrons from ¹⁵O will give an efficient signal when the high energy positrons interact with the detector fill gas. This type of detector requires only light lead shielding and the detector system can be installed very close by to the animal. The proportional counter used in this work was a typical single-wire side-window detector.

MATERIALS AND METHODS

The proportional counter (Fig. 1; type 0460.3 Ar, diameter 27 mm, length 150 mm, fill gas Ar-iC4H10, 400 kPa) and electronics were purchased from Oxford Instruments Analytical Oy, Finland. The detector was equipped with a beryllium window (diameter 20 mm, thickness 500 µm) and was originally intended for analyses of soft X-rays. The blood sampling tube (Teflon, i.d. 1.0 mm, o.d. 1.5 mm) was installed in front of the beryllium window. The counter electronics, preamplifier, linear amplifier and high-voltage power supply were all in the same aluminium box. The counter A/D converter and software for data collection were custom made. The detector was shielded with 50 mm of lead (20 kg). The background count rate was less than 5 cps. Oxygen-15 was produced with the Cyclone 3 cyclotron (IBA, Belgium) of the Turku PET Centre and [¹⁵O]water was produced with a Hidex Radiowater Generator (Hidex Oy, Finland). The performance of the proportional counter was tested with a known activity of [¹⁵O]water solution. The rats were anesthetized with isoflurane and about 50 - 60 MBq [¹⁵O]water (500 µL) was manually injected into the tail vein. A peristaltic pump was used for blood sampling from the tail artery. The blood flow rate through the detector was 500 µL/min. The animals were placed in a PET scanner (HRRT, Siemens) in order to get a reference input function from the hearth.

RESULTS

In Fig. 2 the proportional counter response to ¹⁵O activities in the Teflon tubing is shown. The detector response was linear in the range 15 - 10000kBq/mL which covers well the radioactivity

concentrations which can be measured in rat blood after 60 MBq i.v. injection of [^{15}O]water. In Figs. 3 and 4 blood time-activity curves are shown for [^{15}O]water. Our results show that a simple proportional counter setup can be used for blood time-activity curve measurements in [^{15}O]water PET studies. However, in this preliminary study the blood-pump tubing (i.d. 1.0 mm, length 50 cm) was not optimal. The time delay from the tail artery to the detector was rather high. The time delay and the dispersion of the time-activity curve can be minimized by using a shorter blood-pump tube with a smaller inner diameter.

REFERENCE

1. Jean-Marc Reymond, David Guez, Sophie Kerhoas, Philippe Mangeot, Raphael Boisgard, Sebastien Jan, Bertrand Tavitian and Regine Trebossen, Nuclear Instr. Meth. **A571** (2007) 358–361.

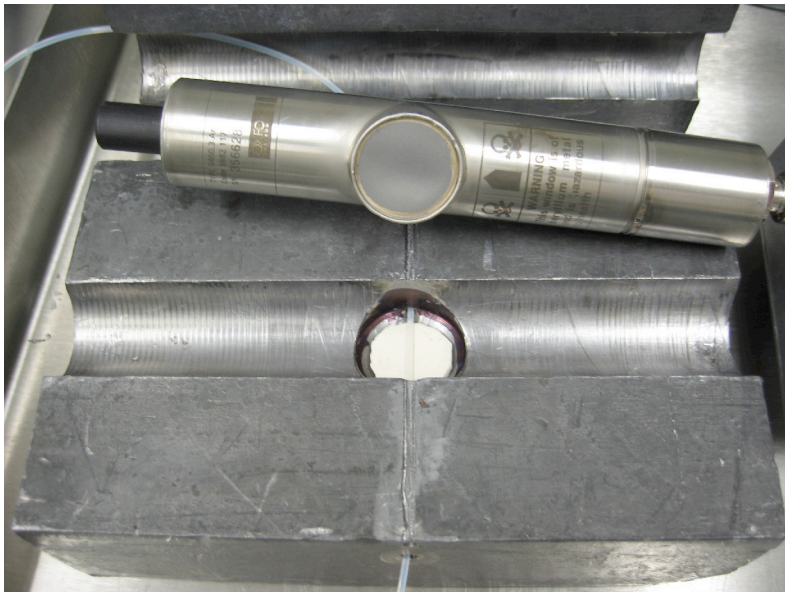


Fig. 1. Proportional counter and lead shield.

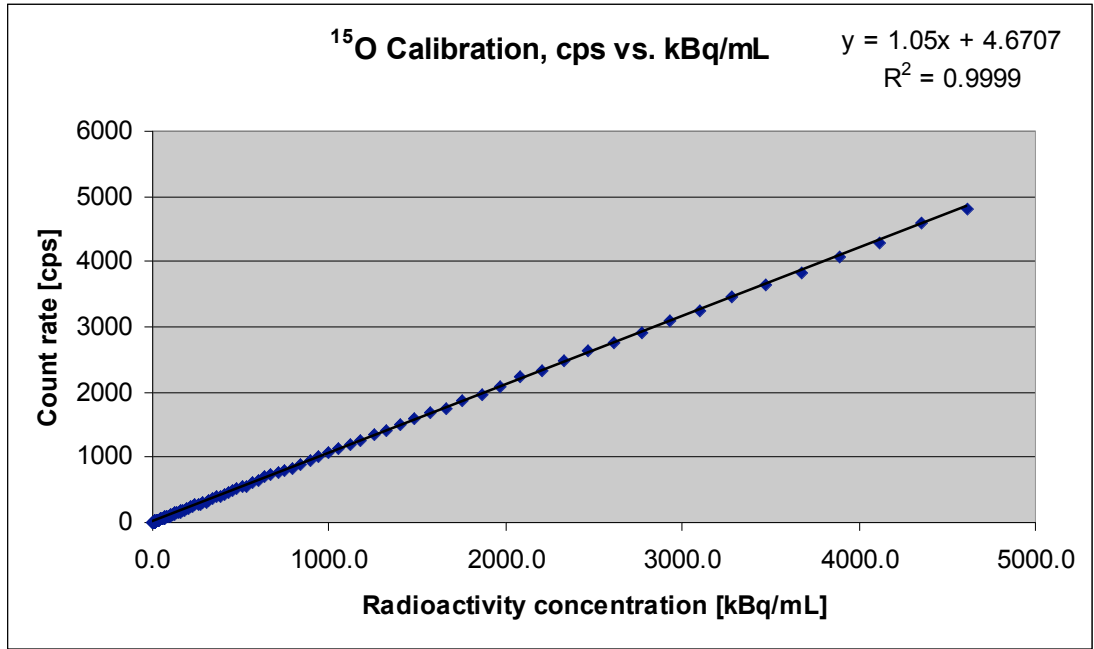


Fig. 2. Proportional counter response to ¹⁵O activity in Teflon tubing.

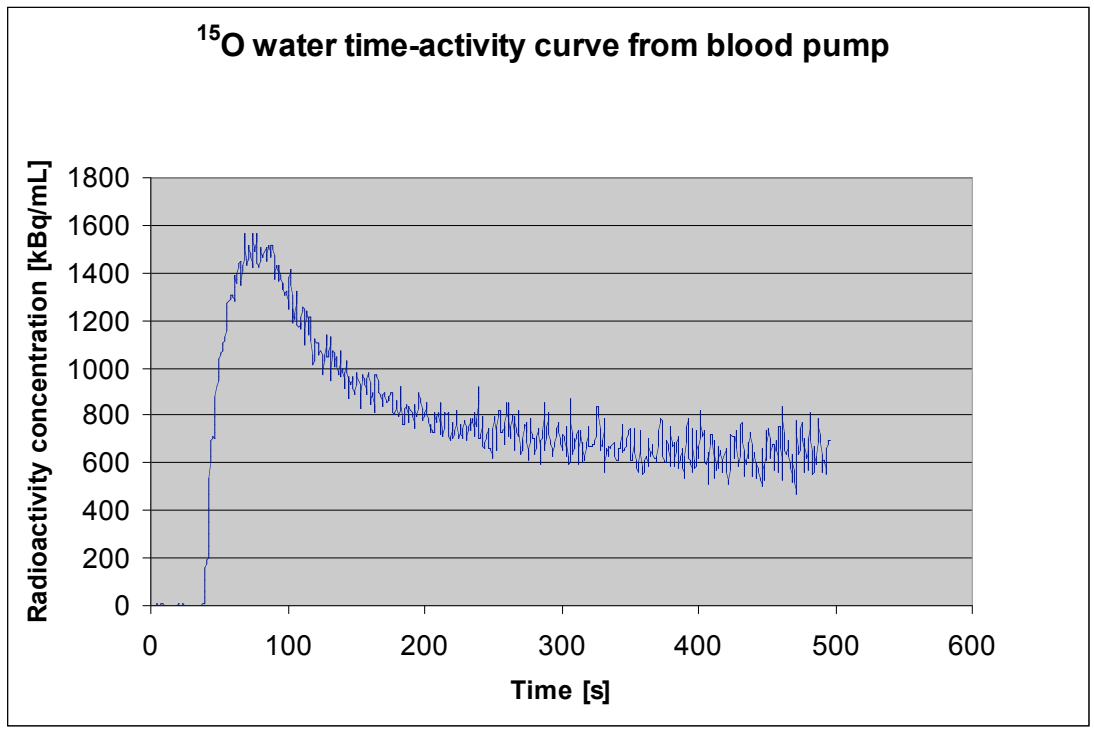


Fig. 3. Tail artery time-activity curve of rat blood measured after administration of 60 MBq [¹⁵O]water.

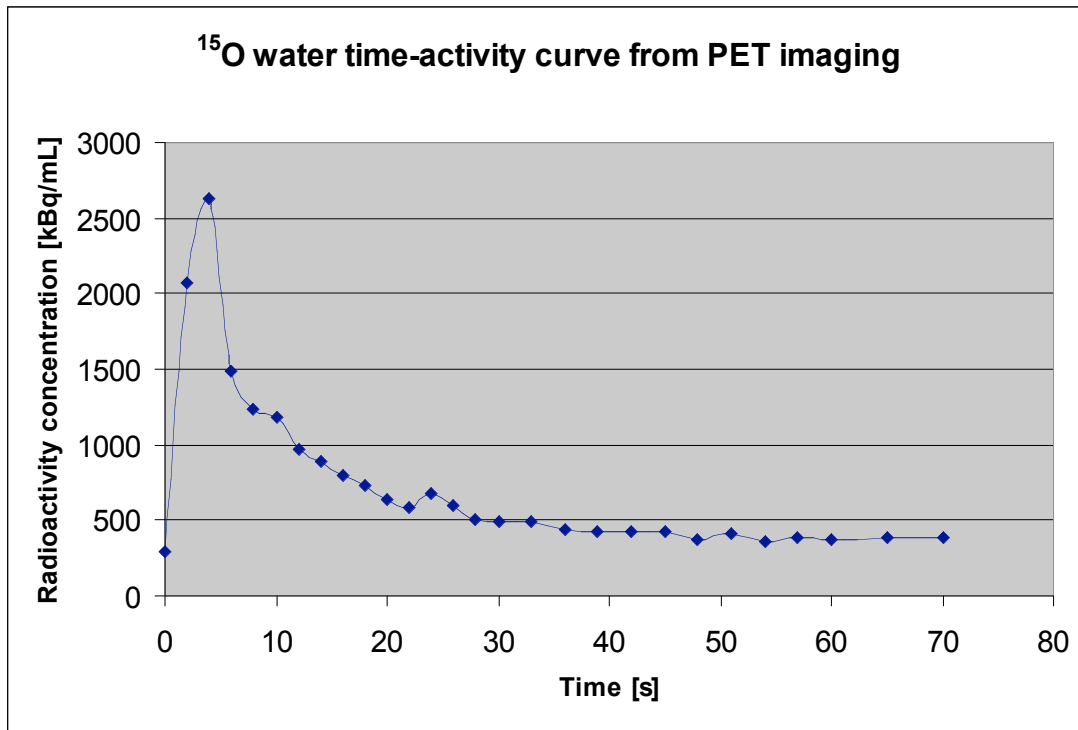


Fig. 4. Myocardium time-activity curve of rat blood measured after administration of 60 MBq ^{15}O water.

Method of distribution of radioactive liquid product from the cyclotron targets to the hotcell labs at the Department of Nuclear Medicine at the University at Buffalo, the State University of New York. Erol Bars, Dr Lynn Kaczmarek.

INTRODUCTION

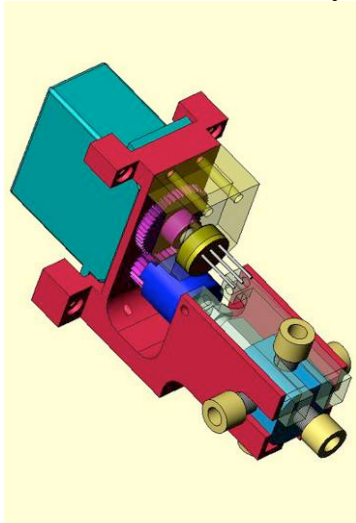
We have designed an automated distribution system to allow us to transfer radioactive liquids from multiple targets to various destinations remotely.

METHOD

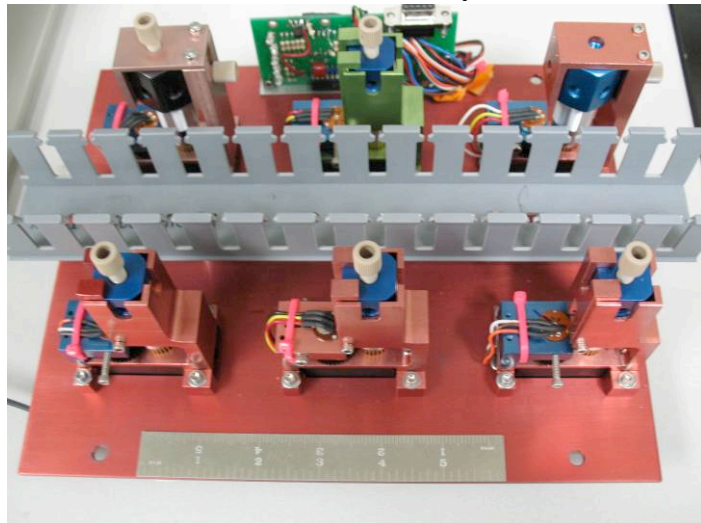
This system is comprised of newly designed software program and hardware. The goal of the design was to provide a system that was shielded from outside radiation, occupying minimal space, at minimal cost.

The system allows the user the ability to install a total of 6 valves, varying from 2-6 ports. Our ^{18}F pathway consists of a 1 way input, 4 output port Hamilton valve coming from the cyclotron targets to the distribution system and 1 way input and 6 output port Hamilton valve from distribution system to various locations throughout facility. These valves are made with Teflon internal parts and have a small dead volume. To drive these valves, a Futaba S3305 hobby servo capable to deliver 8.9kg-cm of torque was used. A small modification was made to these servo's to give it the ability to rotate >320 degrees. A PLC microcontroller was embedded into the system to reduce the size and cost of the system. The Visual Basic GUI employed offers the benefit of a multiple remote control platform network.

Servo-Hamilton Assembly



Manifold of 6 Valves Assembly and microPLC

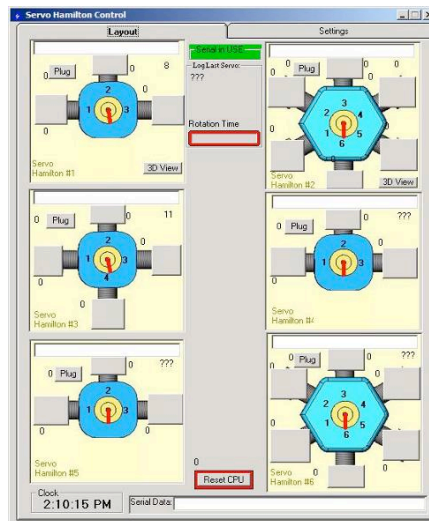


Servo Hamilton Program Main Screen

The microPLC can control up to 6 Valves per one serial connection.

Angular potentiometer detection offers a feed back location of the rotor valve shaft, thus giving the real time port selected. The software is designed in a way to customize all valve key labels and notes. The software is capable of selecting up to 16 manifold uPLC's in one screen.

Servo Hamilton Main Screen software.



CONCLUSION

This system is located in the vault beneath the cyclotron pit and has been successfully employed since February 2008. This user friendly system may be expanded for other uses, such as radiopharmaceutical synthesis.

**Semi-automated process of Choline and acetate module at the Department of Nuclear Medicine at the University at Buffalo, the State University of New York.
Erol Bars, Dr Sajjad**

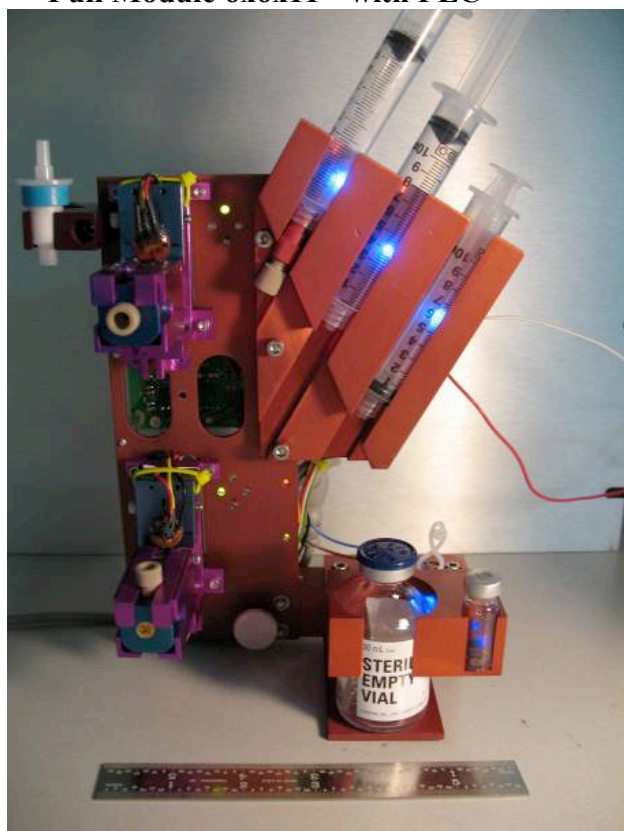
INTRODUCTION

We developed a module designed primarily for C¹¹ compound synthesis but offers the flexibility to use for other research compounds. Our goal was to build a customizable and user friendly system at a low cost.

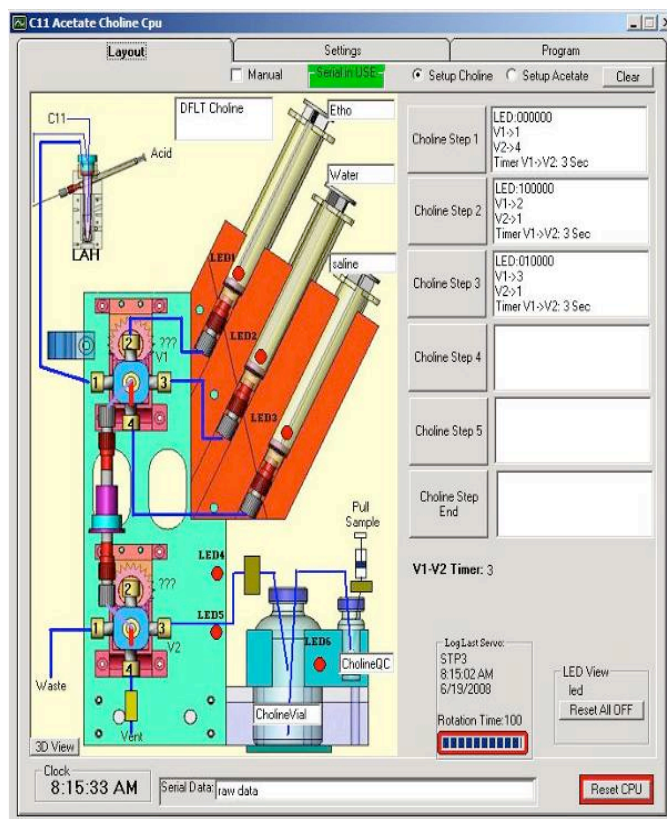
METHOD

The system should be network accessible, small, ergonomic, and reliable. The semi-automated design provides a compact system. The valves are PC base controllable, while the syringes are manually controlled and equipped with LED backlight signal notification. The graphic user interface offers remote access operation from other lab location.

Full Module 6x6x11 ” with PLC



Software Control GUI



Note: The basic process of Choline and Acetate will not be described in this abstract.

CONCLUSION

Designing a module to do R&D compounds is always a challenge. This module offers the chemist the ability to program various procedures and methods, facilitating and expediting the design of a new semi-automated synthesis module.

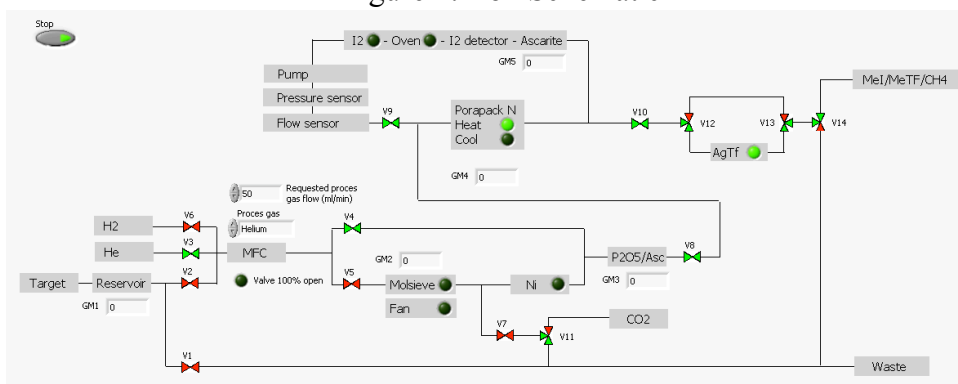
Breaking in a Scansys automated synthesis box with [¹¹C]Methyl Iodide and [¹¹C]Methyl Triflate.

Jonathan W Engle, Todd E Barnhart, Dhanabalan Murali, Nick T Vandehey, Peter Larsen, Robert J Nickles

Objectives: We report the initial experiences of the cyclotron group at the University of Wisconsin-Madison using the Scansys automated synthesis box to produce [¹¹C]CH₃I and [¹¹C]CH₃OTf as preliminary compounds for a variety of clinical and research PET radiotracer syntheses. After minor modifications post-delivery, the Labview-driven box reliably produces 1000 to 4000 mCi/umol specific activities at end of synthesis with average [¹¹C]CH₃I to [¹¹C]CH₃OTf conversion of 57% ± 3% (n=62). For static irradiations of 26-34 minutes with 15 uA of beam yields in initial precursor solution were 147 ± 21 mCi for [¹¹C]CH₃I (n=7) and 101 ± 30 mCi for [¹¹C]CH₃OTf (n=9).

Methods: Between 10 and 24 uA of 11 MeV protons from the CTI RDS 112 prototype are directed onto a pressurized gas target containing a static mixture of 10% H₂ in N₂ gas to make use of the ¹⁴N(p,α)¹¹C reaction. Target valves are then opened and [¹¹C]CH₄ is trapped on a Hayesep column cooled to -180°C with liquid nitrogen, whose flow around the trap is regulated by a novel jet vacuum pump. The circulation loop is closed, the Hayesep is warmed to -10°C, and a two-zone tube furnace is heated, with I₂ volatilized at 60°C and the reaction zone at 760°C. Flushing steps at incrementally elevated Hayesep temperatures serve to remove contaminant NH₃, HI, and unreacted iodine before the Hayesep is finally heated to 200°C to release [¹¹C]CH₃I. If methyl triflate is desired, flow is diverted through an additional furnace packed with silver triflate heated to 210°C before bubbling through precursor in solution. Real-time activities, pressures, and flows are measured, logged, and saved to disc throughout the synthesis.

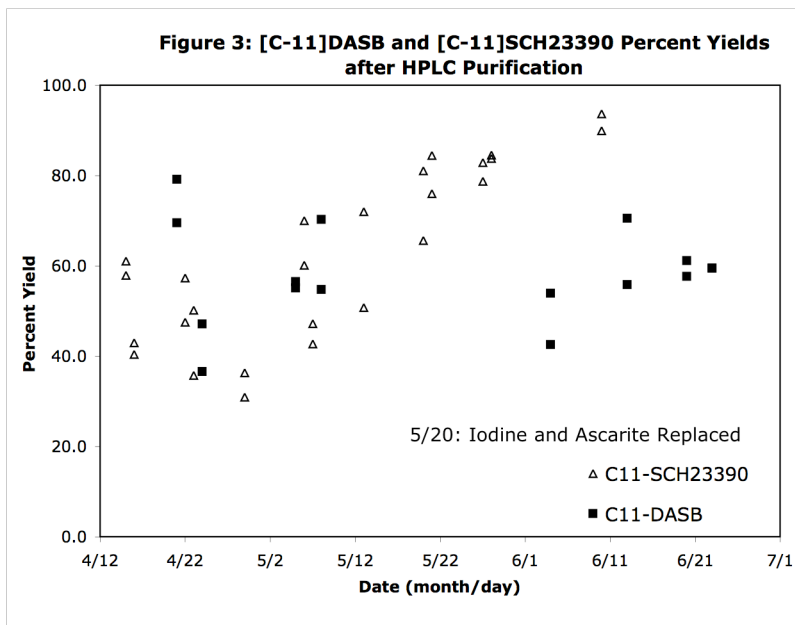
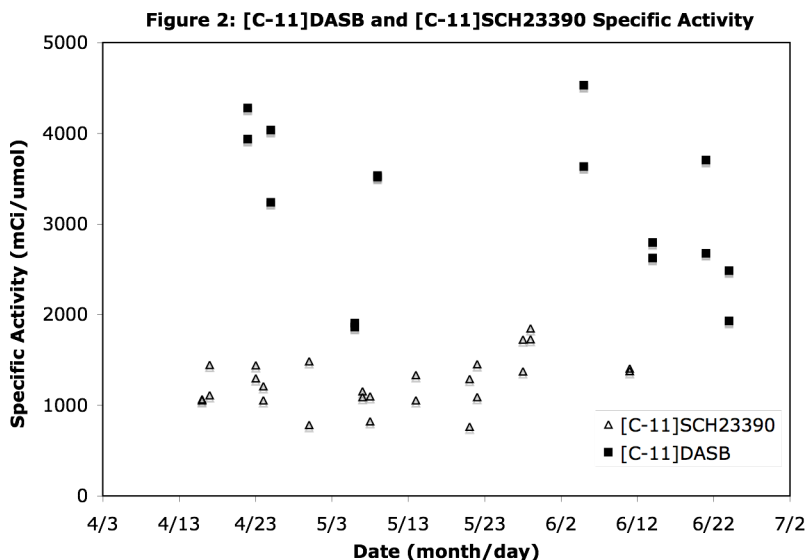
Figure 1: Box Schematic



In three months, the Scansys box has been employed in the production of six different PET radiotracers: ¹¹C-DASB, ¹¹C-SCH23390, ¹¹C-PK11195, ¹¹C-PIB, ¹¹C-FLB457, and ¹¹C-Paraquat. Notable in-house modifications include the use of a wet Ascarite mixture within the loop to trap excess iodine during conversion to [¹¹C]CH₃I, a check valve to prevent backflow into the loop after conversion is complete, an additional P₂O₅ trap in front of the triflate furnace to remove any accumulated moisture prior to triflation, removal of stainless steel materials from post-triflation steps in the synthesis, and

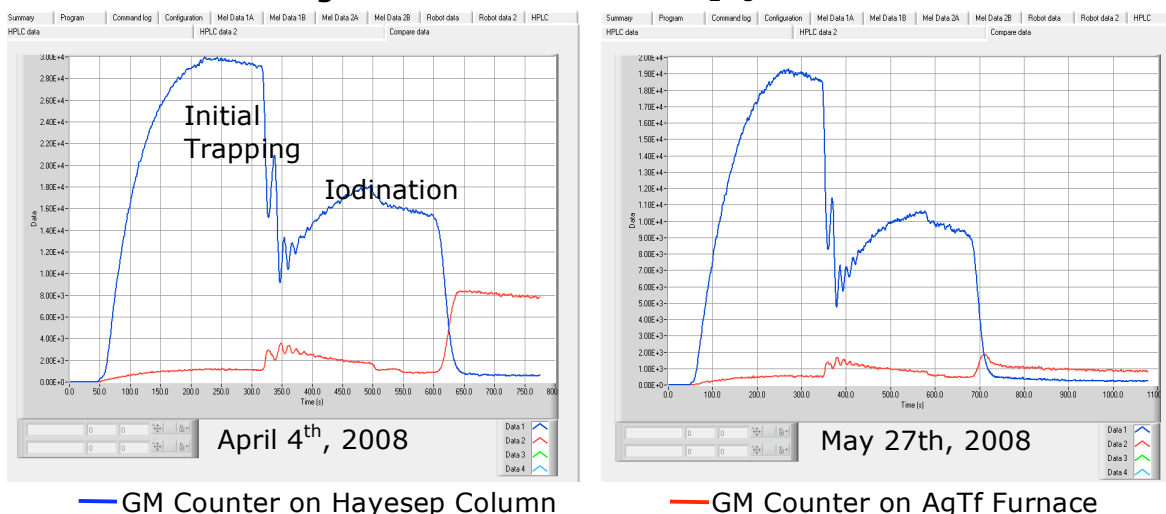
customization of Labview program code to optimize temperatures, flow rates, pressures, and reaction durations during synthesis.

Data: Specific activities of ^{11}C -DASB and ^{11}C -SCH23390 based on available standards are reported below in Figure 2. Figure 3 details percentage yields for the same two tracers after HPLC purification. We noted significant improvement in $[^{11}\text{C}]\text{CH}_3\text{OTf}$ synthesis yields after replacing iodine reservoirs and Ascarite traps within the circulation loop.



Triflation yields also appear directly related to the age of the added P_2O_5 trap as shown in Figure 4. With use, P_2O_5 loses its ability to efficiently remove water, leading to significant trapping of $[^{11}\text{C}]$ in the triflate furnace.

Figure 4: Before and After P₂O₅ Addition



Contamination of the triflate furnace with precursor is possible and has been informally reported by users of the other existing Scansys ¹¹C-synthesis box if needles are inserted into precursor solutions prior to the opening of release valves due to accumulated pressure on the backside of the conversion loop. To prevent such a problem, it is important to establish release flow before any portion of the needle approaches the precursor solution. Stainless steel needles trap large portions of produced [¹¹C]CH₃OTf and must be washed with ethanol and baked dry before each synthesis. The box is regularly conditioned with helium flows of 50 mL/min and cyclic heating of both the Hayesep column and the silver triflate furnace, especially following any maintenance that opens the system to air. This serves to purge atmospheric contaminants and well as cold products, HI or I₂ from previous runs and has kept precursor from changing color (presumably due to either HI or I₂).

Conclusions: The Scansys ¹¹C synthesis box has proven to be an indispensable tool in radiotracer synthesis and development at the University of Wisconsin, and transition from our two homemade synthesis systems, used with much success for the past four years, has been facile. Failed syntheses have, without exception, been due to testing modifications or operator error. In total, the box has produced 9.9 Ci of [¹¹C]CH₃I and [¹¹C]CH₃OTf trapped in precursor solutions in its first three months of operation and it has opened the door to reliable, high yield ¹¹C at our institution.

Literature Cited:

- Larsen P, Ulin J, Dahlstrom K, and Jensen M (1997) Synthesis of [¹¹C]Iodomethane by Iodination of [¹¹C]Methane Appl. Radiat. Isot. 48,53-157.
- Jewett DM (1992) A Simple Synthesis of [¹¹C]Methyl Triflate Appl. Radiat. Isot. 43, 1383-1385.
- Vandehey NT, Barnhart TE, Dallas CB, Nickles RJ, Oakes TR, Roberts AD, Converse AK (2004) Design of an automated chemistry rig for production of [¹¹C]CH₃I [abstract, poster]. Workshop on Targetry and Target Chemistry 10.